Appendix A

Examples of Uniform Time-Delay Embedding

Two examples regarding the methodology of uniform time-delay embedding are presented: (A.1) using a 20 sample length vector, and (A.2) using a time series from horizontal movement of a triaxial accelerometer.

A.1 20 sample length vector.

For this example, it has been proposed to work with a vector $\{\boldsymbol{x}_n\}_{n=1}^{20}$ with a sample length $N = 20$ in order to implement an uniform time-delay embedding matrix, $\boldsymbol{X}_{\tau}^{m}$, with embedding dimension of $m = 5$ and delay dimension of $\tau = 3$ (Eq. (3.4)).The representation of the uniform time-delay embedding matrix $\boldsymbol{X}_3^5$ is as follows

$$\boldsymbol{X}_{\boldsymbol{3}}^{\boldsymbol{5}} = \begin{pmatrix} \tilde{\boldsymbol{x}}_n \\ \tilde{\boldsymbol{x}}_{n-3} \\ \tilde{\boldsymbol{x}}_{n-6} \\ \tilde{\boldsymbol{x}}_{n-9} \\ \tilde{\boldsymbol{x}}_{n-12} \end{pmatrix}^{\mathsf{T}} \tag{A.1}$$

The dimension of the uniform time-delay embedding matrix is defined by $N-(m-1)\tau$ rows and m columns. $N-(m-1)\tau$ is also the sample length of the delayed copies of $\boldsymbol{x}_n$ which is equal to eight $(20-((5-1)*3)=8)$. Therefore, $\boldsymbol{X}_3^5$ can be explicitly represented as

$$\boldsymbol{X}_3^5 = \begin{pmatrix} x_1 & x_2 & x_3 & x_4 & x_5 & x_6 & x_7 & x_8 \\ x_4 & x_5 & x_6 & x_7 & x_8 & x_9 & x_{10} & x_{11} \\ x_7 & x_8 & x_9 & x_{10} & x_{11} & x_{12} & x_{13} & x_{14} \\ x_{10} & x_{11} & x_{12} & x_{13} & x_{14} & x_{15} & x_{16} & x_{17} \\ x_{13} & x_{14} & x_{15} & x_{16} & x_{17} & x_{18} & x_{19} & x_{20} \end{pmatrix}^{\mathsf{T}} \tag{A.2}$$

After transposing $\boldsymbol{X}_3^5$, one can see that the ranges of values of the uniform time-delay embedded matrix are between $((m-1)\tau)+1$ to N (for this example from 13 to 20):

$$\boldsymbol{X}_3^5 = \begin{pmatrix} x_1 & x_4 & x_7 & x_{10} & x_{13} \\ x_2 & x_5 & x_8 & x_{11} & x_{14} \\ x_3 & x_6 & x_9 & x_{12} & x_{15} \\ x_4 & x_7 & x_{10} & x_{13} & x_{16} \\ x_5 & x_8 & x_{11} & x_{14} & x_{17} \\ x_6 & x_9 & x_{12} & x_{15} & x_{18} \\ x_7 & x_{10} & x_{13} & x_{16} & x_{19} \\ x_8 & x_{11} & x_{14} & x_{17} & x_{20} \end{pmatrix} = \begin{pmatrix} \boldsymbol{X}[13] \\ \boldsymbol{X}[14] \\ \boldsymbol{X}[15] \\ \boldsymbol{X}[16] \\ \boldsymbol{X}[17] \\ \boldsymbol{X}[18] \\ \boldsymbol{X}[19] \\ \boldsymbol{X}[20] \end{pmatrix}. \tag{A.3}$$

A.2 Time series for horizontal movement of a triaxial accelerometer.

In this example, it is considered a time series of a triaxial accelerometer (Figure A.1(C)), captured from repetitions of a horizontal trajectory (Figure A.1(A)) performed by user (Figure A.1(B)). From Figure A.1(C)) is evidently that the $A_y(n)$ is the most affected axis of the accelerometer due to the movement's characteristics in the horizontal trajectory. With that in mind, $A_y(n)$ is selected as the input time series for the uniform time-delay embedding theorem.

Considering that the sample rate of the data is 50 Hz, it has been proposed to work with a vector of sample length of $N = 1000$ which corresponds to 20 seconds of data. Then, with minimum embedding parameters $m = 7$ and $\tau = 11$, the dimensions of the uniform time-delay embedding matrix, $\boldsymbol{A_y}_{11}^7$, are 934 ($N - (m-1)\tau$) rows and 7 (m)

columns. ${\boldsymbol{A}_{\boldsymbol{y}}}^{7}_{11}$ is therefore represented as follows:

$$
{\boldsymbol{A}_{\boldsymbol{y}}}^{7}_{11} = \begin{pmatrix} A_y(n) \\ A_y(n-11) \\ A_y(n-22) \\ A_y(n-33) \\ A_y(n-44) \\ A_y(n-55) \\ A_y(n-66) \end{pmatrix}^{\mathsf{T}} = \begin{pmatrix} a_y(1) & \dots & a_y(934) \\ a_y(12) & \dots & a_y(945) \\ a_y(23) & \dots & a_y(956) \\ a_y(34) & \dots & a_y(967) \\ a_y(45) & \dots & a_y(978) \\ a_y(56) & \dots & a_y(989) \\ a_y(67) & \dots & a_y(1000) \end{pmatrix}^{\mathsf{T}} \tag{A.4}
$$

$$
{\boldsymbol{A}_{\boldsymbol{y}}}^{7}_{11} = \begin{pmatrix} a_y(1) & a_y(12) & a_y(23) & a_y(34) & a_y(45) & a_y(56) & a_y(67) \\ \vdots & \vdots & \vdots & \vdots & \vdots & \vdots & \vdots \\ a_y(934) & a_y(945) & a_y(956) & a_y(967) & a_y(978) & a_y(989) & a_y(1000) \end{pmatrix} \tag{A.5}
$$

$$
{\boldsymbol{A}_{\boldsymbol{y}}}^{7}_{11} = \begin{pmatrix} {\boldsymbol{A}_{\boldsymbol{y}}}^{7}_{11}[67] \\ \vdots \\ {\boldsymbol{A}_{\boldsymbol{y}}}^{7}_{11}[1000] \end{pmatrix}. \tag{A.6}
$$

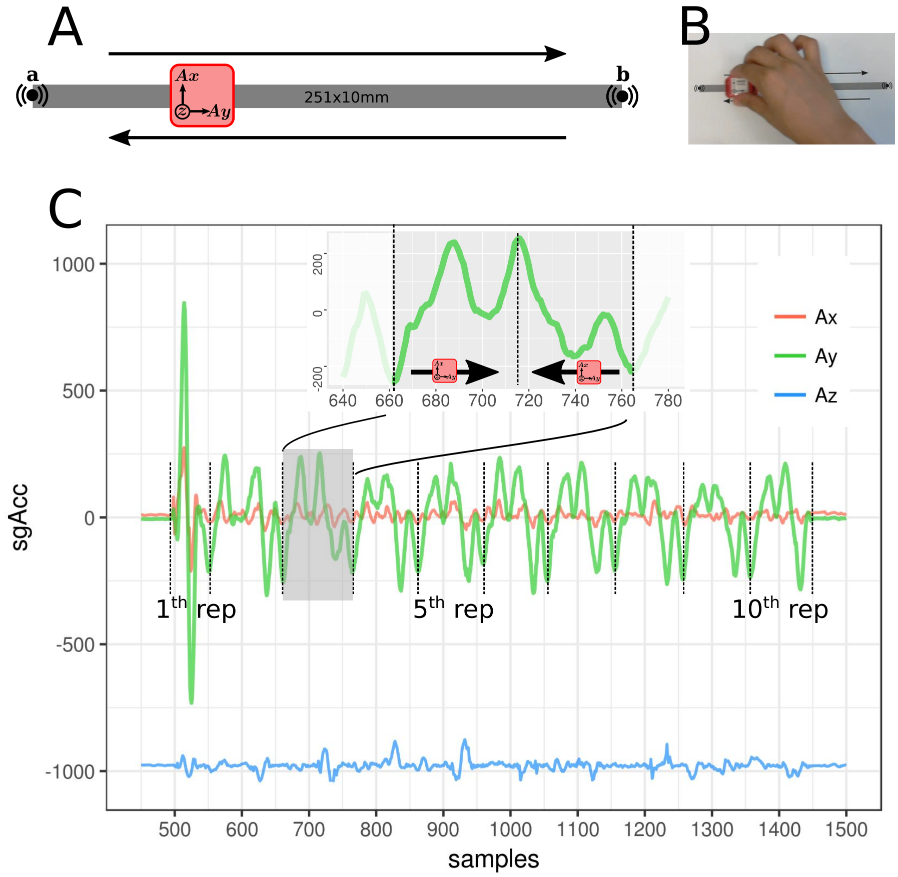

Fig. A.1 **Example of time series with an IMU** (A). Triaxial accelerometer (in red) is moved repetitively across a line of 251 mm from point **a** to **b** and then from **b** to **a**. The points **a** and **b** indicate when a click sound is produced. (B). Person's hand holding and moving the sensor horizontally across the line. (C). Time series for the triaxial accelerometer ($A_x(n)$, $A_y(n)$, $A_z(n)$) for ten repetitive horizontal movements across a line. The top time series only shows A_y axis which corresponds to one cycle of the horizontal movement and the black arrows represent the movement's direction of the accelerometer with respect to the produced time series.

Appendix B

Equipment

B.1 NeMEMsi IMU sensors

For this thesis, data were collected using NeMEMsi sensors that provide 3D accelerometer, 3D magnetometer, 3D gyroscope and quaternions (Comotti et al., 2014). Figure B.1 shows NeMEMsi sensor. It is important to note that NeMEMsi sensors were tested against the state-of-the-art device MTi-30 IMU from xsense. The comparison values between NeMEMsi and MTi-30 in terms of standard deviation of the noise of each component of the Euler angles at a stated state are lower than 0.1 degrees. Additionally, the NeMEMsi provide not only to have a lower-power consumption but also the smaller dimensions against other state-of-the-art brands of IMUs. In the following sections, some features of the NeMENsi IMU are presented. See Comotti et al. (2014) for further details.

Sample rate and power consumption

Data streaming can be set up to be streamed at 25 Hz, 50 Hz and 100Hz which affects the power consumption from 29mAh, 32mAh and 35mAh, respectively. For this thesis, the sample rate were set up to 50 Hz.

Sensors

The outputs of the NeMEMsi sensor includes:

Orientation

* Euler angles (Yaw, Pitch and Roll).
* Quaternions.

Accelerometer (Linear acceleration)

* Raw and calibrated XYZ measurement from ±2 / ±4 / ±6 / ±8 / ±16

Gyroscope (Rate of turn)

* Raw and calibrated XYZ measurement from ±245 / ±500 / ±2000 degrees per second.

Magnetometer (Magnetic field)

* Raw and calibrated XYZ measurement from ±4 / ±8 / ±12 / ±16 gauss.

Microprocessor

* Architecture: ARM 32-bit Cortex M4 CPU with FPU and DSP instructions
* Max.frequency: 100MHz

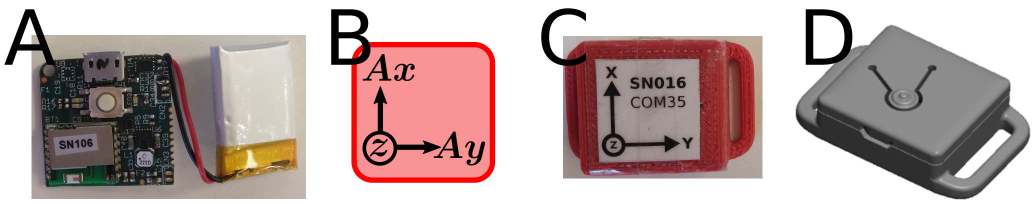

Fig. B.1 **Inertial Measurement Sensor** (A) Printed Circuit Board (PCB) with 165mAh battery, (B) axis orientation, (C) real case, and (D) 3D model for the case.

* Memory Size: 512 Kbytes
* RAM: 128 Kbytes SRAM

Connectivity

* Bluetooth: Class 2, bluetooth 3.0
* Range: 10 m
* Transmission rate: Up to 560 kbps with Service Port to Port
* Multipoint: Up to 7 slaves

Form factor

* Electronics physical dimension: 25L x 25W x 4H (mm)
* Electronics Weight: 3.3 gr
* Dimension with battery and casing: 42L x 28W x 11.5 (mm)
* Weight with batter and casing: 15 gr

B.1.1 Issues with IMUs

For the experiment of human-image imitation activities where eight activities were performed per participant, it has been observed that time synchronisation had issues because of the drift in time for time series data (2 minutes of data collection). Additionally, these experiments had problems with disconnections to bluetooth module. In contrast, for the human-humanoid imitation activities where only four activities were performed per participant (1 minutes of data collection), data collection of time series had fewer issues with regard to the drift in time and bluetooth data streaming.

B.2 Time-series preprocessing

The following sections explain how the organising data in multidimensional arrays, data synchronisation, data Synchronisation, and time alignment are computed. Code and data for the following sections is available at .

B.2.1 Organising Data in Multidimensional Arrays

Scripts in MATLAB were created to synchronise the data using the clock drift and clock offset values which were provided for each of the NeMEMSi sensors. Then the data from each sensor is aligned in time using using `finddelay()` and `alignsignals()`.

B.2.2 Data Synchronisation

To find the delay between two two sensors that were attached to the same place of the body parts, a function called `finddelayMX()` was created. Such function computes the autocorrelation between two signals using (xcorr()) then the maximum value of the autocorrleation function is extracted to create a delay between the values of maximum index in the autocorrelation function and the length of the first signal.

The function `alignsignalsMX()` was used to align two signals based on `finddelayMX()`. The function `alignsignalsMX()` use six inputs of which sA and sB are for the sensors, windowframe for the information of the signal is extracted from another activities, the MainAxis of which the signal are going to be extracted, the truncate delay that is created to synchronise the signals adding an extra delay that is based on the length of previous signals and tuning delay that can be useful to tune the delay in the case of the delay is not appropriate when the signals are too noisy. Then, `aligntwosignals()` is applied to align only two signals. The inputs of `aligntwosignals()` are X and Y for the input vectors, truncate delay for the previous delay of two signals and tuning delay in case that signals are two noise and the xcorr fail to find an appropriate delay.

B.2.3 Time Alignment

Given four vectors of time t_1, t_2, t_3, t_4, the minimum and maximum values were extracted for the start time of the four sequence of time, it was also extracted the minimum and maximum values to the end of each of the four sequences of time. However, after aligning the vectors it has then been noticed that there were different values of length across vectors i.e., $1880, 1986, 1987, 1988$. Therefore the length for the second vector was used as the primary length because is the one that presents the minimum value of the three maximum lengths. Then `interp1(x,v,vq,'phchip')` was used to interpolate the length of each of the vectors, for example: $1986, 1986, 1986, 1986$. It has been chosen `phchip` function since the interpolation present values for each of the points as oppose to `linear` function which create NA values.

B.3 NAO – humanoid robot

A NAO humanoid robot version 04 from SoftBank (Fig. B.2) was used for the experiments of human-humanoid interaction. NAO were programmed for simple horizontal and vertical arm movements using Choregraphe, an API to program NAO, and then interpolated values of the animation were exported to a python script.

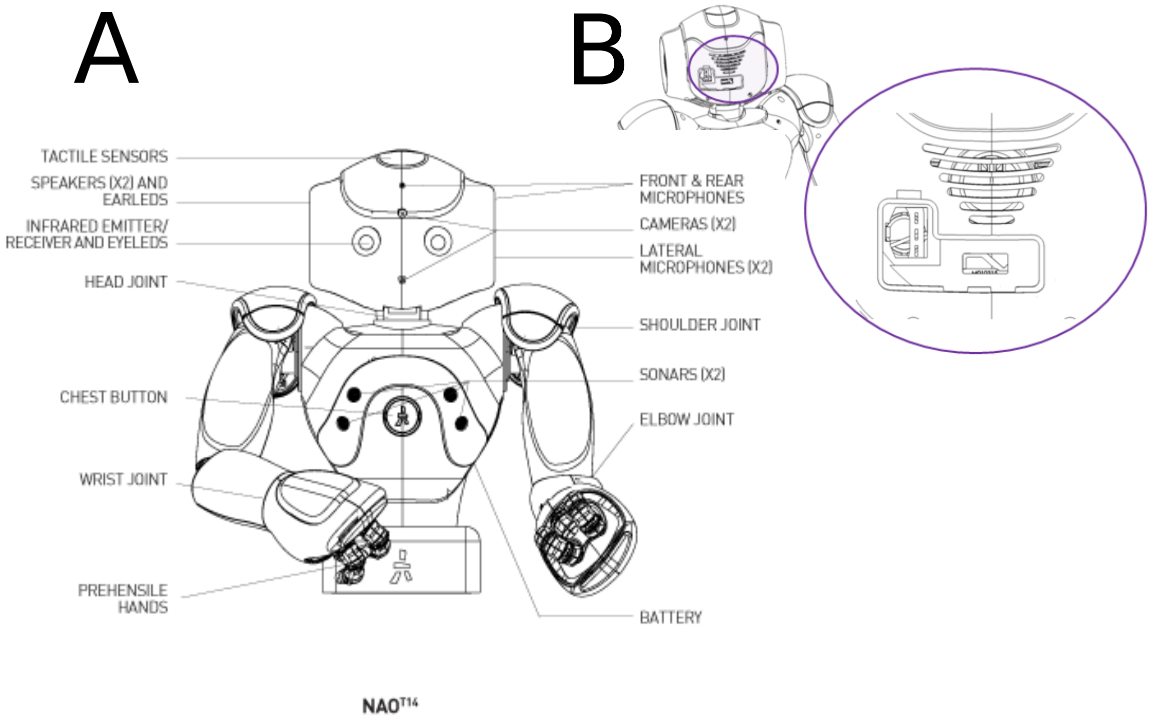

Fig. B.2 **NAO, humanoid robot from SoftBank.** (A) NAO body type T4 with its parts, and (B) back design of NAO version 04.

Appendix C

Experiment Design

C.1 Experiment Check List

Figure C.1 shows the experiment check list for the experiments which consist of: 1. Participant Information, 2. Setting up sensors, 3. Experiments, 4. Stop sensors, and 5. Extra notes.

C.2 Information Sheet

Figures C.2, C.3, C.4 and C.5 show a google form for the Online Participation Sheet.

Experiment Check List. Participant: p____

Human-Humanoid Imitation Activities

1. Information

◯ 1.1 Participant Information Sheet ◯ 1.2 Anthropometric Data

◯ 1.3 Sitting the participant on the Chair

◯ 1.4 Start Recording Video ◯ 1.5 Show participant p__ to the camera

2. Setting Up Sensors

Status HII	**Description**	**Status HRI**
☐	Create Data Path	☐
☐	Open Muse Applications	☐
☐	Turn ON the sensors	☐
☐	Pair the sensor [sensor number and port number]	☐
☐	Set the sampling rate to 50 Hz	☐
☐	Open settings for Time Sync parameters	☐
☐	Compute the Time Sync parameters	☐
☐	PrintScreen the Time Sync parameters and Save Capture	☐
☐	Close settings and set parameters	☐
☐	Start Recording data	☐
☐	Shake all sensors	☐

◯ 2.1.a Attach Sensors to the Participant (check sensor orientation) ◯ 2.1.b Attach Sensors to the Robot (check sensor orientation)

◯ 2.1.a Attach Sensors to the Participant (check sensor orientation) ◯ 2.2.b Attach Sensors to the Participant (check sensor orientation)

3. Experiment

◯ 3.1.a Human-Image Int [NO BEAT]

Status	**Description**
☐	Hor Normal
☐	Ver Normal
☐	Hor Fast
☐	Ver Fast

◯ 3.2.b Human-Robot Int [BEAT]

Status	**Description**
☐	**./HN.sh p__**
☐	**./VN.sh p__**
☐	**./HF.sh p__**
☐	**./VF.sh p__**

◯ 3.2.a Human-Image Int [BEAT]

Status	**Description**
☐	**aplay HN_beat.wav**
☐	**aplay VN_beat.wav**
☐	**aplay HF_beat.wav**
☐	**aplay VF_beat.wav**

4. Stop

◯ 4.1.a Stop Sensor Recording ◯ 4.1.b Stop Sensor Recording

◯ 4.2.a Save Data ◯ 4.2.b Save Data

◯ 4.3.a Disconect Sensors ◯ 4.3.b Disconect Sensors

◯ 4.4 Stop Video Recording

5. Notes

Fig. C.1 **Experiment Check List.**

25/10/2018 A Study of Movement Variability in Human-Humanoid Interaction Activities

A Study of Movement Variability in Human-Humanoid Interaction Activities

*Required

Introduction

The aim of this study is to explore how participant's performance of simple movements affects the movement variablity in the follwoing conditions: a) following an image while not hearing a beat and while hearing a beat; and b) following a humanoid-robot while not hearing a beat and while hearing a beat.

The estimated time for the study is between 40 to 45 minutes.

Miguel P. Xochicale [http://mxochicale.github.io/]
Doctoral Researcher in Human-Robot Interaction
School of Electronic, Electrical and System Engineering
University of Birmingham, UK

1. Online Participant Information Sheet

Who will conduct the research?

The study is conducted by Miguel P. Xochicale as part of his PhD degree in Electronic, Electrical and System Engineering at the University of Birmingham. The research is supervised by Professor Chirs Baber and Professor Martin Russell in the Electronic, Electrical and System Engineering department at the University of Birmingham.

What is the purpose of the research?

The aim of this study is to explore how participant's performance of simple movements affects the movement variablity in the follwoing conditions: a) following an image while not hearing a beat and while hearing a beat; and b) following a humanoid-robot while not hearing a beat and while hearing a beat.

What will happen during the experiment?

During the experiment you will be asked to wear two inertial sensors in your right hand and you will perform 10 repetitions for horizontal and vertical arm movements in six conditions:

Condition 1. Following an image while NOT hearing a beat
Condition 2. Following an image while hearing a slow beat rate
Condition 3. Following an image while hearing a fast beat rate

(a 5 minutes break will be given at this point)

Condition 4. Following a humanoid-robot while NOT hearing a beat
Condition 5. Following a humanoid-robot while hearing a slow beat rate
Condition 6. Following an image while hearing a fast beat rate.

https://docs.google.com/forms/d/1dPN6D_S3CRg4pkDYplfDg6fSnh6FaQ4Z7M0xl_11Fq4/edit 1/4

Fig. C.2 **Participant Information Sheet (p. 1/4)**

What type of data will be collected during the experiment?

Three types of dada will be collected:
i) Data from inertial sensors will be collected. Each inertial sensor has a accelerometer, magnetomer, gyroscope.
ii) Audio from a microphone to record the movements of the humanoid-robot.
iii) A video will be recorded for visualisation and demonstration purposes (let me know if you are uncomfortable with the video recording).

What happens to the data collected?

The data will be analysed in order to explore how participant's performance of simple movements affects the movement variablity in the previous six conditions of movement.

How Is Confidentiality Maintained in the experiment?

The law called the Data Protection Act (1998) tells us how to keep your information secure.

Your data will be treated as confidential and you will be assigned a unique identifying code which will be used to identify your data. If you have decided to provide your name and email address, it will remain confidential and we will
not give your details to anyone else. No other personal data will be recorded about participants (no ethnicity, address, telephone number, etc.)

What is the duration of the experiment?

The estimated time for the study is between 40 to 45 minutes.

Where the experiment will be conducted?

The experiment will be conducted in room N310 which is in third floor at Gisbert Kapp Building (G8), University of Birmingham.

Will the results of this research be published?

Data collected will be used for conference and journal publications and the PhD thesis results.

Will be compensation for participating?

You are invited to participate in this study but will receive no compensation.

Can I withdrawal from the experiment after given my consent?

Yes, you can withdrawal from the experiment at any time after given your consent which might be either before the start of your experiment session, during the session, or after finishing the session. In case of withdrawal, all your data will be discarded and will not be used anywhere in the study.

Fig. C.3 **Participant Information Sheet (p. 2/4)**

25/10/2018 A Study of Movement Variability in Human-Humanoid Interaction Activities

Contact Details

If you have any questions about the project, you can contact Miguel by e-mail or telephone, using the details provided below:

Doctoral Researcher: Miguel P. Xochicale [map479@bham.ac.uk].
Deparment: School of Electronic Electrical and Systems Engineering

Primary Supervisor: Professor Chirs Baber [c.baber@bham.ac.uk]
Deparment: School of Electronic Electrical and Systems Engineering

Secondary Supervisor: Professor Martin Russell [m.j.russell@bham.ac.uk]
Deparment: School of Electronic Electrical and Systems Engineering

1. **Statement of understanding/consent** *
Tick all that apply.

☐ I confirm that I have read and understand the participant information online sheet for this study. I have had the opportunity to aks questions if necessary and have had these answered satisfactorily.

☐ I understand that I am able to withdraw from the experiment at any time without giving any reason. If I withdraw my data will be removed from the study and will be destroyed.

☐ I understand that my personal data will be processed for the purposes detailed above, in accordance witht he Data Protection Act 1998.

☐ Based upon the above, I agree to take part in this study.

2. **Your Name** *

3. **Email** *

2. Antropometric Data

4. **Participant Number (e.g. p11)** *

5. **What is your gender?** *
Mark only one oval.

◯ Male
◯ Female

6. **What is your age in years?** *

7. **What is your handeness?** *
Mark only one oval.

◯ Left
◯ Right

https://docs.google.com/forms/d/1dPN6D_S3CRg4pkDYplfDg6fSnh6FaQ4Z7M0xl_11Fq4/edit 3/4

Fig. C.4 **Participant Information Sheet (p. 3/4)**

25/10/2018 A Study of Movement Variability in Human-Humanoid Interaction Activities

8. **Have you received formal music training?** *
Mark only one oval.

- No
- Yes (less than 5 years)
- Yes (more than 5 years)

9. **What is your arm lenght in centimetres?** *
Mark only one oval.

- Less than 45
- 45
- 46
- 47
- 48
- 49
- 50
- 51
- 52
- 53
- 54
- 55
- 56
- 57
- 58
- 59
- 60
- More than 60

10. **What is your height in centimeters?** *

11. **What is your weight in kilograms?** *

Powered by
Google Forms

https://docs.google.com/forms/d/1dPN6D_S3CRg4pkDYpIfDg6fSnh6FaQ4Z7M0xl_11Fq4/edit 4/4

Fig. C.5 **Participant Information Sheet (p. 4/4)**

Appendix D

Additional Results for HII experiment

D.1 Time Series

Figures D.1 D.2, and D.3 show time series for horizontal arm movements and figures D.4, D.5, D.6 show time series for vertical arm movements. Time series are only for a window size of 10 seconds window length. For the remained window lengths, the reader is welcome to download the data and code at Xochicale (2018). See Appendix F for details on how code and data is organised and how results can be replicated.

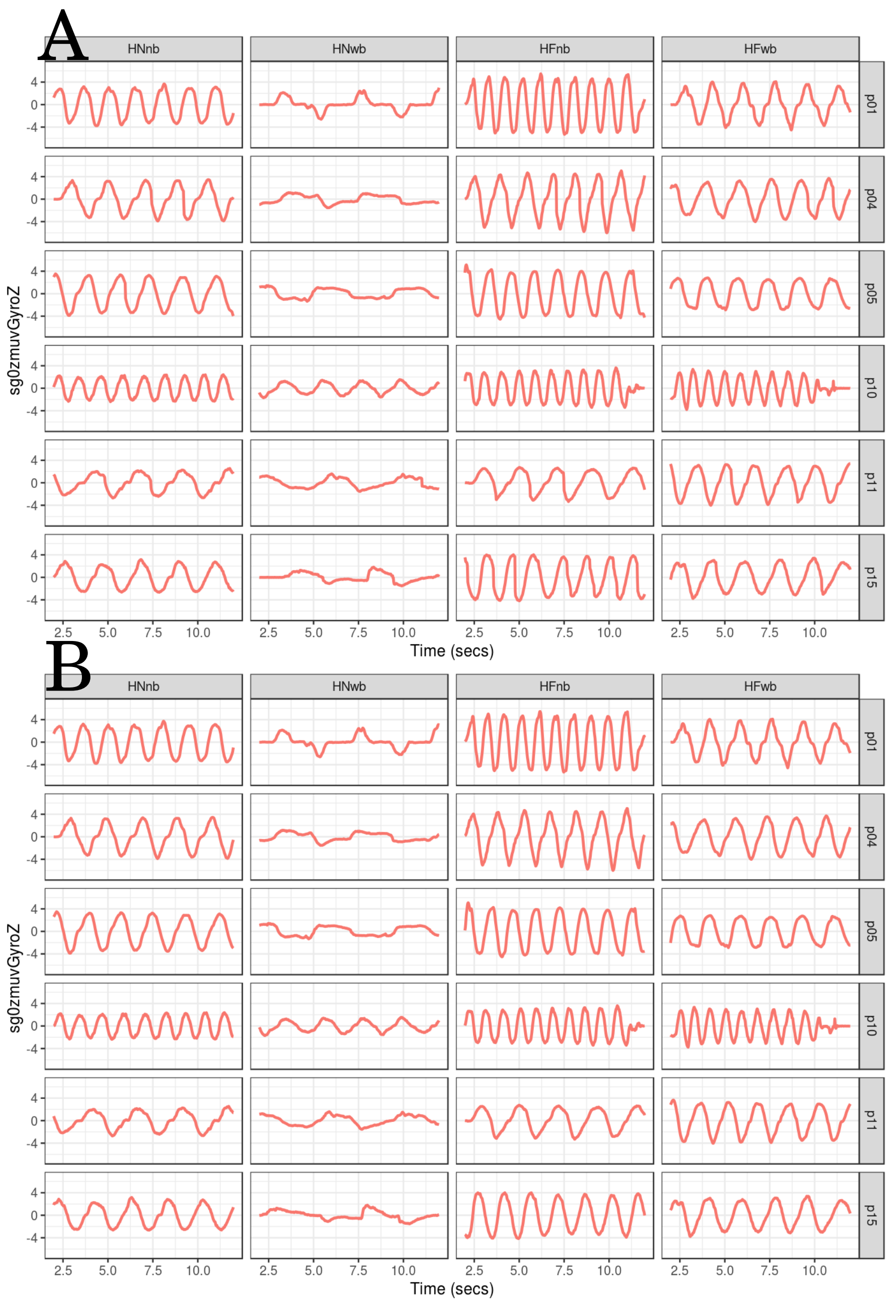

Fig. D.1 **Time series for horizontal arm movements (sg0)** Time series for sg0GyroZ are for six participants ($p01$, $p04$, $p05$, $p10$, $p11$, $p15$) for horizontal movements in normal and faster velocity with no beat (HNnb, HFnb) and with beat (HNwb, HFwb) using the normalised GyroZ axis (zmuvGyroZ). Two sensors were attached to the wrist of the participants (HS01, HS02), where plots in (A) are from human sensor HS01 and plots in (B) are from human sernso HS02. R code to reproduce the figure is available at .

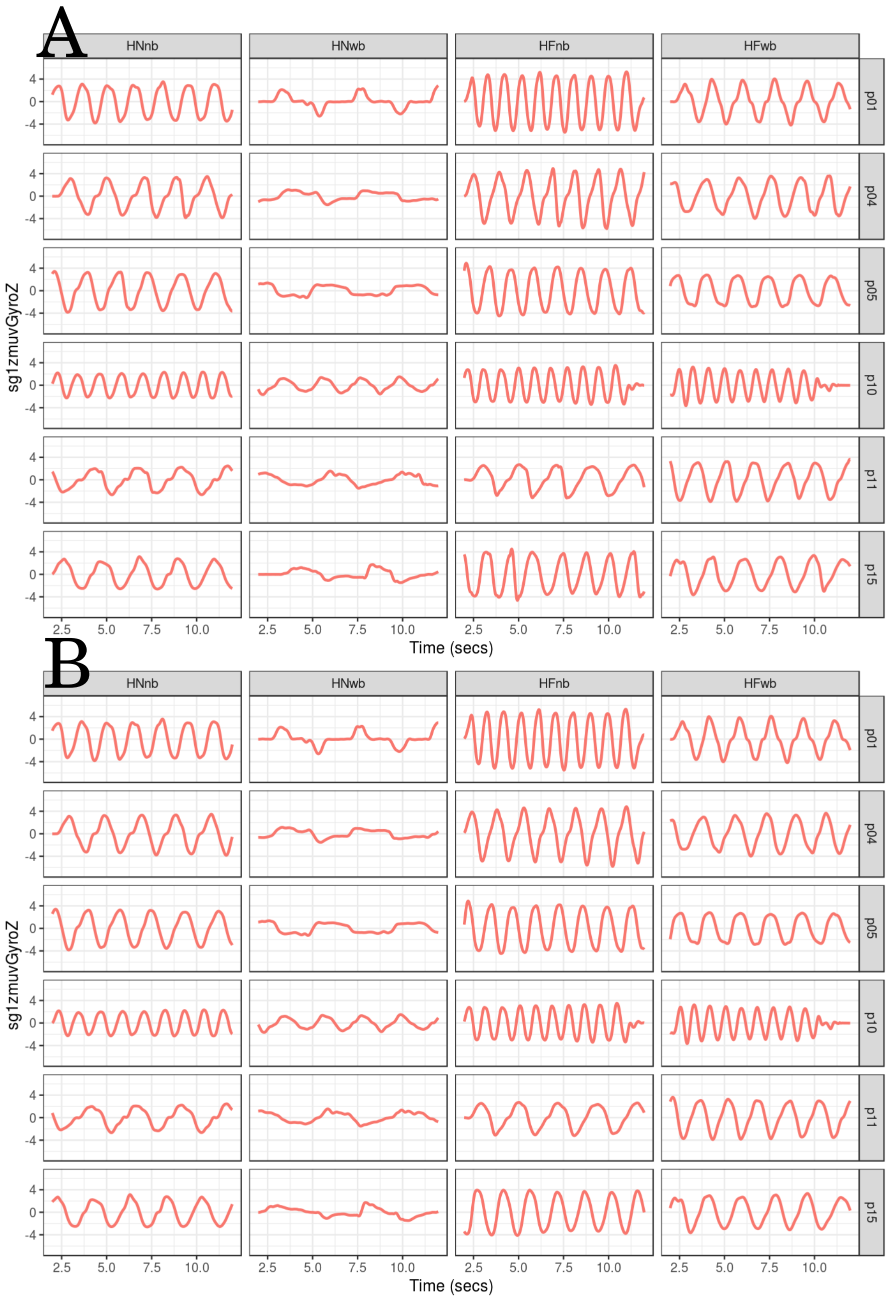

Fig. D.2 **Time series for horizontal arm movements (sg1)** Time series for sg1GyroZ for six participants ($p01$, $p04$, $p05$, $p10$, $p11$, $p15$) for horizontal movements in normal and faster velocity with no beat (HNnb, HFnb) and with beat (HNwb, HFwb) using the normalised GyroZ axis (zmuvGyroZ). Two sensors were attached to the wrist of the participants (HS01, HS02), where plots in (A) are from human sensor HS01 and plots in (B) are from human sernso HS02. R code to reproduce the figure is available at .

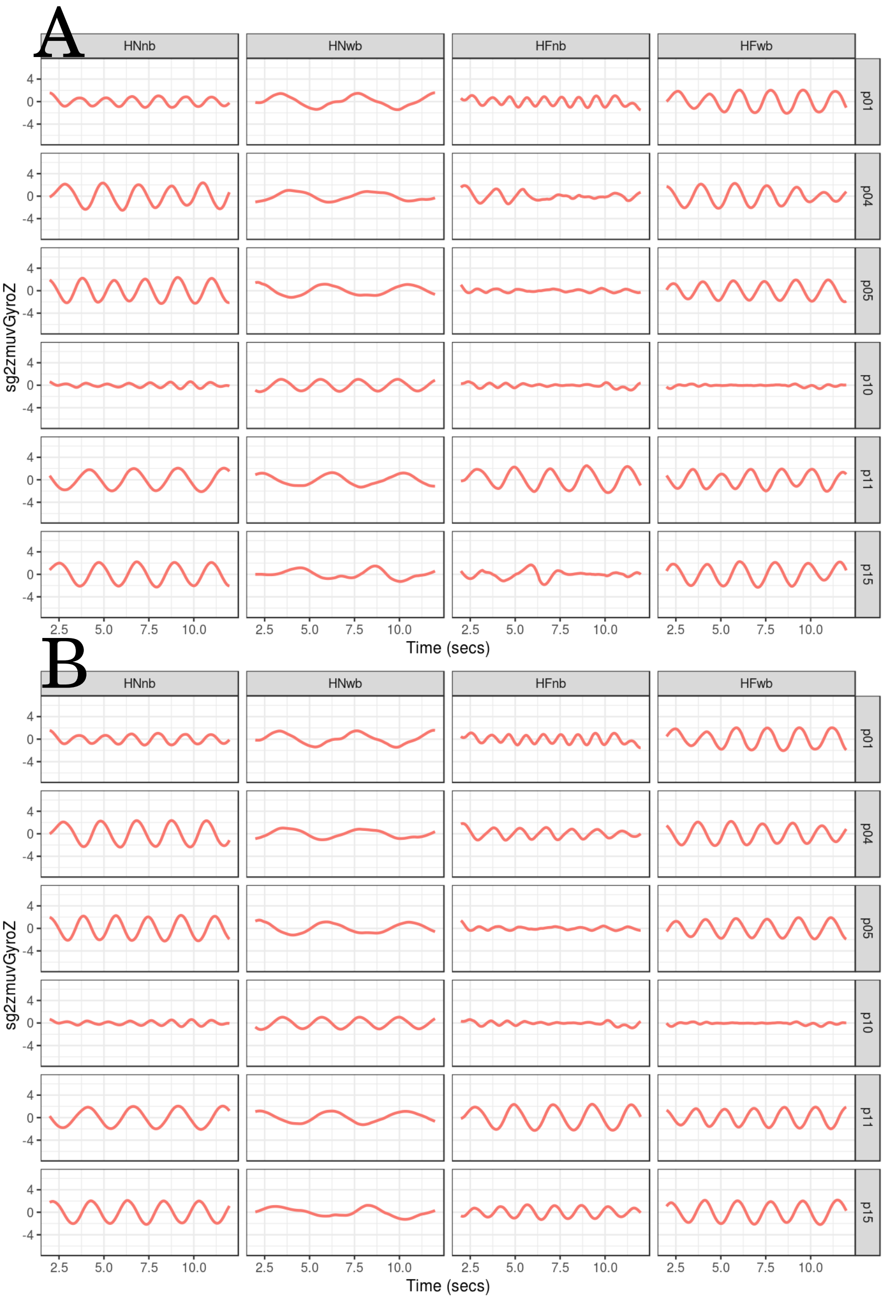

Fig. D.3 **Time series for horizontal arm movements (sg2)** Time series for sg2GyroZ for six participants ($p01$, $p04$, $p05$, $p10$, $p11$, $p15$) for horizontal movements in normal and faster velocity with no beat (HNnb, HFnb) and with beat (HNwb, HFwb) using the normalised GyroZ axis (zmuvGyroZ). Two sensors were attached to the wrist of the participants (HS01, HS02), where plots in (A) are from human sensor HS01 and plots in (B) are from human sernso HS02. R code to reproduce the figure is available at .

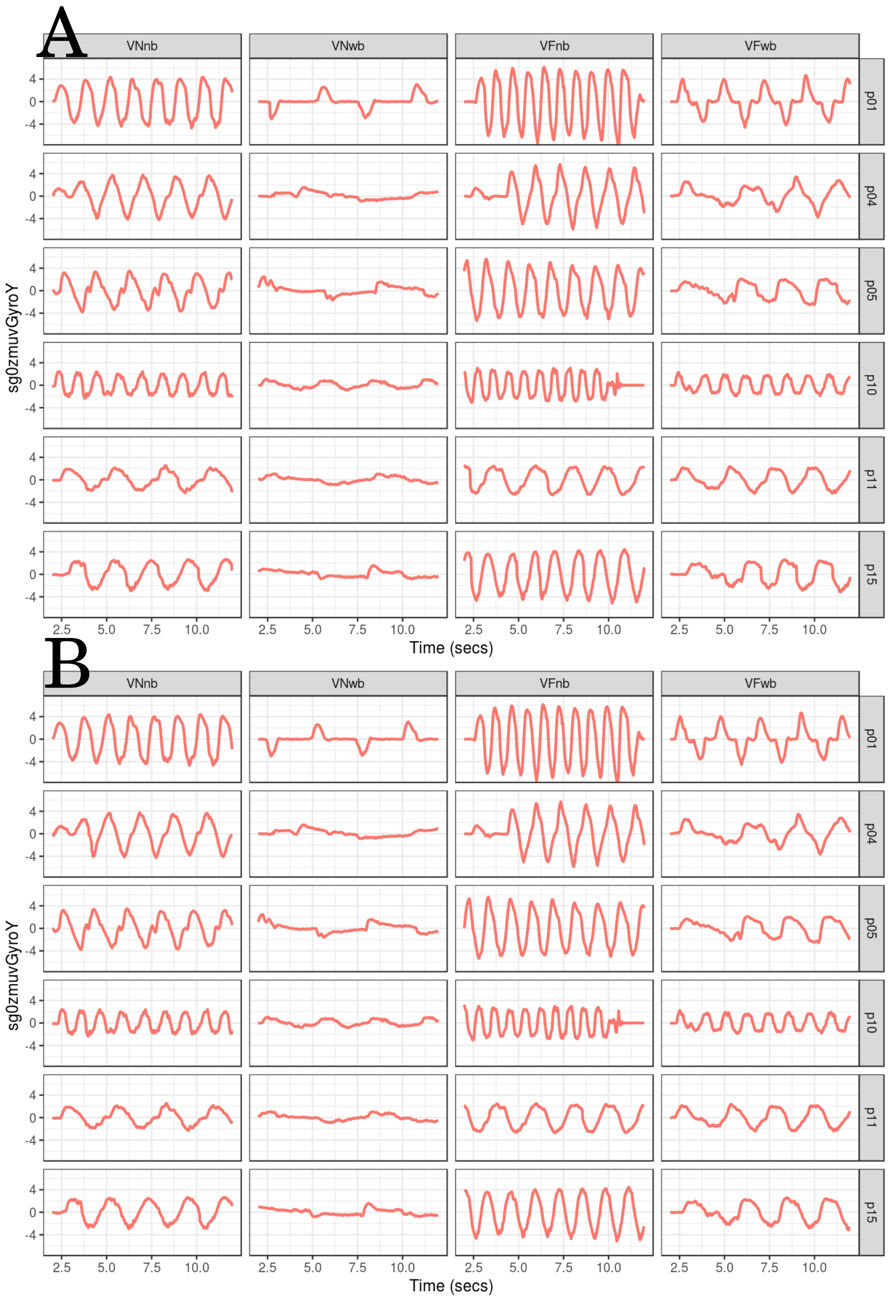

Fig. D.4 **Time series for vertical arm movements (sg0)** Time series for sg0GyroY are for six participants (p01, p04, p05, p10, p11, p15) for vertical movements in normal and faster velocity with no beat (VNnb, VFnb) and with beat (VNwb, VFwb) using the normalised GyroZ axis (zmuvGyroY). Two sensors were attached to the wrist of the participants (HS01, HS02), where plots in (A) are from human sensor HS01 and plots in (B) are from human sernso HS02. R code to reproduce the figure is available at .

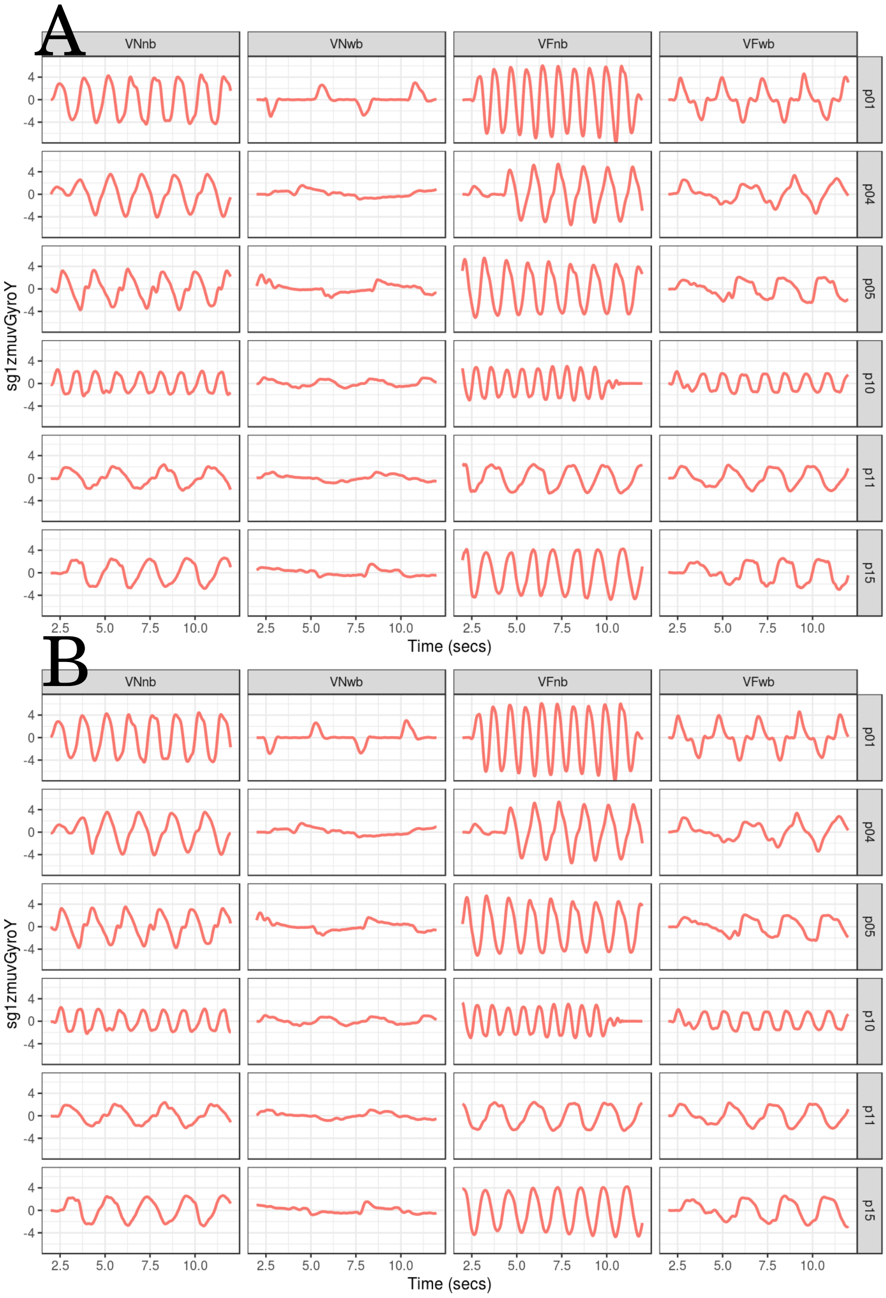

Fig. D.5 **Time series for vertical arm movements (sg1)** Time series for sg1GyroY for six participants (p01, p04, p05, p10, p11, p15) for vertical movements in normal and faster velocity with no beat (VNnb, VFnb) and with beat (VNwb, VFwb) using the normalised GyroZ axis (zmuvGyroY). Two sensors were attached to the wrist of the participants (HS01, HS02), where plots in (A) are from human sensor HS01 and plots in (B) are from human sernso HS02. R code to reproduce the figure is available at .

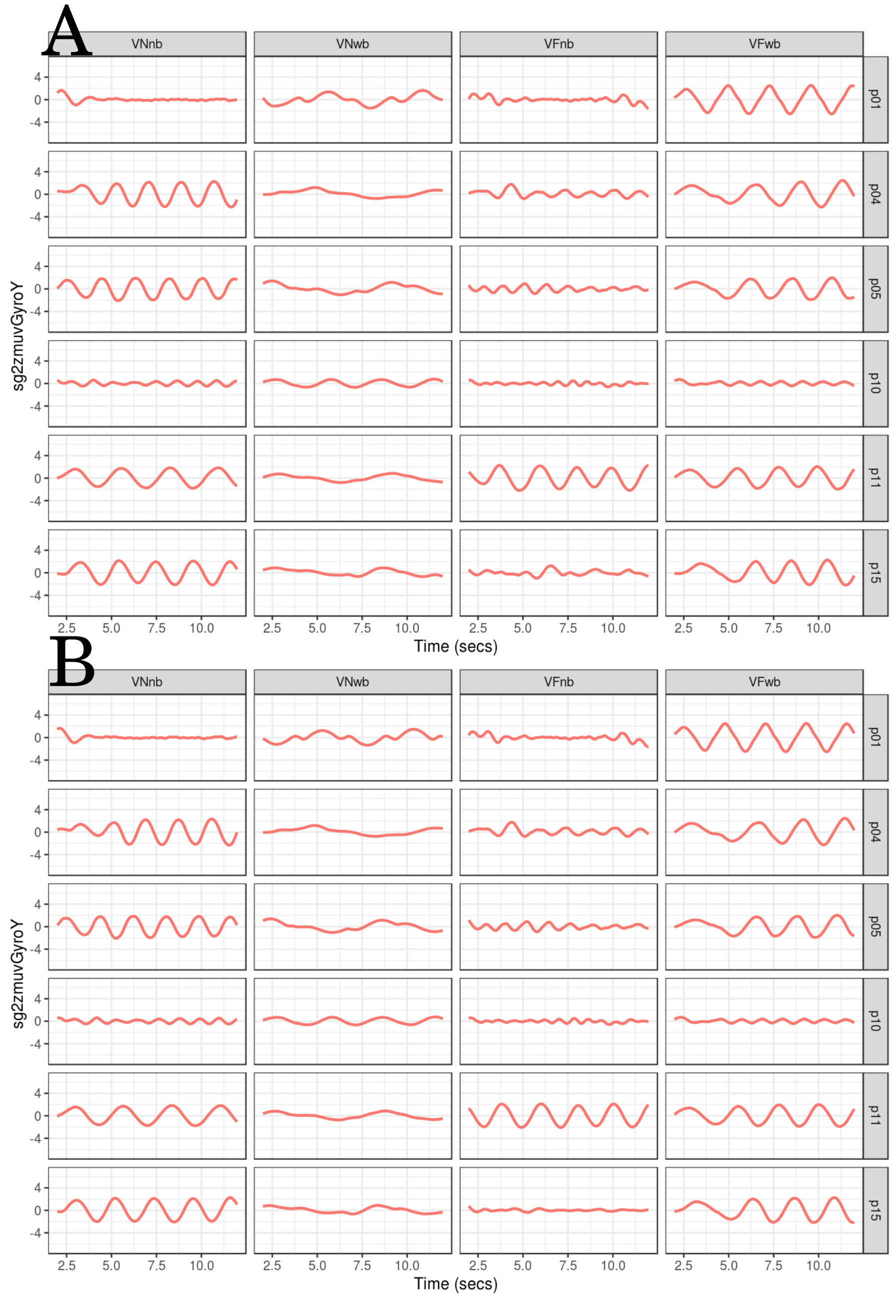

Fig. D.6 **Time series for vertical arm movements (sg2)** Time series for sg2GyroY for six participants ($p01$, $p04$, $p05$, $p10$, $p11$, $p15$) for vertical movements in normal and faster velocity with no beat (VNnb, VFnb) and with beat (VNwb, VFwb) using the normalised GyroY axis (zmuvGyroY). Two sensors were attached to the wrist of the participants (HS01, HS02), where plots in (A) are from human sensor HS01 and plots in (B) are from human sernso HS02. R code to reproduce the figure is available at .

D.2 Embedding parameters

D.2.1 Minimum dimension embedding values

Values of minimum embedding dimensions for horizontal normal arm movements with no beat (HNnb) and horizontal faster arm movements with no beat (HFnb) are shown in Fig D.7 which values of minimum embedding dimensions present a fluctuation of values between four and seven over six participants. It can also be noted a slightly variation of minimum embedding dimension values over participants when comparing HS01 and HS02 (Fig D.7(A, B)). With regards to the smoothness of the time series, the minimum embedding values are also smoothed showing less variations of values over six participants (Fig D.7).

Values of minimum embedding dimension for horizontal normal arm movements with beat (HNwb) and horizontal faster arm movements with beat (HFwb) are shown in Fig D.8 where is shown a fluctuations of values for minimum embedding dimension between five and seven. Similarly as in Fig D.7, Fig D.8 show changes of minimum embedding dimension between participants and the smoothness of the time series also affects the smoothness of minimum embedding dimension values.

Values of minimum embedding dimension for vertical arm movements with no beat are shown in Figs D.9(A, B) where the smoothness of the time series have little effect on the minimum embedding dimension values, whereas smoothness of time series affects the smoothness of the minimum embedding values for vertical faster arm movements with no beats (Fig D.9(C, D)).

Fig D.10 shows the variation of minimum embedding values for vertical arm movements with beat where the smoothness of the time series affects both vertical normal and vertical faster movements with a slight decrease on each of the values as the smoothness increase.

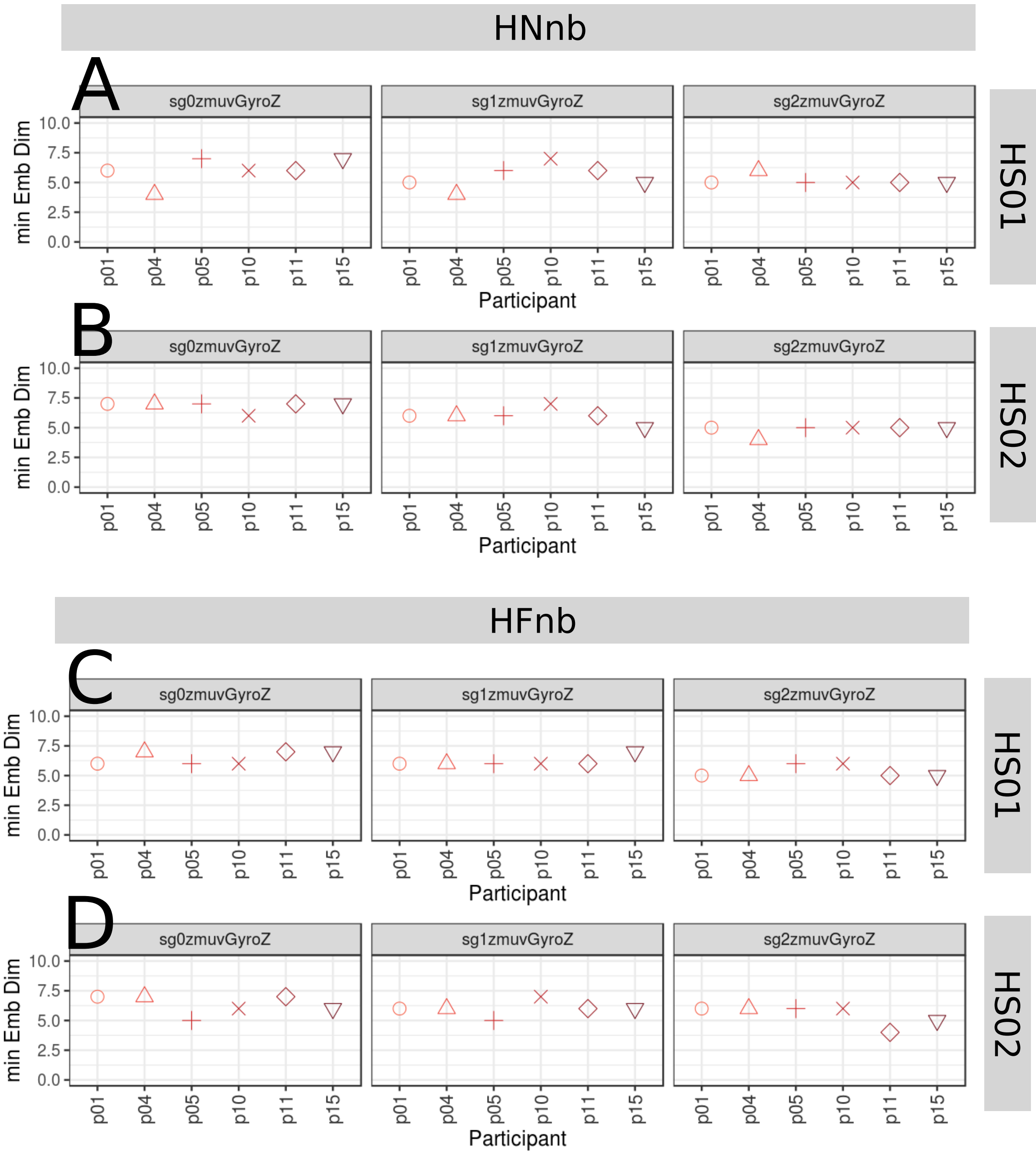

Fig. D.7 **Minimum embedding dimensions for horizontal arm movements (no beat).** (A, B) Horizontal Normal with no beat (HNnb), and (C, D) Horizontal Faster with no beat (HFnb) movements. (A, C) Sensor 01 attached to the participant (HS01), and (B, D) sensor 02 attached to the participant (HS02). Minimum embedding dimensions are for six participants (p01, p04, p05, p10, p11, p15) with three smoothed signals (sg0zmuvGyroZ, sg1zmuvGyroZ and sg2zmuvGyroZ) and window lenght of 10-sec (500 samples). R code to reproduce the figure is available at .

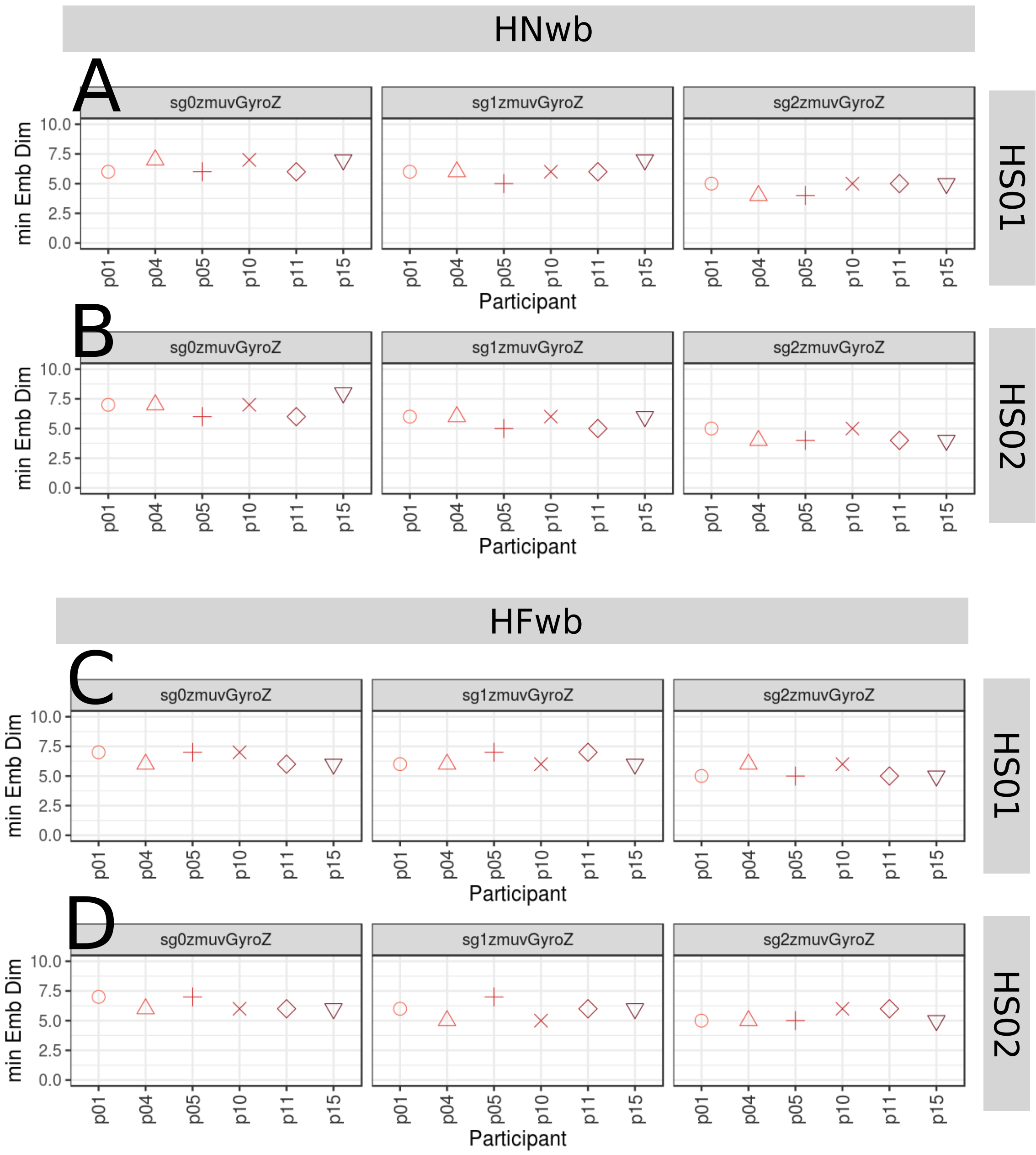

Fig. D.8 **Minimum embedding dimensions for horizontal arm movements (with beat).** (A, B) Horizontal Normal with beat (HNwb), and (C, D) Horizontal Faster with beat (HFwb) movements. (A, C) Sensor 01 attached to the participant (HS01), and (B, D) sensor 02 attached to the participant (HS02). Minimum embedding dimensions are for six participants (p01, p04, p05, p10, p11, p15) with three smoothed signals (sg0zmuvGyroZ, sg1zmuvGyroZ and sg2zmuvGyroZ) and window lenght of 10-sec (500 samples). R code to reproduce the figure is available at .

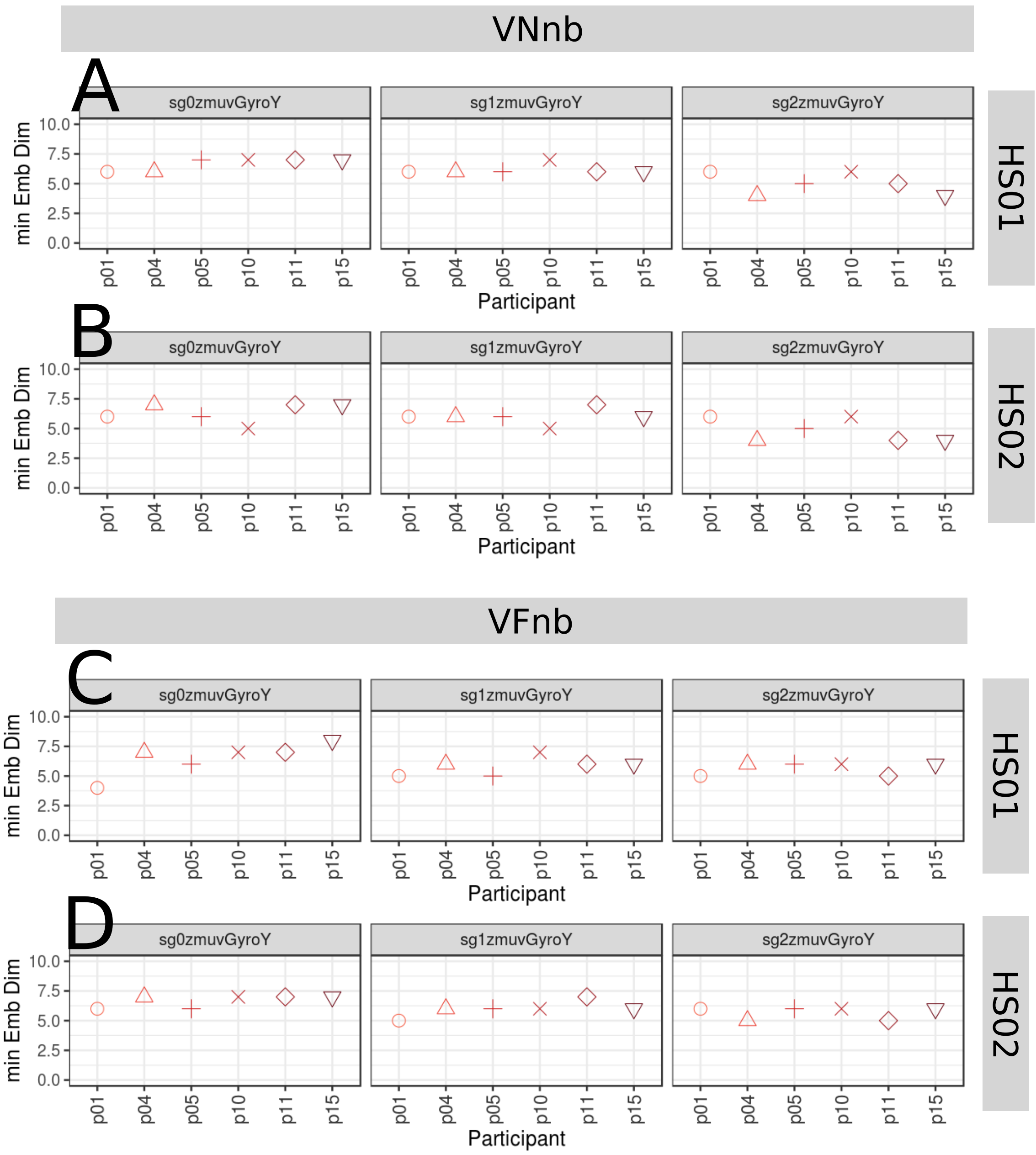

Fig. D.9 **Minimum embedding dimensions for vertical arm movements (no beat).** (A, B) Vertical Normal with no beat (VNnb), and (C, D) Vertical Faster with no beat (VFnb) movements. (A, C) Sensor 01 attached to the participant (HS01), and (B, D) sensor 02 attached to the participant (HS02). Minimum embedding dimensions are for six participants (p01, p04, p05, p10, p11, p15) with three smoothed signals (sg0zmuvGyroZ, sg1zmuvGyroZ and sg2zmuvGyroZ) and window lenght of 10-sec (500 samples). R code to reproduce the figure is available at .

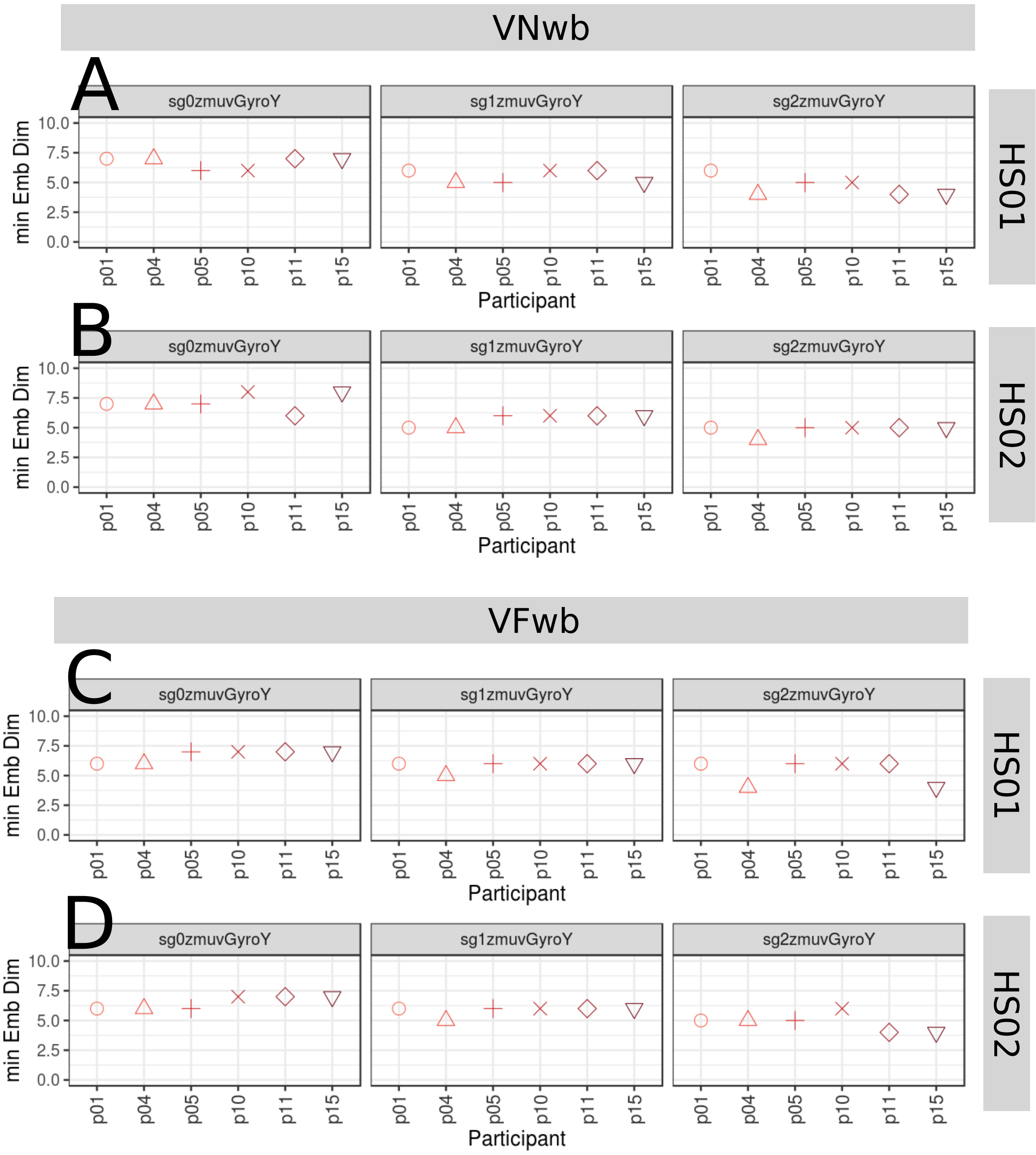

Fig. D.10 **Minimum embedding dimensions for vertical arm movements (with beat).** (A, B) Vertical Normal with beat (VNwb), and (C, D) Vertical Faster with beat (VFwb) movements. (A, C) Sensor 01 attached to the participant (HS01), and (B, D) sensor 02 attached to the participant (HS02). Minimum embedding dimensions are for six participants (p01, p04, p05, p10, p11, p15) with three smoothed signals (sg0zmuvGyroZ, sg1zmuvGyroZ and sg2zmuvGyroZ) and window lenght of 10-sec (500 samples). R code to reproduce the figure is available at .

D.2.2 Minimum delay embedding values

The general behavior for horizontal and vertical arm movements with regards to the smoothness of the time series is that the first minimum AMI values increase as the increase of the smoothness which is due to smoothed AMI curves (Figs D.11, D.12, D.13 and D.14).

Fluctuations of minimum AMI values from sensor HS01 are more evident than for sensor HS02 for horizontal normal arm movements with no beat (Fig D.11(A, B)), whereas fluctuations of minimum AMI values from sensors HS01 and HS02 for horizontal faster arm movements with no beat appear to be similar (Fig D.11(C, D)). Similarly, fluctuations of minimum AMI values are more evidently for horizontal normal arm movements with beat (Fig D.12(A, B)) than horizontal faster arm movements with beat (Fig D.12(C, D)).

As smoothness increase, minimum AMI values for vertical normal arm movements with no beat appear to fluctuate more (Figs D.13(A, B)) than vertical faster arm movements with no beat (Figs D.13(C, D)), whereas for vertical normal and vertical faster arm movements with beat the fluctuation of minimum AMI values is more evidently, specially when comparing vertical normal arm movements (Figs D.14(A, B)) with vertical faster arm movements (Figs D.14(C, D)).

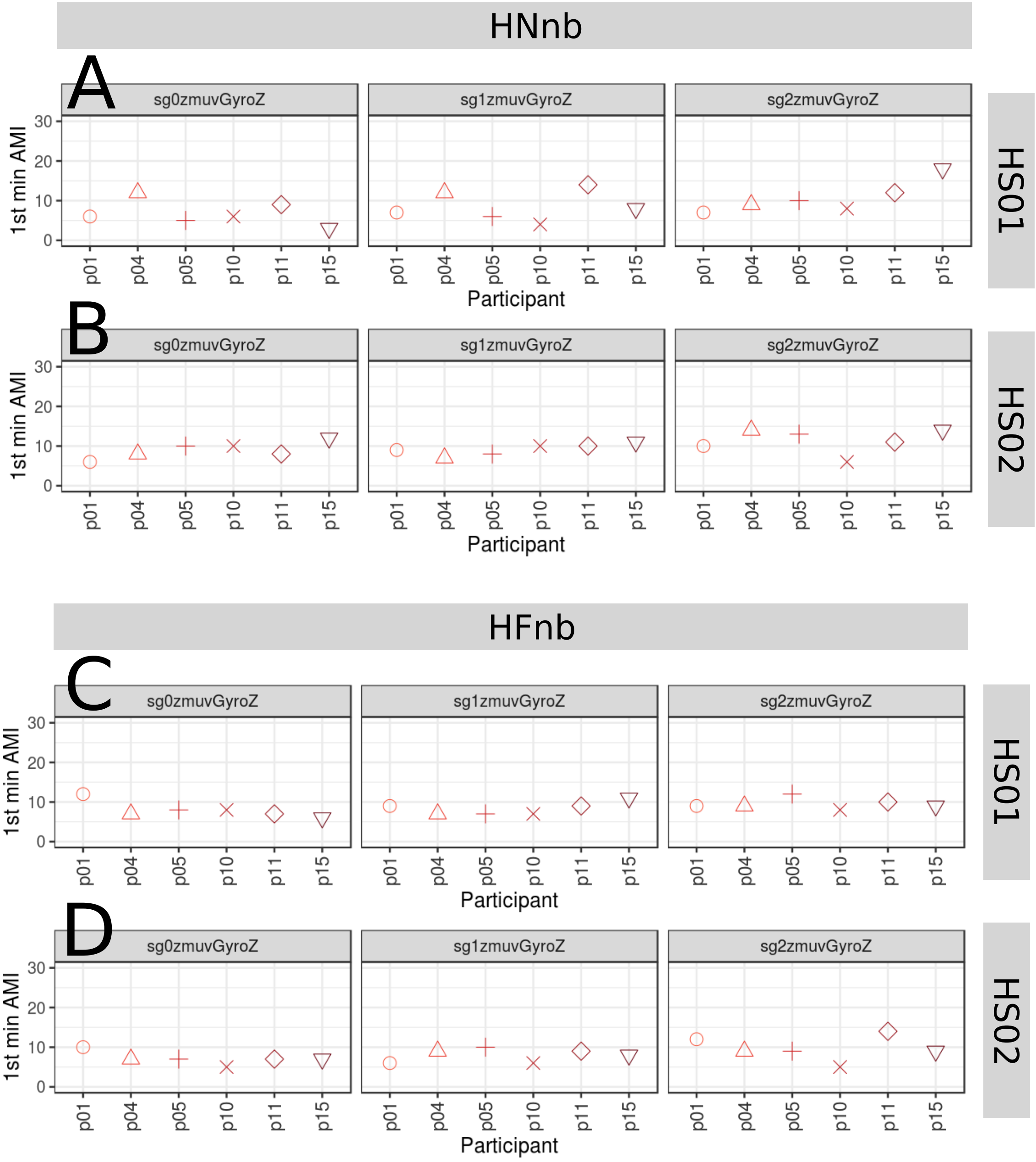

Fig. D.11 **First minimum AMI values for horizontal arm movements (no beat).** (A, B) Horizontal Normal with no beat (HNnb), and (C, D) Horizontal Faster with no beat (HFnb) movements. (A, C) Sensor attached to the participant (HS01), and (B, D) sensor attached to the participant (HS02). First minimum AMI values are for six participants (p01, p04, p05, p10, p11, p15) with three smoothed signals (sg0zmuvGyroZ, sg1zmuvGyroZ and sg2zmuvGyroZ) and window lenght of 10-sec (500 samples). R code to reproduce the figure is available at .

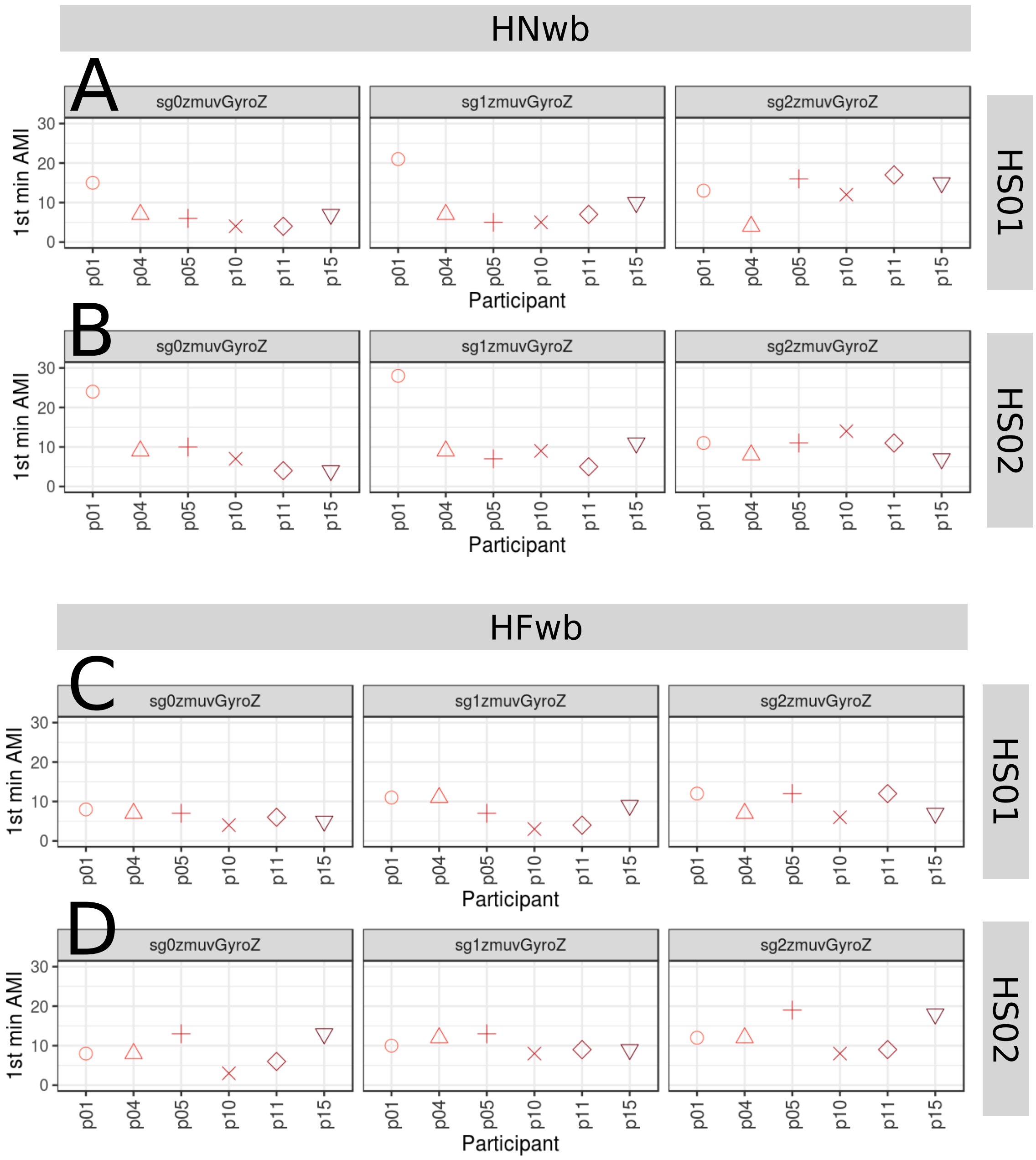

Fig. D.12 **First minimum AMI values for horizontal arm movements (with beat).** (A, B) Horizontal Normal with beat (HNwb), and (C, D) Horizontal Faster with beat (HFwb) movements. (A, C) Sensor attached to the participant (HS01), and (B, D) sensor attached to the participant (HS02). First minimum AMI values are for six participants (p01, p04, p05, p10, p11, p15) with three smoothed signals (sg0zmuvGyroZ, sg1zmuvGyroZ and sg2zmuvGyroZ) and window lenght of 10-sec (500 samples). R code to reproduce the figure is available at .

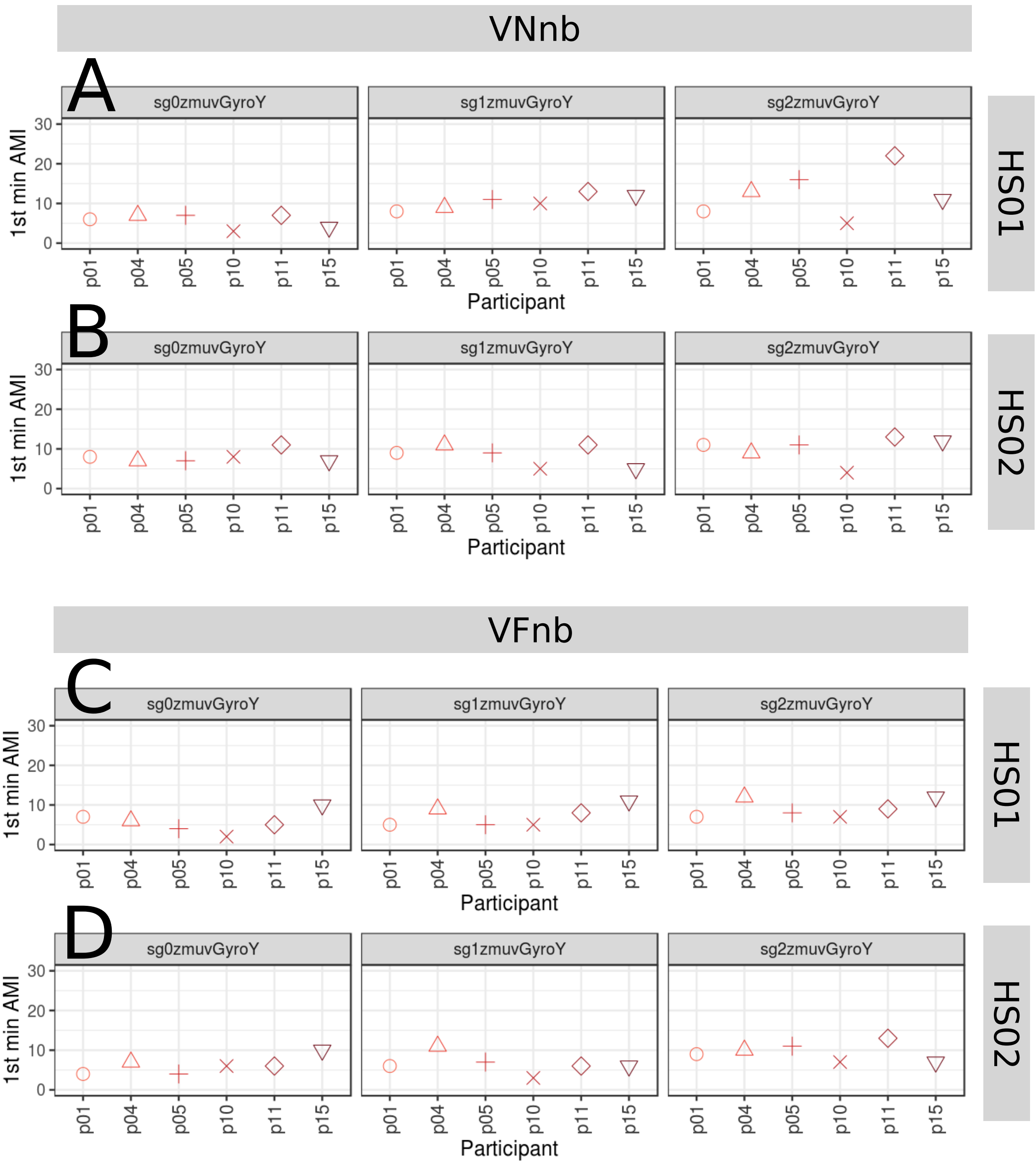

Fig. D.13 **First minimum AMI values for vertical arm movements (no beat).** (A, B) Vertical Normal with no beat (VNnb), and (C, D) Vertical Faster with no beat (VFnb) movements. (A, C) Sensor attached to the participant (HS01), and (B, D) sensor attached to the participant (HS02). First minimum AMI values are for six participants (p01, p04, p05, p10, p11, p15) with three smoothed signals (sg0zmuvGyroZ, sg1zmuvGyroZ and sg2zmuvGyroZ) and window lenght of 10-sec (500 samples). R code to reproduce the figure is available at .

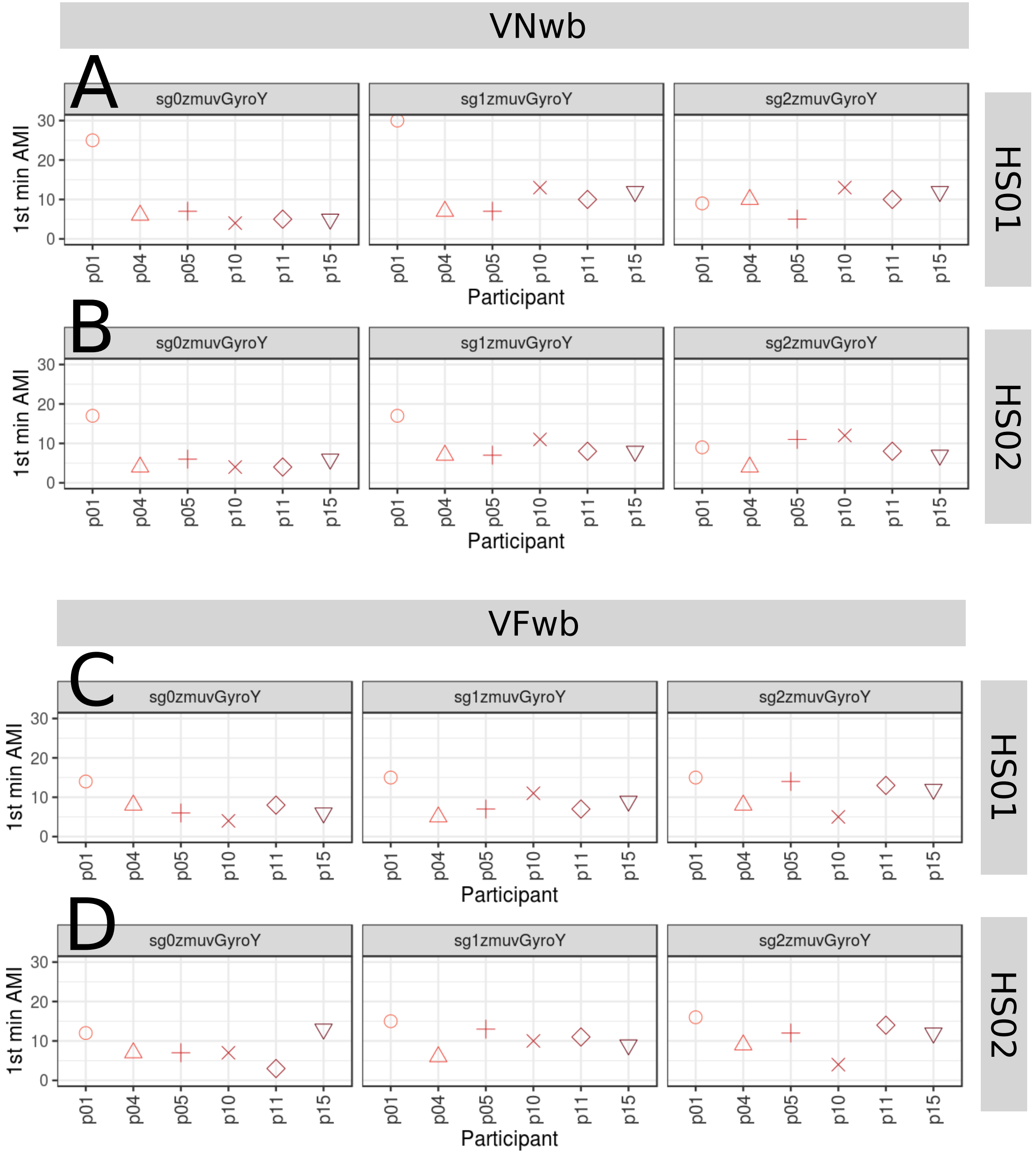

Fig. D.14 **First minimum AMI values for vertical arm movements (with beat).** (A, B) Vertical Normal with beat (VNwb), and (C, D) Vertical Faster with beat (VFwb) movements. (A, C) Sensor attached to the participant (HS01), and (B, D) sensor attached to the participant (HS02). First minimum AMI values are for six participants (p01, p04, p05, p10, p11, p15) with three smoothed signals (sg0zmuvGyroZ, sg1zmuvGyroZ and sg2zmuvGyroZ) and window lenght of 10-sec (500 samples). R code to reproduce the figure is available at .

D.3 RSSs

The following Figs. D.17, D.18, D.15, D.16, D.21, D.22, D.19, D.20 illustrate reconstructed state spaces of participant $p04$ with a window length size of 500 samples. We refer the reader to download the data and code at Xochicale (2018) for the remained window size lengths and other participants.

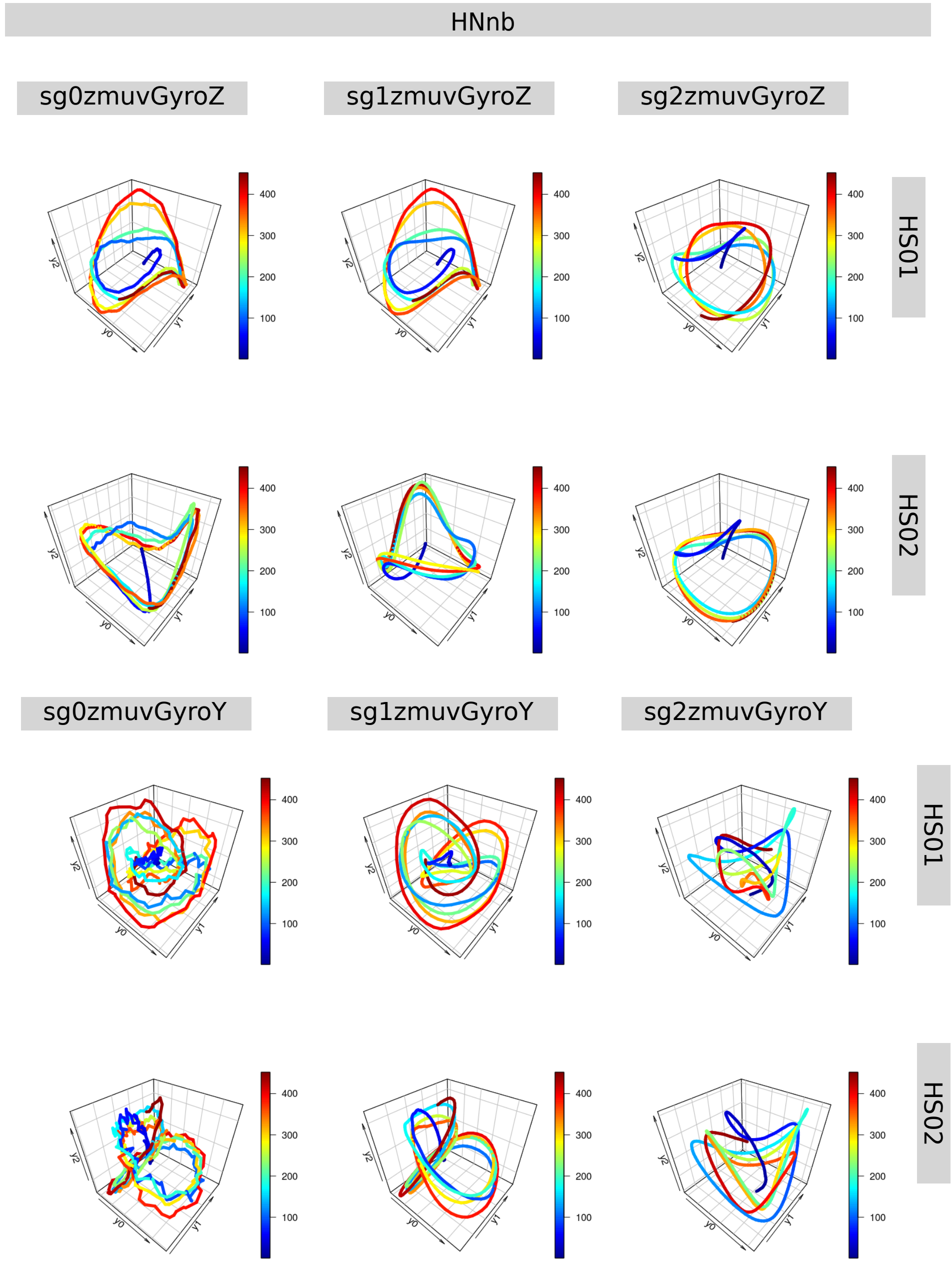

Fig. D.15 **RSSs for horizontal normal arm movements (no beat).** Reconstructed state spaces of participant $p04$ with time series for raw-normalised (sg0), normalised-smoothed 1 (sg1) and normalised-smoothed 2 (sg2), with sensors attached to the participant (HS01, HS02). Reconstructed state spaces were computed with embedding parameters $\overline{m_0} = 6$, $\overline{\tau_0} = 10$. R code to reproduce the figure is available at .

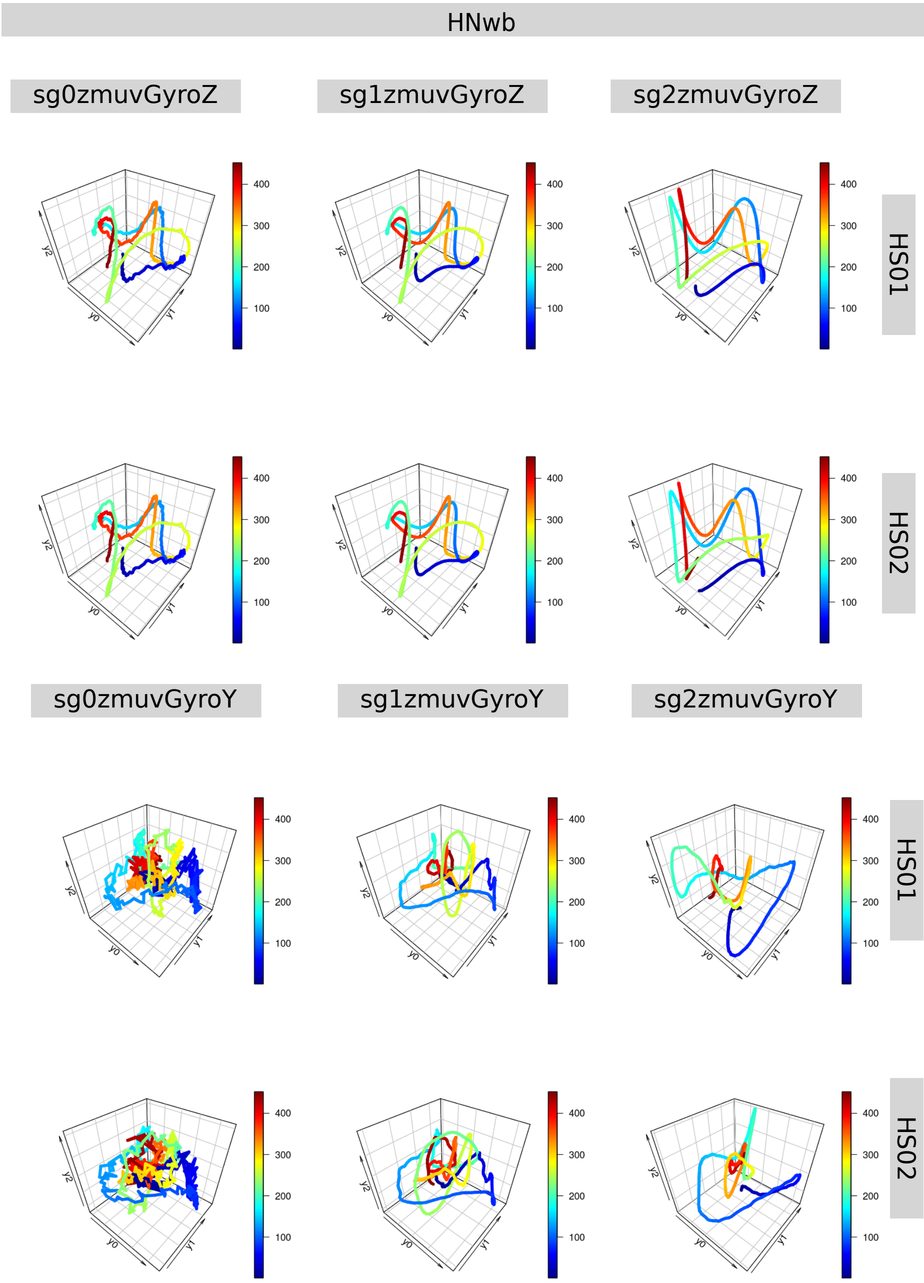

Fig. D.16 **RSSs for horizontal normal arm movements (with beat).** Reconstructed state spaces of participant $p04$ with time series for raw-normalised (sg0), normalised-smoothed 1 (sg1) and normalised-smoothed 2 (sg2), with sensors attached to the participant (HS01, HS02). Reconstructed state spaces were computed with embedding parameters $\overline{m_0} = 6$, $\overline{\tau_0} = 10$. R code to reproduce the figure is available at .

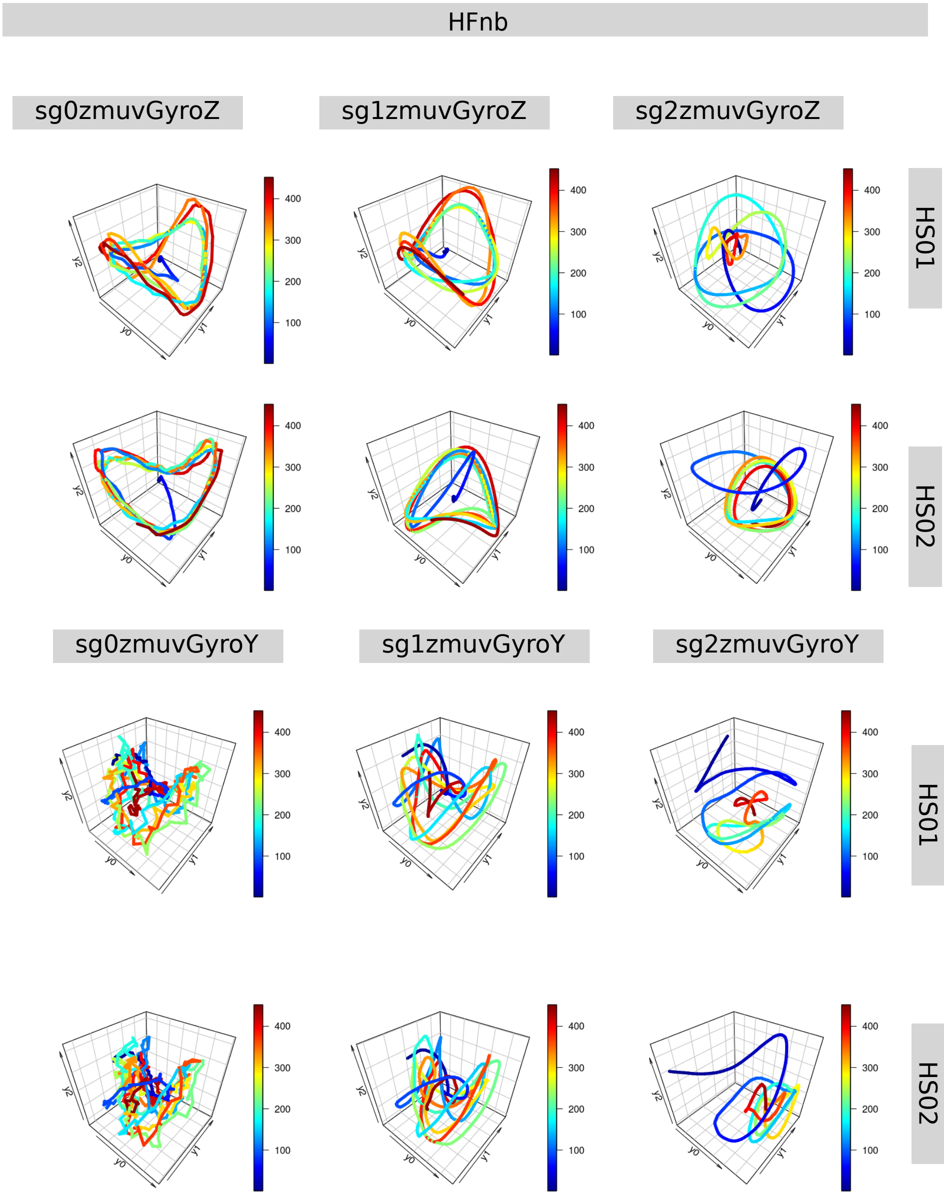

Fig. D.17 **RSSs for horizontal faster arm movements (no beat).** Reconstructed state spaces of participant $p04$ with time series for raw-normalised (sg0), normalised-smoothed 1 (sg1) and normalised-smoothed 2 (sg2), with sensors attached to the participant (HS01, HS02). Reconstructed state spaces were computed with embedding parameters $\overline{m_0} = 6$, $\overline{\tau_0} = 10$. R code to reproduce the figure is available at .

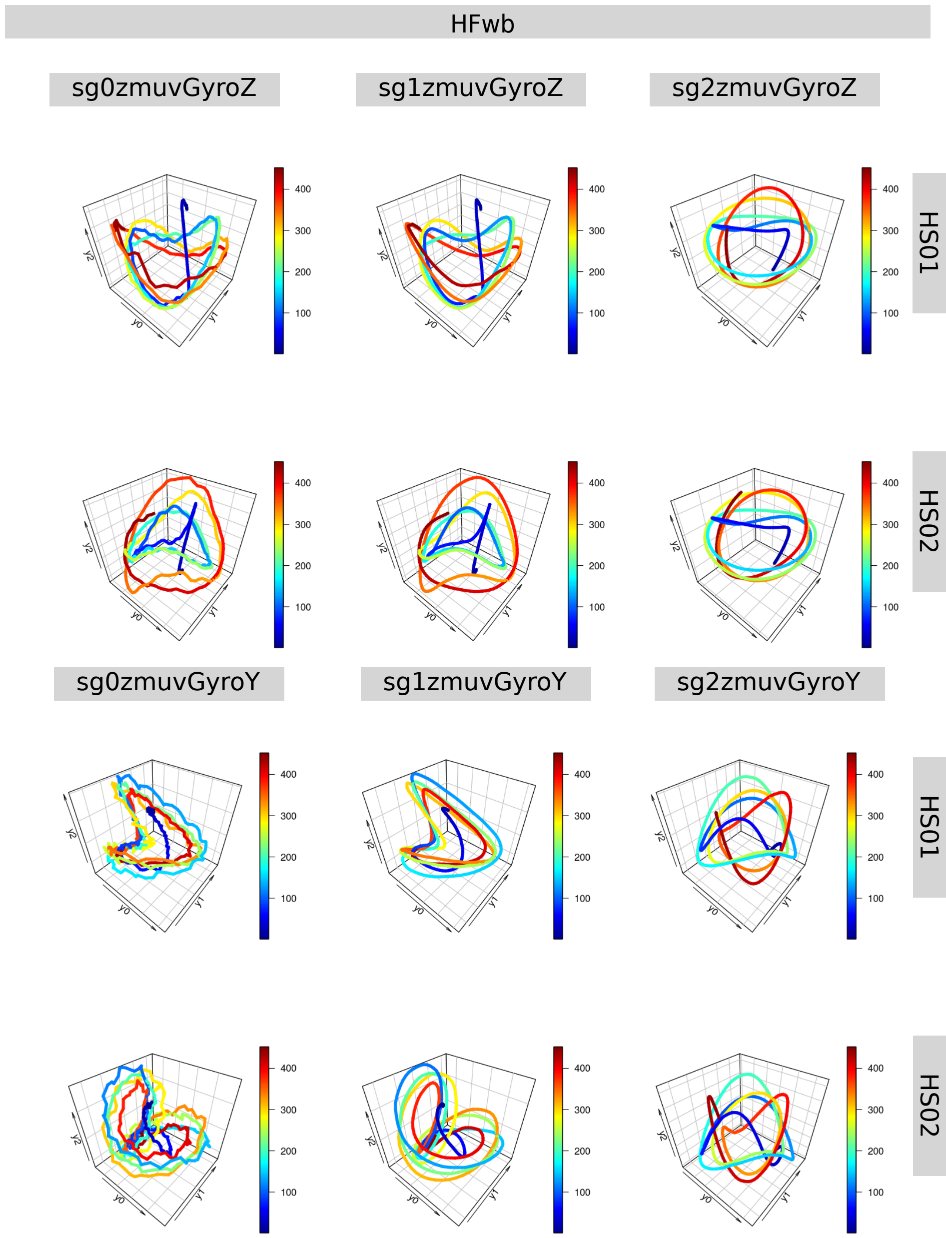

Fig. D.18 **RSSs for horizontal faster arm movements (with beat).** Reconstructed state spaces of participant $p04$ with time series for raw-normalised (sg0), normalised-smoothed 1 (sg1) and normalised-smoothed 2 (sg2), with sensors attached to the participant (HS01, HS02). Reconstructed state spaces were computed with embedding parameters $\overline{m_0} = 6$, $\overline{\tau_0} = 10$. R code to reproduce the figure is available at .

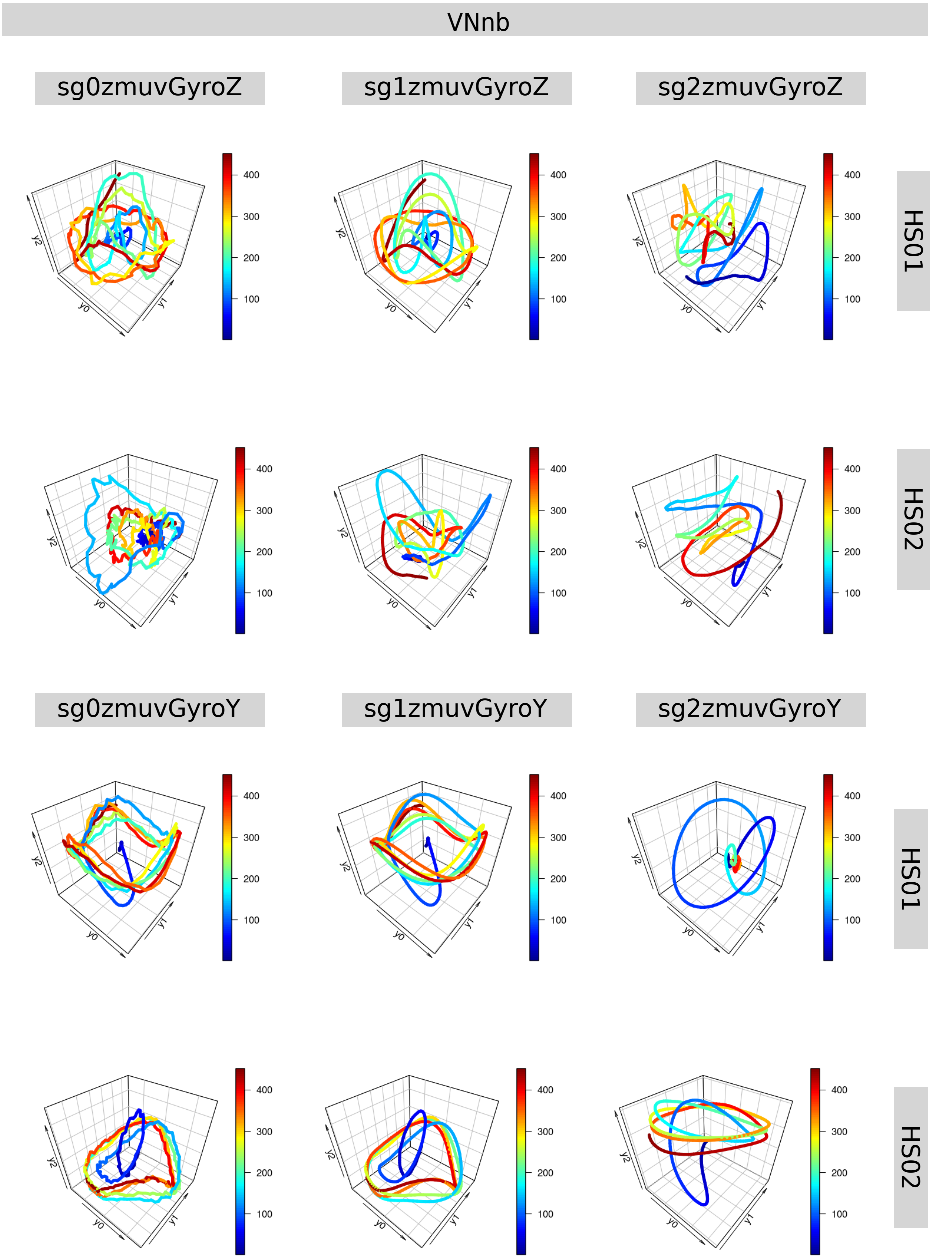

Fig. D.19 **RSSs for vertical normal arm movements (no beat).** Reconstructed state spaces of participant $p04$ with time series for raw-normalised (sg0), normalised-smoothed 1 (sg1) and normalised-smoothed 2 (sg2), with sensors attached to the participant (HS01, HS02). Reconstructed state spaces were computed with embedding parameters $\overline{m_0} = 6$, $\overline{\tau_0} = 10$. R code to reproduce the figure is available at .

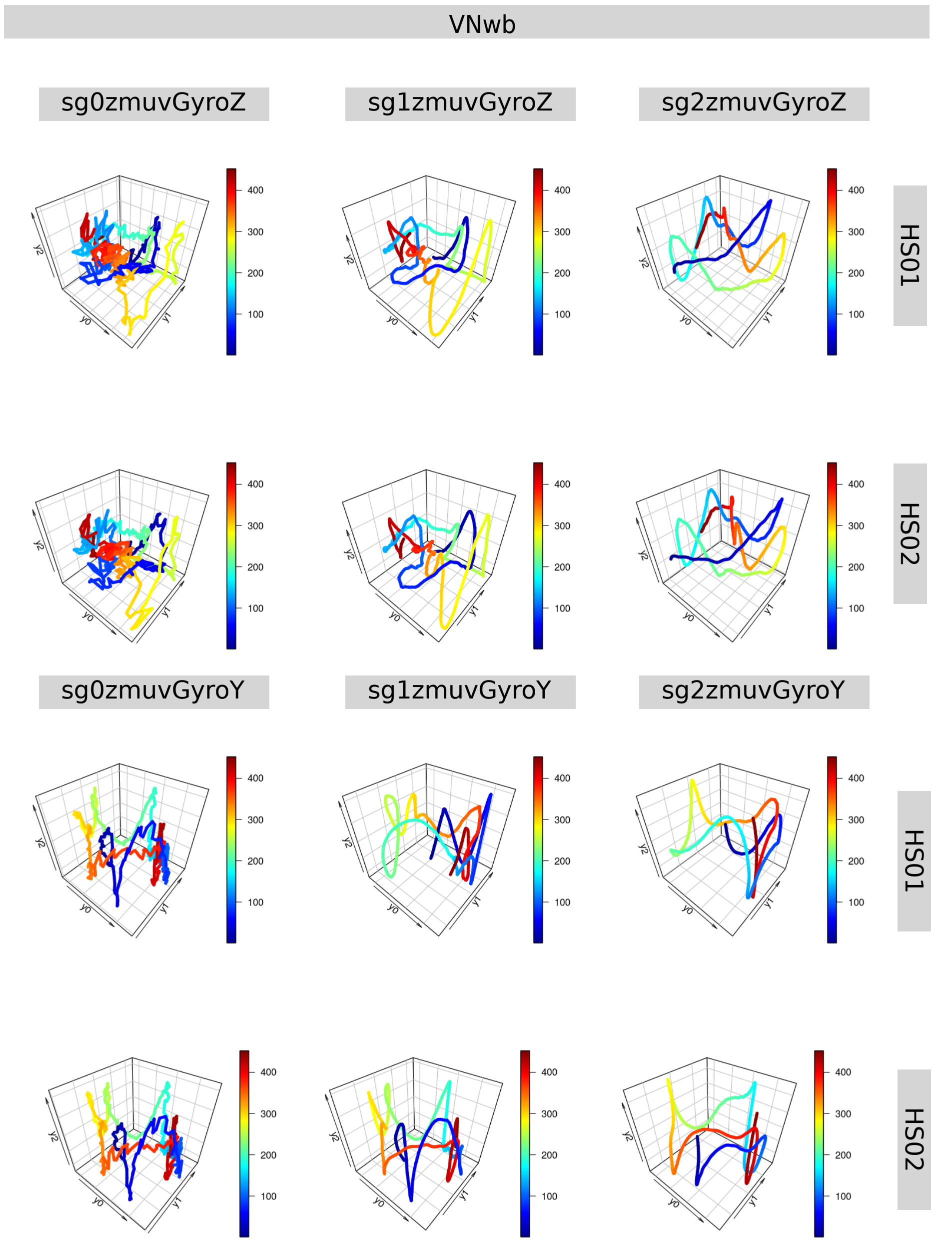

Fig. D.20 **RSSs for vertical normal arm movements (with beat).** Reconstructed state spaces of participant $p04$ with time series for raw-normalised (sg0), normalised-smoothed 1 (sg1) and normalised-smoothed 2 (sg2), with sensors attached to the participant (HS01, HS02). Reconstructed state spaces were computed with embedding parameters $\overline{m_0} = 6$, $\overline{\tau_0} = 10$. R code to reproduce the figure is available at .

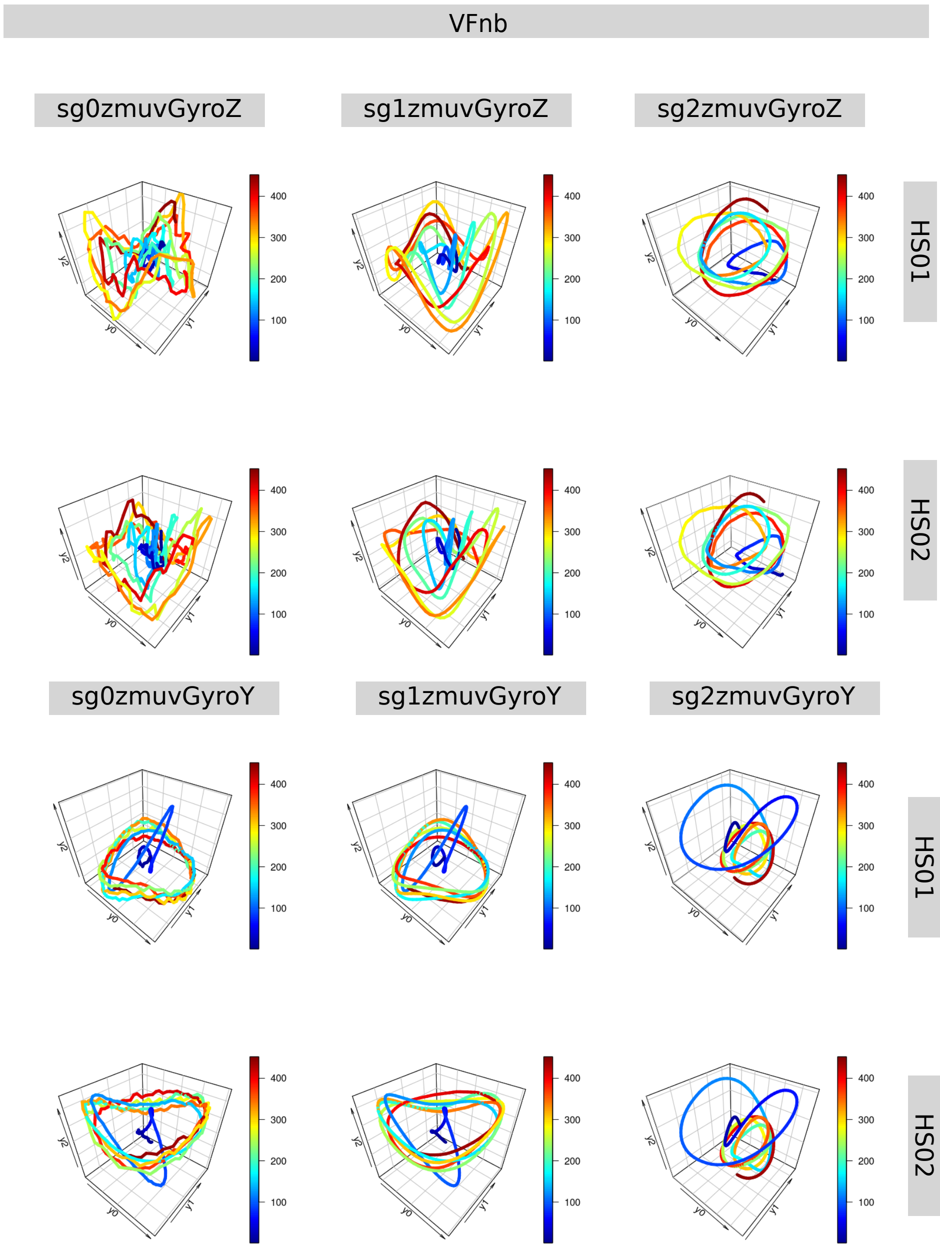

Fig. D.21 **RSSs for vertical faster arm movements (no beat).** Reconstructed state spaces of participant $p04$ with time series for raw-normalised (sg0), normalised-smoothed 1 (sg1) and normalised-smoothed 2 (sg2), with sensors attached to the participant (HS01, HS02). Reconstructed state spaces were computed with embedding parameters $\overline{m_0} = 6$, $\overline{\tau_0} = 10$. R code to reproduce the figure is available at .

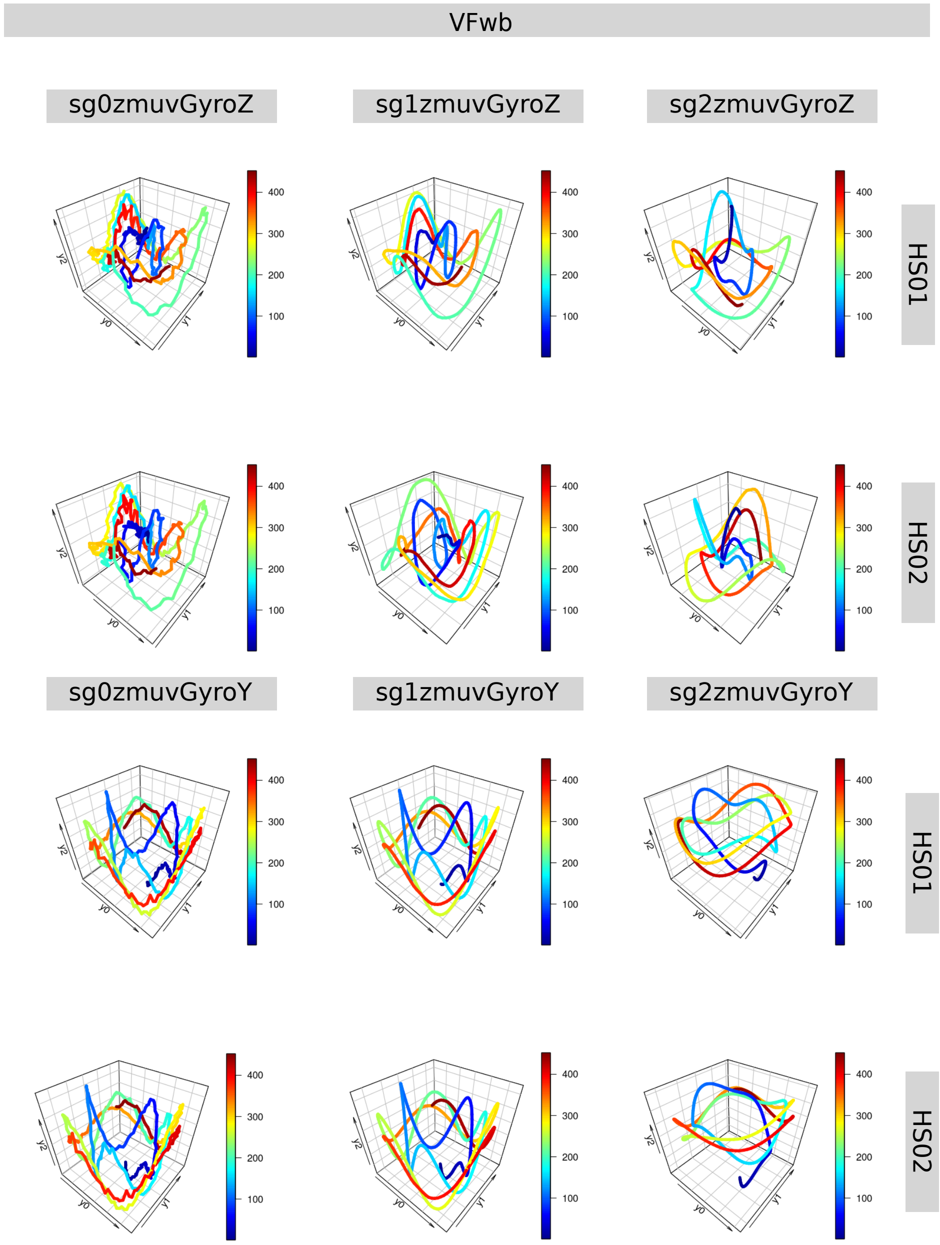

Fig. D.22 **RSSs for vertical faster arm movements (with beat).** Reconstructed state spaces of participant $p04$ with time series for raw-normalised (sg0), normalised-smoothed 1 (sg1) and normalised-smoothed 2 (sg2), with sensors attached to the participant (HS01, HS02). Reconstructed state spaces were computed with embedding parameters $\overline{m_0} = 6$, $\overline{\tau_0} = 10$. R code to reproduce the figure is available at .

D.4 RPs

The following Figs. D.24, D.23, D.26, D.25 illustrate reconstructed state spaces of participant $p04$ with a window length size of 500 samples. We refer the reader to download the data and code at Xochicale (2018) for the remained window size lengths and other participants.

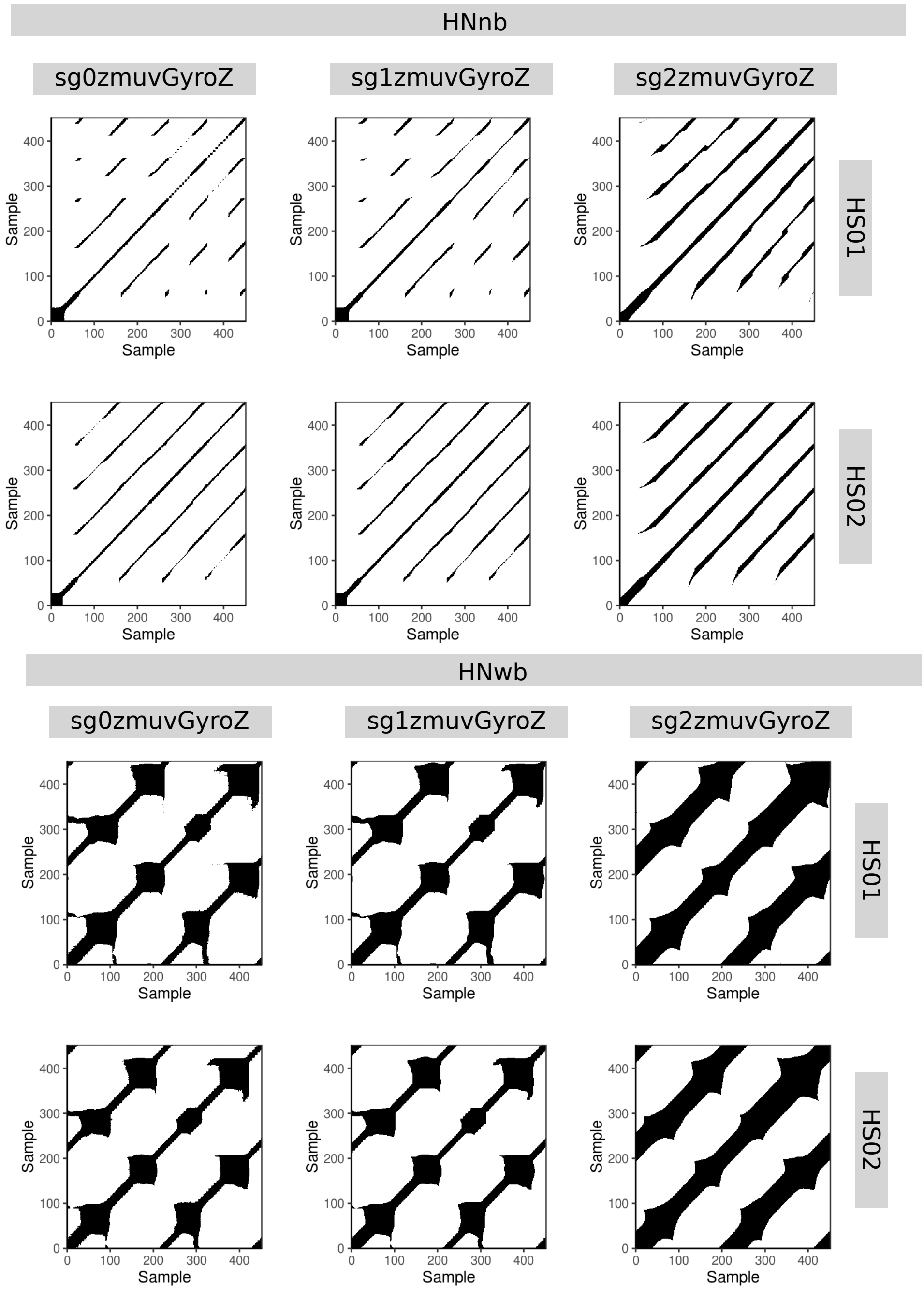

Fig. D.23 **RPs for horizontal normal arm movements.** Recurrence plots of participant $p04$ for horizontal normal movements with no beat (HNnb) and horizontal normal movements with beat (HFwb). Time series for raw-normalised (sg0zmuvGyroZ), normalised-smoothed 1 (sg1zmuvGyroZ) and normalised-smoothed 2 (sg2zmuvGyroZ) with sensors attached to the participant (HS01, HS02). Recurrence plots were computed with embedding parameters $\overline{m_0} = 6$, $\overline{\tau_0} = 10$ and recurrence threshold $\epsilon = 1$. R code to reproduce the figure is available at .

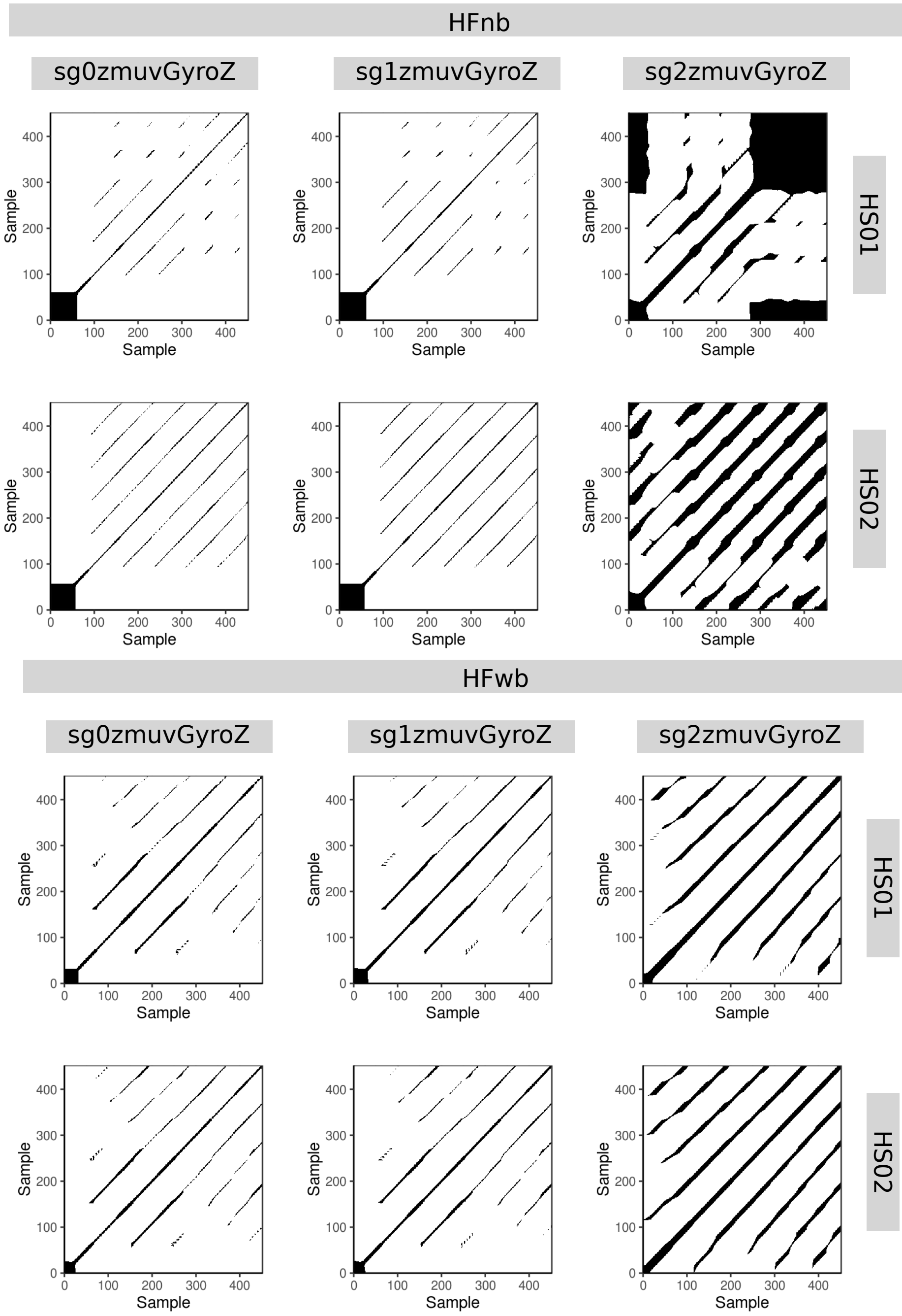

Fig. D.24 **RPs for horizontal faster arm movements.** Recurrence plots of participant $p04$ for horizontal faster movements with no beat (HNnb) and horizontal faster movements with beat (HFwb). Time series for raw-normalised (sg0zmuvGyroZ), normalised-smoothed 1 (sg1zmuvGyroZ) and normalised-smoothed 2 (sg2zmuvGyroZ) with sensors attached to the participant (HS01, HS02). Recurrence plots were computed with embedding parameters $\overline{m_0} = 6$, $\overline{\tau_0} = 10$ and recurrence threshold $\epsilon = 1$. R code to reproduce the figure is available at .

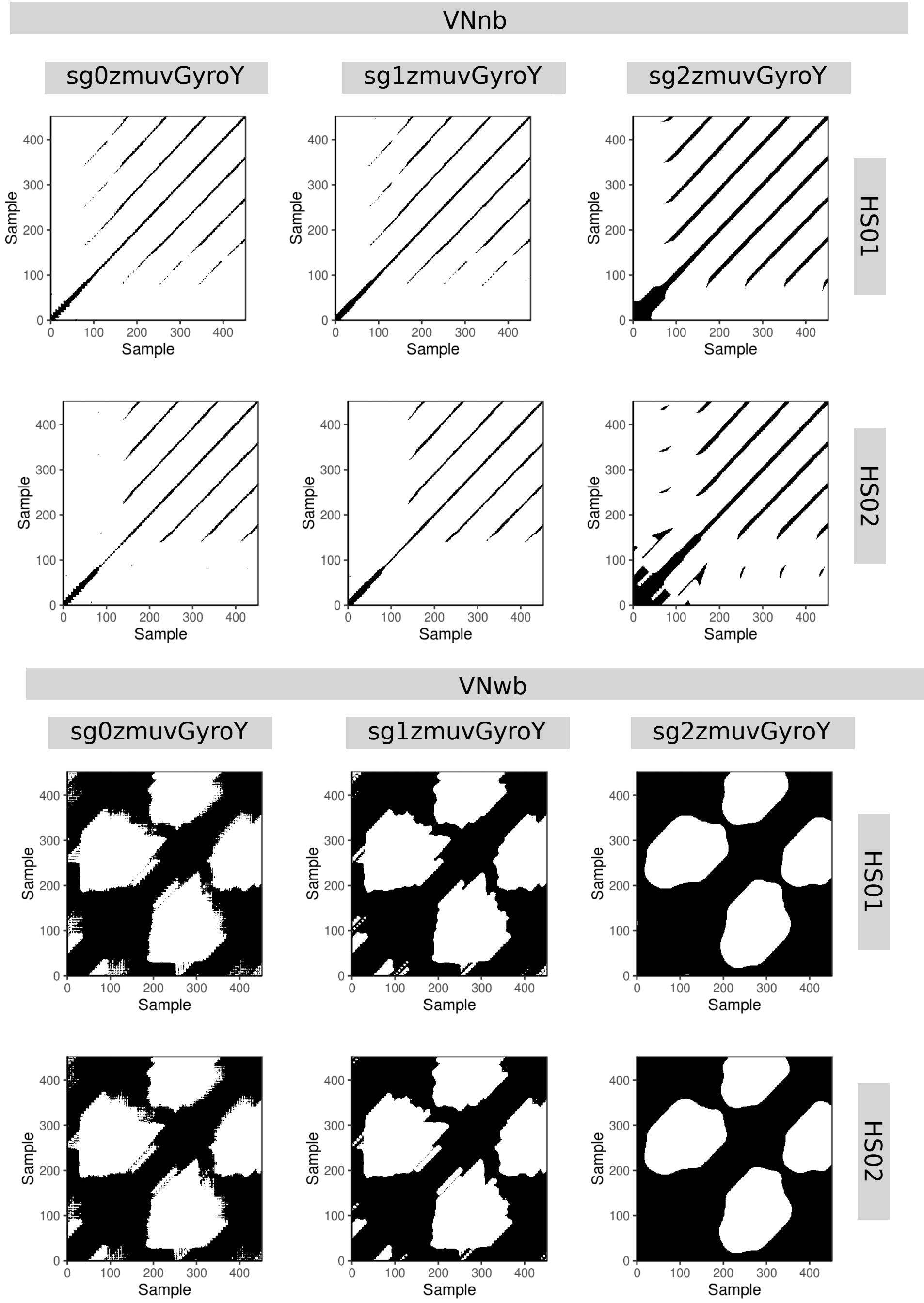

Fig. D.25 **RPs for vertical normal arm movements.** Recurrence plots of participant $p04$ for horizontal normal movements with no beat (VNnb) and horizontal normal movements with beat (VFwb). Time series for raw-normalised (sg0zmuvGyroY), normalised-smoothed 1 (sg1zmuvGyroY) and normalised-smoothed 2 (sg2zmuvGyroY) with sensors attached to the participant (HS01, HS02). Recurrence plots were computed with embedding parameters $\overline{m_0} = 6$, $\overline{\tau_0} = 10$ and recurrence threshold $\epsilon = 1$. R code to reproduce the figure is available at .

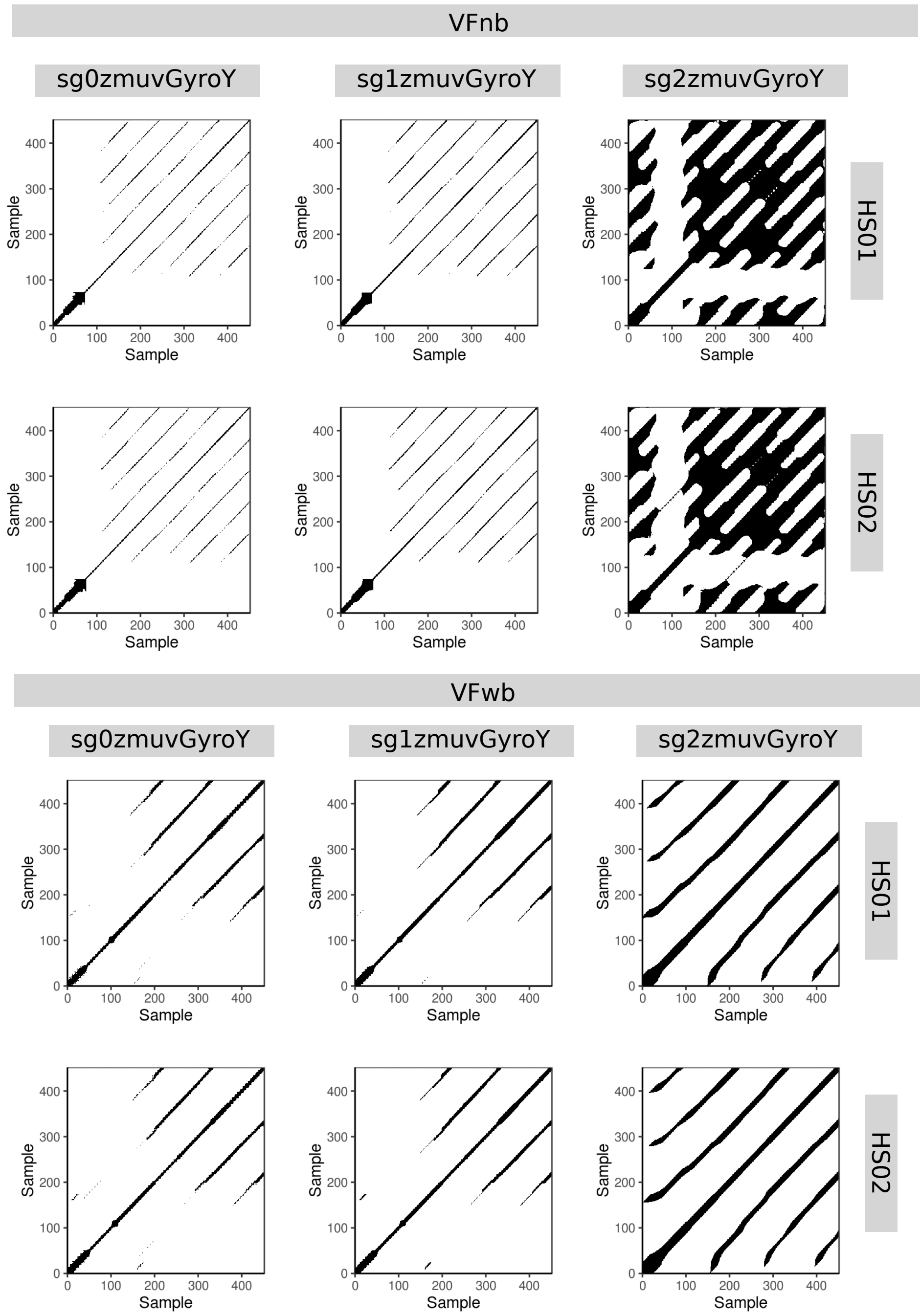

Fig. D.26 **RPs for vertical faster arm movements.** Recurrence plots of participant $p04$ for horizontal faster movements with no beat (VNnb) and horizontal faster movements with beat (VFwb). Time series for raw-normalised (sg0zmuvGyroY), normalised-smoothed 1 (sg1zmuvGyroY) and normalised-smoothed 2 (sg2zmuvGyroY) with sensors attached to the participant (HS01, HS02). Recurrence plots were computed with embedding parameters $\overline{m_0} = 6$, $\overline{\tau_0} = 10$ and recurrence threshold $\epsilon = 1$. R code to reproduce the figure is available at .

D.5 RQAs

D.5.1 REC values

Figs D.27 and D.28 show REC values, representing the % of black dots in the RPs, for vertical and horizontal arm movements.

It can be noted in Fig D.27 that REC values present little differences when comparing sensor HS01 and HS02. Similarly, considering the smoothness of the time series, REC values for participants appear to be similar in each of the activities (HNnb, HNwb, HFnb, HFwb) for sg0zmuvGyroZ and sg1zmuvGyroZ, while REC values for sg2zmuvGyroZ appear to fluctuate a bit more. With regards to the type of activity, horizontal arm movements with beat (HNwb) appear to fluctuate more than other activities (HNnb, HFnb, HFwb). Also RET values appear to fluctuate more and be greater for faster arm movements whereas RET values for normal arm movements appear to be constant (Fig D.27).

Figs D.28 show RET values for vertical arm movements. It can be noted that RET values appear to be similar for sensors HS01 and HS02 and the smoothness effect in REC values is more evident for sg2zmuvGyroY than REC values for sg0zmuvGyroY and sg1zmuvGyroY. RET values appear to fluctuate more for vertical normal arm movements with beat (VNwb) than other activities (VNnb, VFnb, VFwb) and RET values for VNnb, VFnb and VFwb appear to be constant and show little fluctuation between participants.

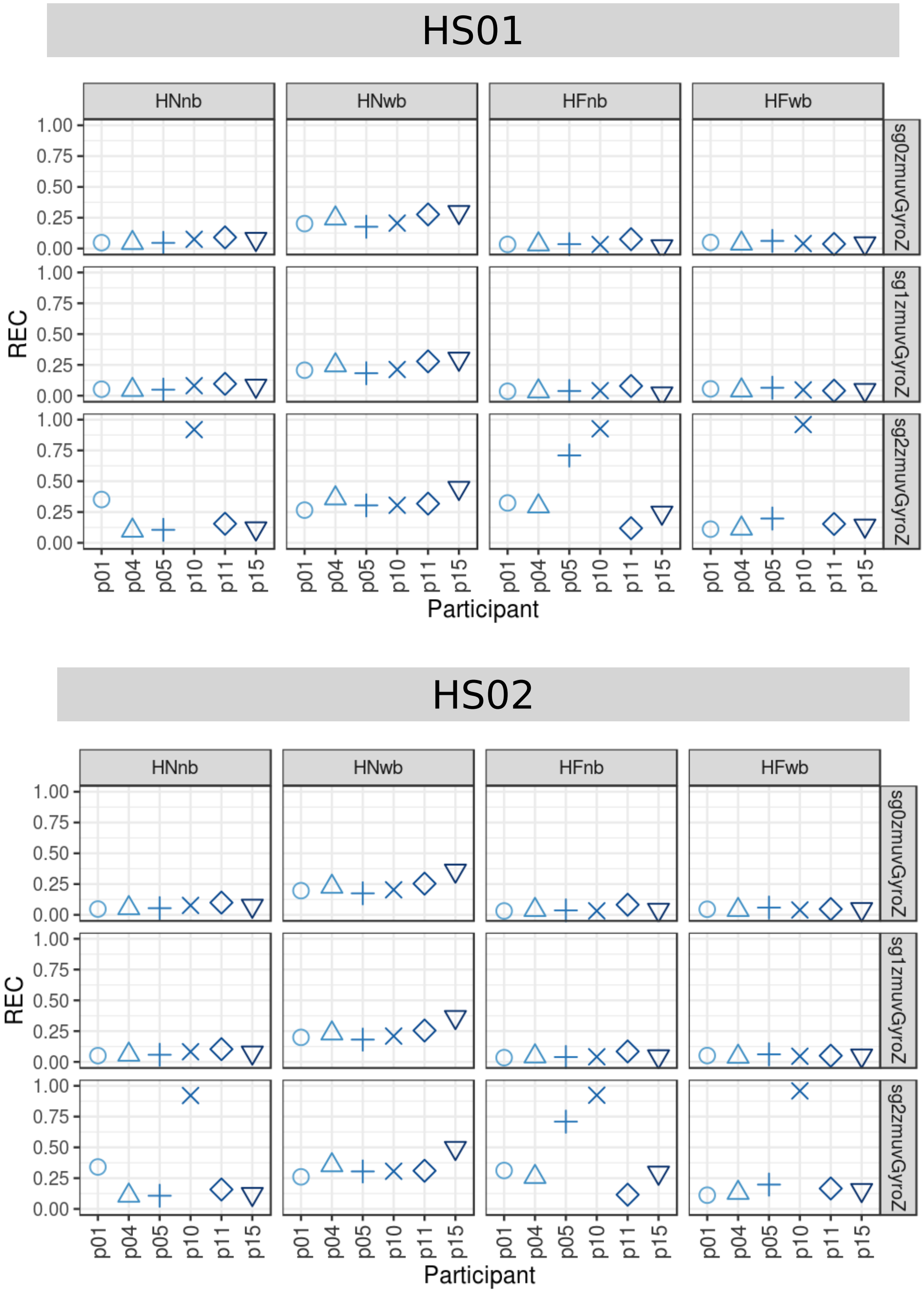

Fig. D.27 **REC values for horizontal arm movements.** REC values (representing % of black dots in the RPs) for 6 participants performing horizontal arm movements (HNnb, HNwb, HFnb, HFwb) for sensors HS01, HS02 and three smoothed-normalised axis of GyroZ (sg0zmuvGyroZ, sg1zmuvGyroZ and sg2zmuvGyroZ). REC values were computed with embedding parameters $\overline{m_0} = 6$, $\overline{\tau_0} = 10$ and recurrence threshold $\epsilon = 1$. R code to reproduce the figure is available at .

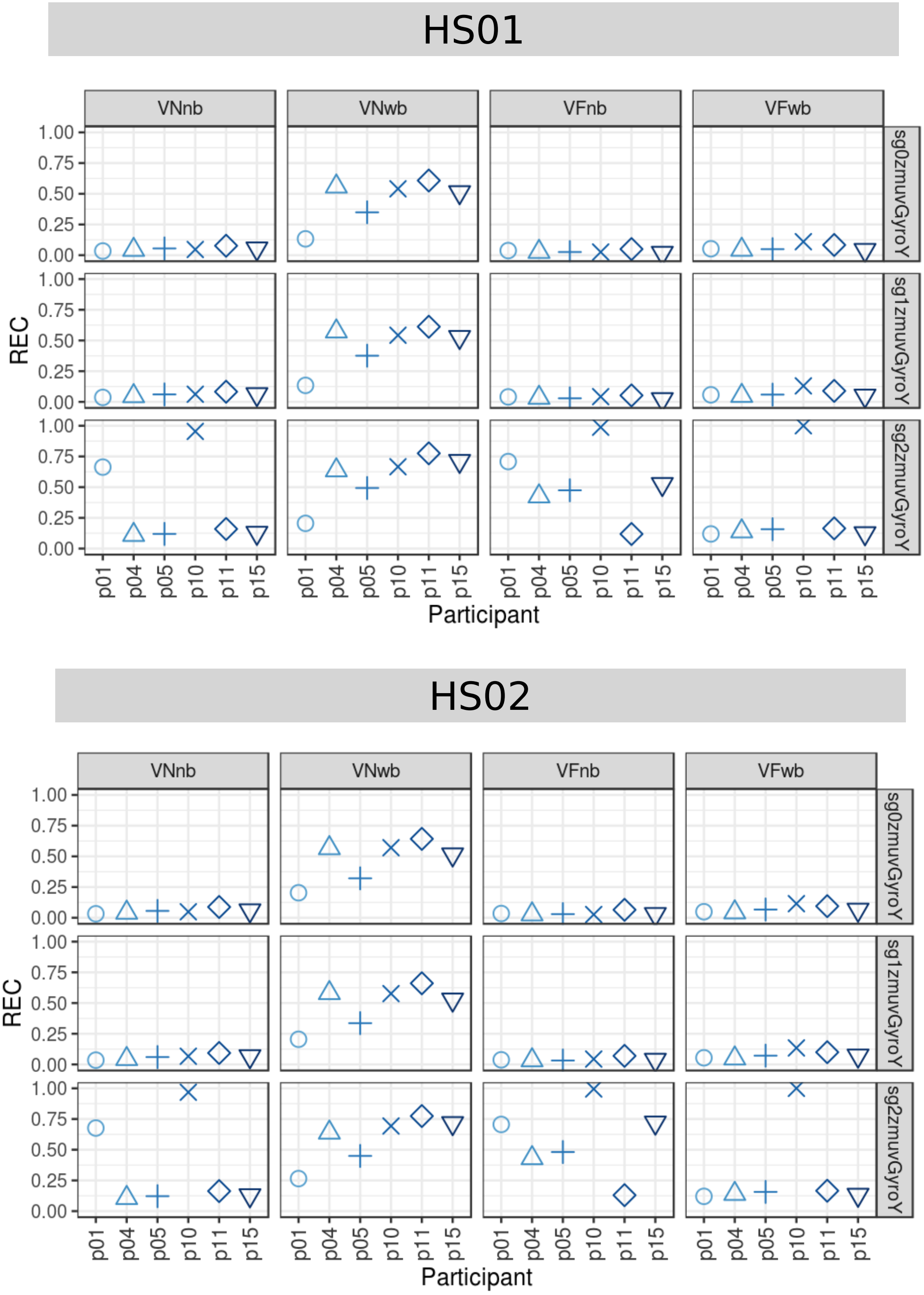

Fig. D.28 **REC values for vertical arm movements.** REC values (representing % of black dots in the RPs) for 6 participants performing vertical arm movements (VNnb, VNwb, VFnb, VFwb) for sensors HS01, HS02 and three smoothed-normalised axis of GyroZ (sg0zmuvGyroZ, sg1zmuvGyroZ and sg2zmuvGyroZ). REC values were computed with embedding parameters $\overline{m_0} = 6$, $\overline{\tau_0} = 10$ and recurrence threshold $\epsilon = 1$. R code to reproduce the figure is available at .

D.5.2 DET values

DET values appear to be constant for any source of time series (Figs D.29 and D.30). For both horizontal and vertical arm movements, the increase of smoothness of time series appear to affect the smoothness of DET values by making them to appear more similar as the smoothness increase. Additionally, it can be noted more fluctuations of DET values for faster activities (HFnb, HFwb) than normal activities (HNnb, HNwb), specifically for sg0zmuvGyroY (Figs D.29, D.30).

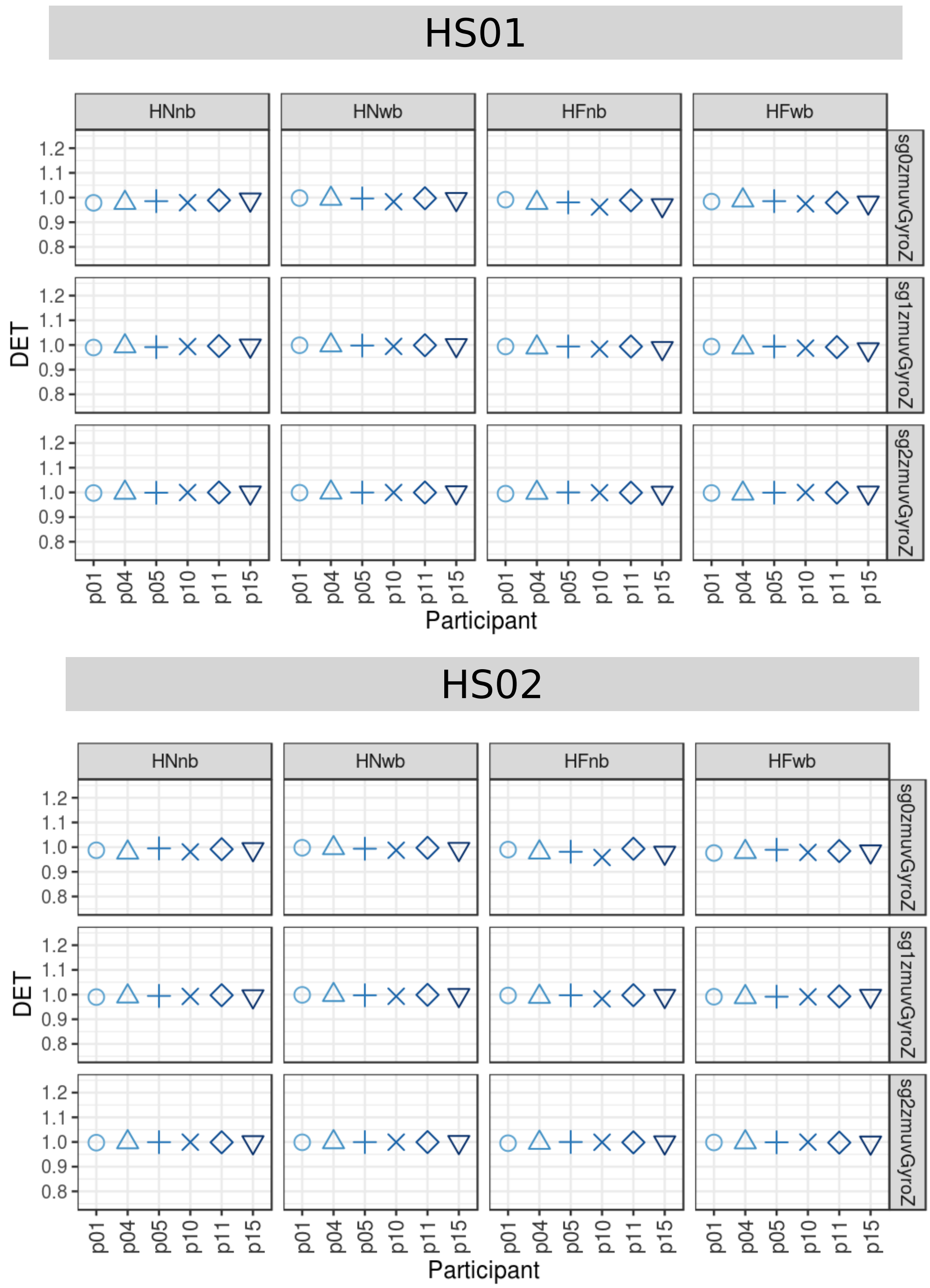

Fig. D.29 **DET values for horizontal arm movements.** DET values (representing predictability and organisation of the RPs) for 6 participants performing horizontal arm movements (HNnb, HNwb, HFnb, HFwb) for sensors HS01, HS02 and three smoothed-normalised axis of GyroZ (sg0zmuvGyroZ, sg1zmuvGyroZ and sg2zmuvGyroZ). DET values were computed with embedding parameters $\overline{m_0} = 6$, $\overline{\tau_0} = 10$ and recurrence threshold $\epsilon = 1$. R code to reproduce the figure is available at .

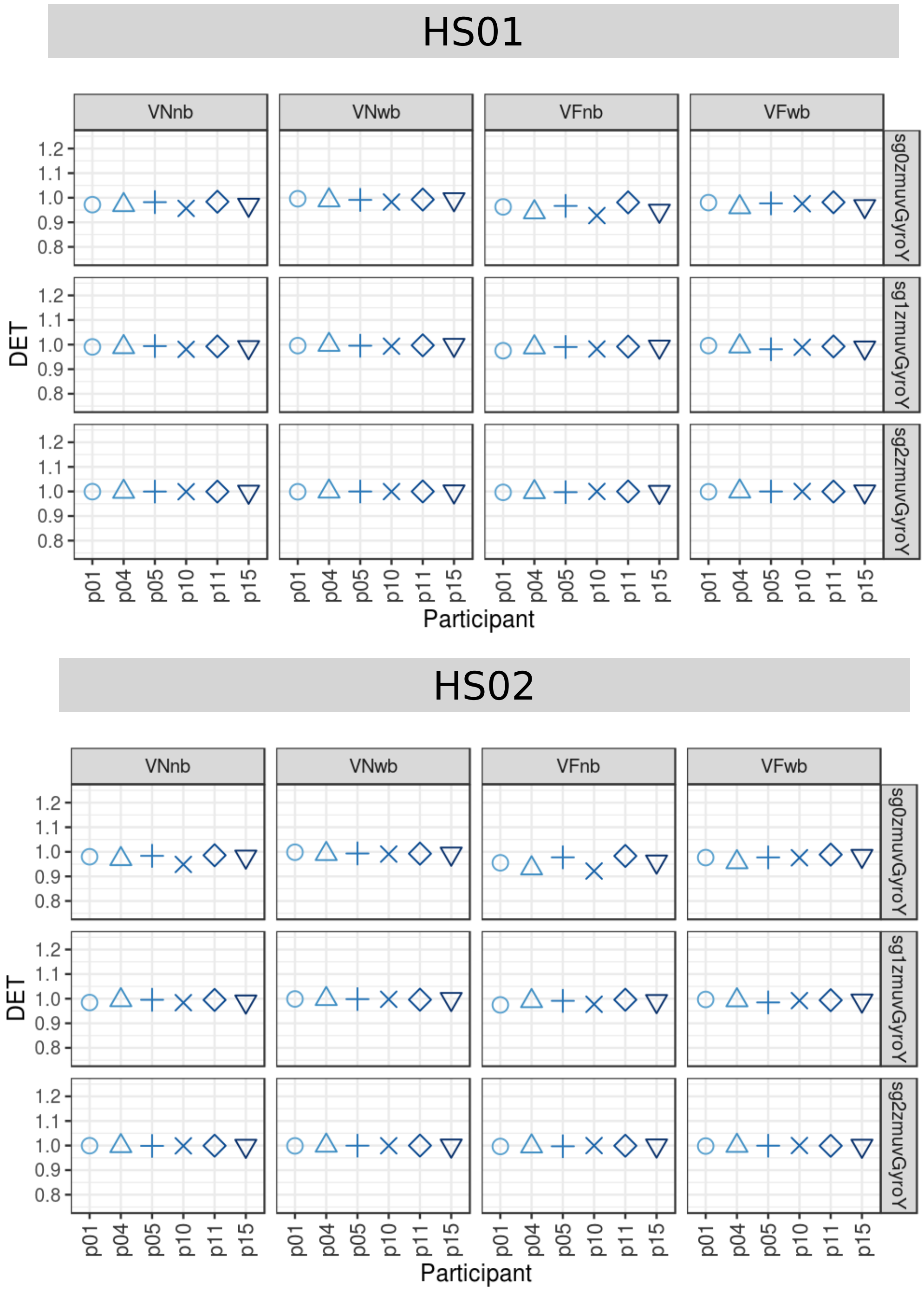

Fig. D.30 **DET values for vertical arm movements.** DET values (representing predictability and organisation of the RPs) for 6 participants performing vertical arm movements (VNnb, VNwb, VFnb, VFwb) for sensors HS01, HS02 and three smoothed-normalised axis of GyroY (sg0zmuvGyroY, sg1zmuvGyroY and sg2zmuvGyroY). DET values were computed with embedding parameters $\overline{m_0} = 6$, $\overline{\tau_0} = 10$ and recurrence threshold $\epsilon = 1$. R code to reproduce the figure is available at .

D.5.3 RATIO values

RATIO values for horizontal and vertical arm movements are shown in Figs D.31 and D.32.

The fluctuation of RATIO values for horizontal faster arm movements appear to be more notable than RATIO values for horizontal normal arm movements. RATIO values appear to be constant for activity HNwb than other activities (HNnb, HFnb, HFwb). Regarding the smoothness of time series, RATIO values appear to have similar values for sg0zmuvGyroZ and sg1zmuvGyroZ while RATIOS values are more uniform for sg2zmuvGyroZ. With regards to type of sensor, RET values appear to be similar for HS01 and HS02 with the exception of $p15$ in HFnb activity (Figs D.31).

Figs D.32 show RATIO values for vertical arm movements. The fluctuation of RATIO values appears to be constant for the activity VNwb whereas other RATIO values for other activities (VNnb, VFnb, VFwb) appear to fluctuate more. The smoothness of the time series affects only the RATIO values for sg2zmuvGyroY as these appear to be constant, while RET values for sg0zmuvGyroY and sg1zmuvGyroZ appear to have the similar RATIO values. Additionally, RATIO values for type of sensors HS01 and HS02 appear to show similar values as well, with the exception of $p15$ in the VFnb activity.

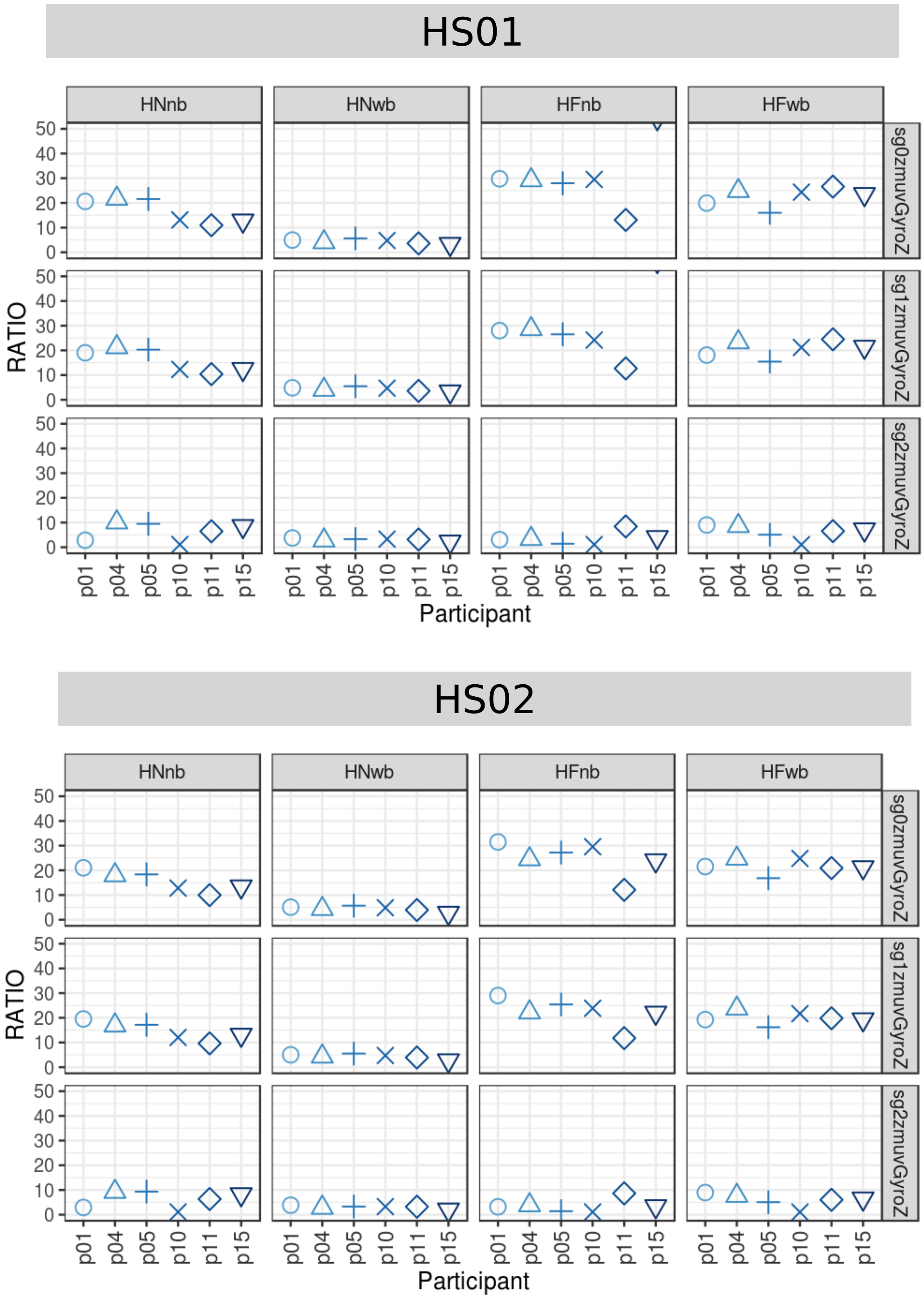

Fig. D.31 **RATIO values for horizontal arm movements.** RATIO values, representing dynamic transitions, for 6 participants performing horizontal arm movements (HNnb, HNwb, HFnb, HFwb) with sensors HS01, HS02 and three smoothed-normalised axis of GyroZ (sg0zmuvGyroZ, sg1zmuvGyroZ and sg2zmuvGyroZ). RATIO values were computed with embedding parameters $\overline{m_0} = 6$, $\overline{\tau_0} = 10$ and recurrence threshold $\epsilon = 1$. R code to reproduce the figure is available at .

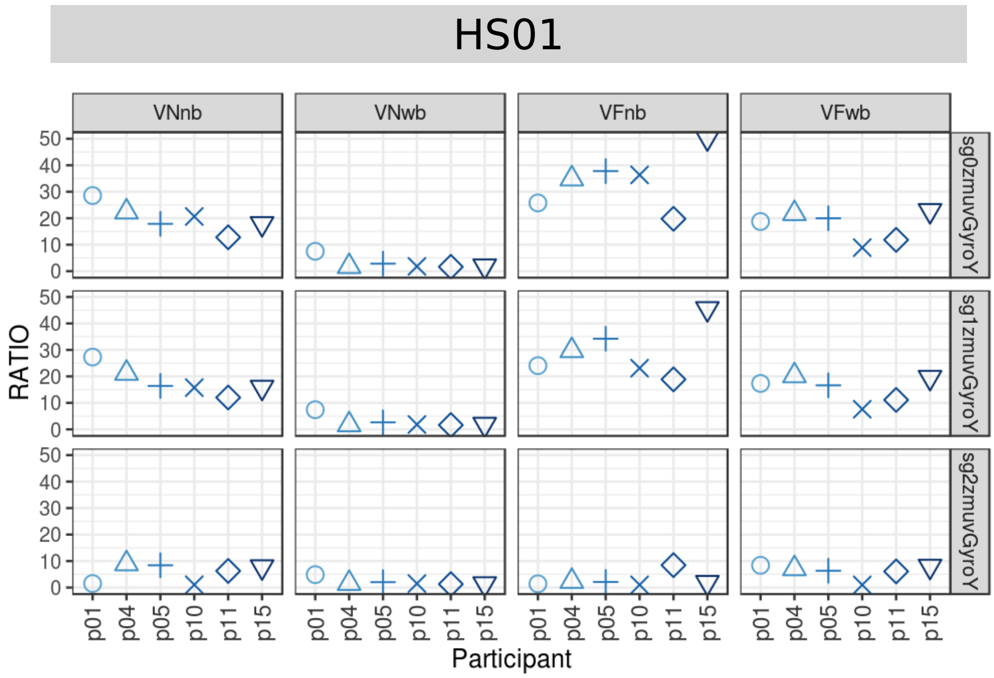

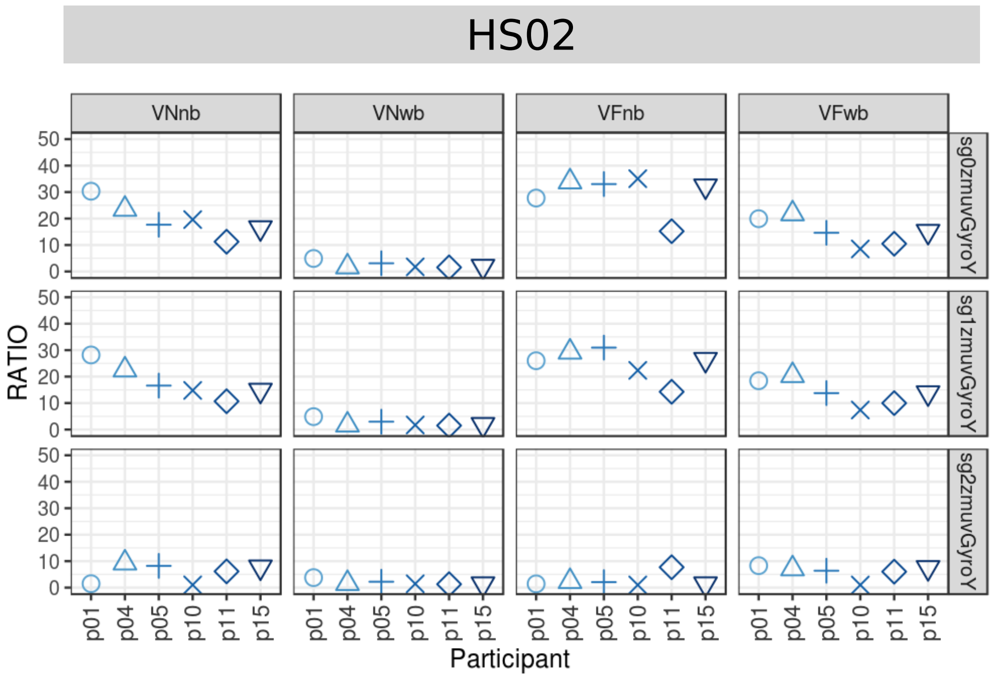

Fig. D.32 **RATIO values for vertical arm movements.** RATIO values, representing dynamic transitions, for 6 participants performing vertical arm movements (VNnb, VNwb, VFnb, VFwb) with sensors HS01, HS02 and three smoothed-normalised axis of GyroY (sg0zmuvGyroY, sg1zmuvGyroY and sg2zmuvGyroY). RATIO values were computed with embedding parameters $\overline{m_0} = 6$, $\overline{\tau_0} = 10$ and recurrence threshold $\epsilon = 1$. R code to reproduce the figure is available at .

D.5.4 ENTR values

ENTR values for horizontal and vertical arm movements are shown in Figs D.33 and D.34.

Figs D.33 show ENTR values for horizontal arm movements. ENTR values appear to be similar for sg0zmuvGyroZ and sg1zmuvGyroZ and oscillate between 2 to 4, while ENTR values for sg2zmuvGyroZ appear to show similar fluctuations but with higher ENTR values oscillating between 3.5 to 5 with the exception of $p10$ with activities VNnb and VFwb for sg2zmuvGyroY which ENTR values are slightly out of range. ENTR values appear to be similar for sensor HS01 and HS02.

Figs D.34 show ENTR values for vertical arm movements. ENTR values for sg0zmuvGyroY and sg1zmuvGyroY appear to show the same values and oscillate between 2 to 4, while ENTR values appear to oscillate between 3.5 to 5 with the exception of $p10$ with activities VNnb and VFwb for sg2zmuvGyroY which ENTR values are out of range. ENTR values for sensor HS01 and HS02 appear to show the same values.

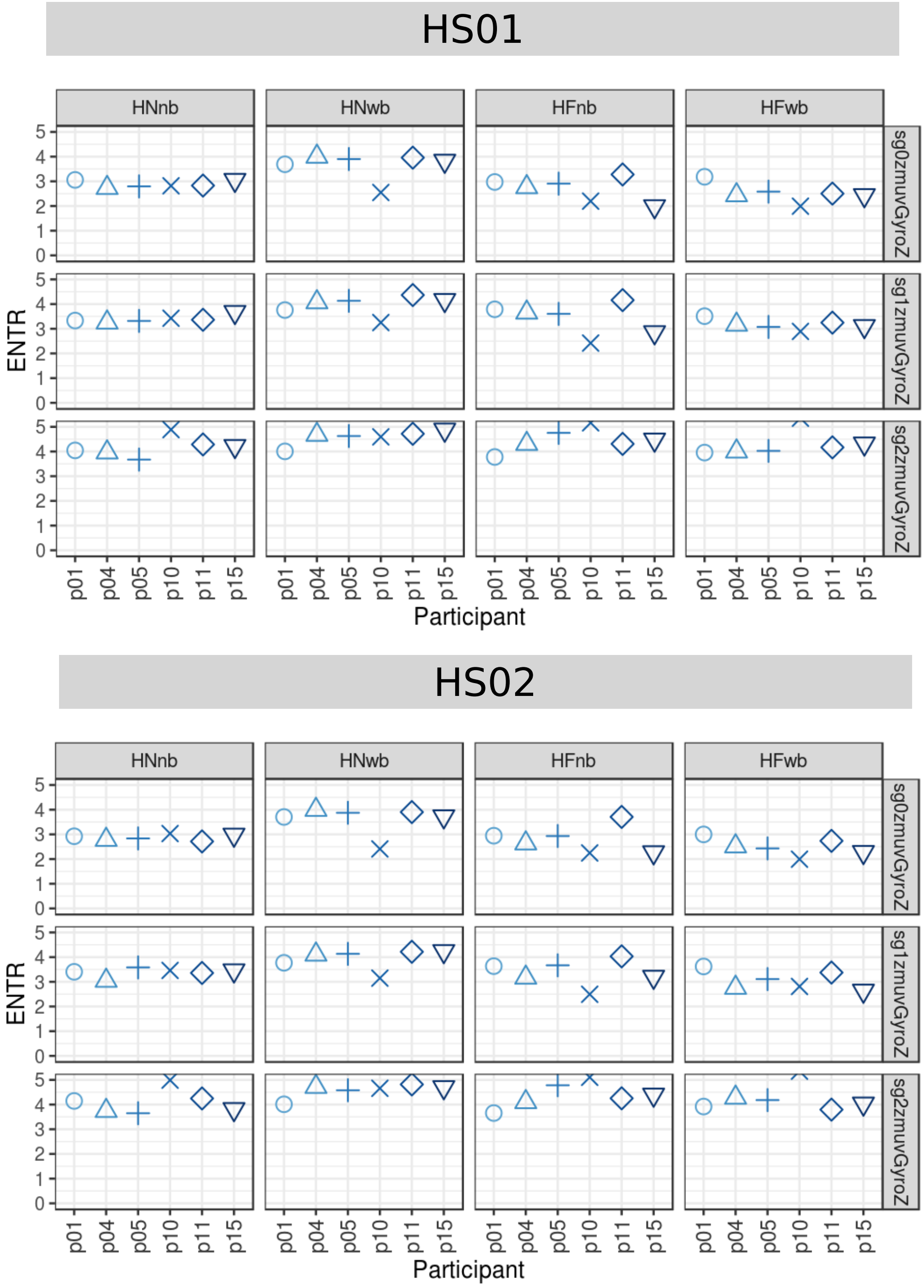

Fig. D.33 **ENTR values for horizontal arm movements.** ENTR values (representing the complexity of the deterministic structure in time series) for 6 participants performing horizontal arm movements (HNnb, HNwb, HFnb, HFwb) for sensors HS01, HS02 and three smoothed-normalised axis of GyroZ (sg0zmuvGyroZ, sg1zmuvGyroZ and sg2zmuvGyroZ). ENTR values were computed with embedding parameters $\overline{m_0} = 6$, $\overline{\tau_0} = 10$ and recurrence threshold $\epsilon = 1$. R code to reproduce the figure is available at .

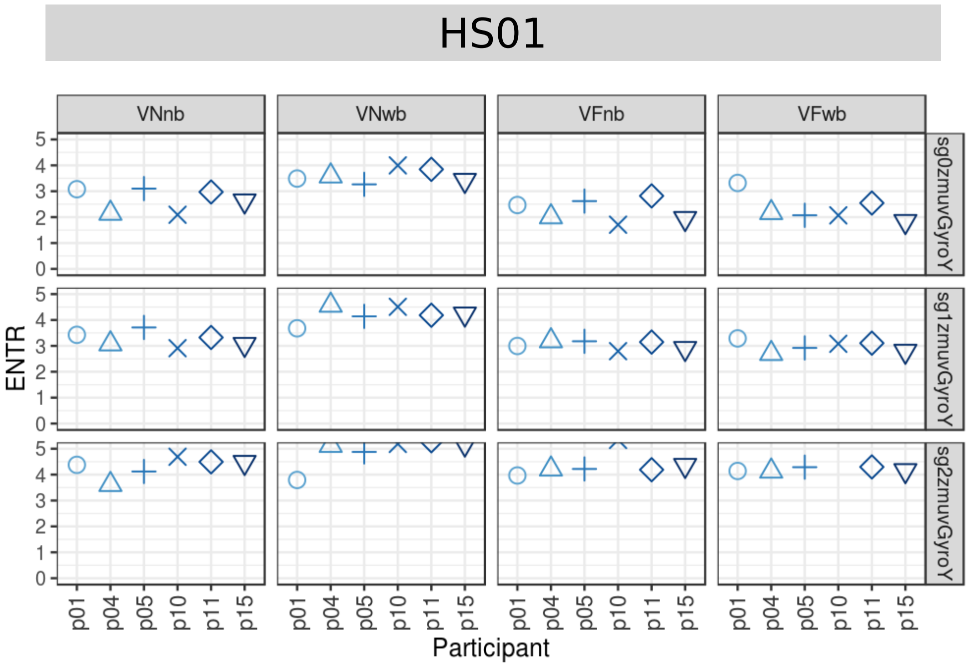

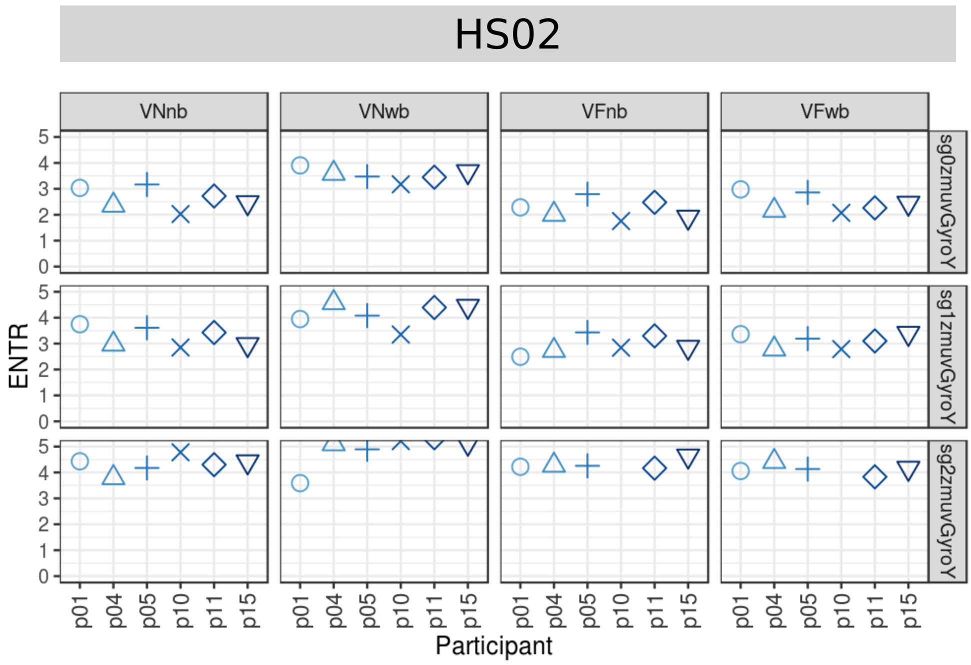

Fig. D.34 **ENTR values for vertical arm movements.** ENTR values (representing the complexity of the deterministic structure in time series) for 6 participants performing vertical arm movements (VNnb, VNwb, VFnb, VFwb) for sensors HS01, HS02 and three smoothed-normalised axis of GyroY (sg0zmuvGyroY, sg1zmuvGyroY and sg2zmuvGyroY). ENTR values were computed with embedding parameters $\overline{m_0} = 6$, $\overline{\tau_0} = 10$ and recurrence threshold $\epsilon = 1$. R code to reproduce the figure is available at .

Appendix E

Additional results for HHI experiment

E.1 Time Series

Time series for twenty participants with a window length size of 500 samples of horizontal arm movements (Figs. E.1, E.2, E.3) and vertical arm movements (Figs. E.4, E.5, E.6). For the remained window lengths, the reader is welcome to download the data and code at Xochicale (2018). See Appendix F for details on how code and data is organised and how results can be replicated.

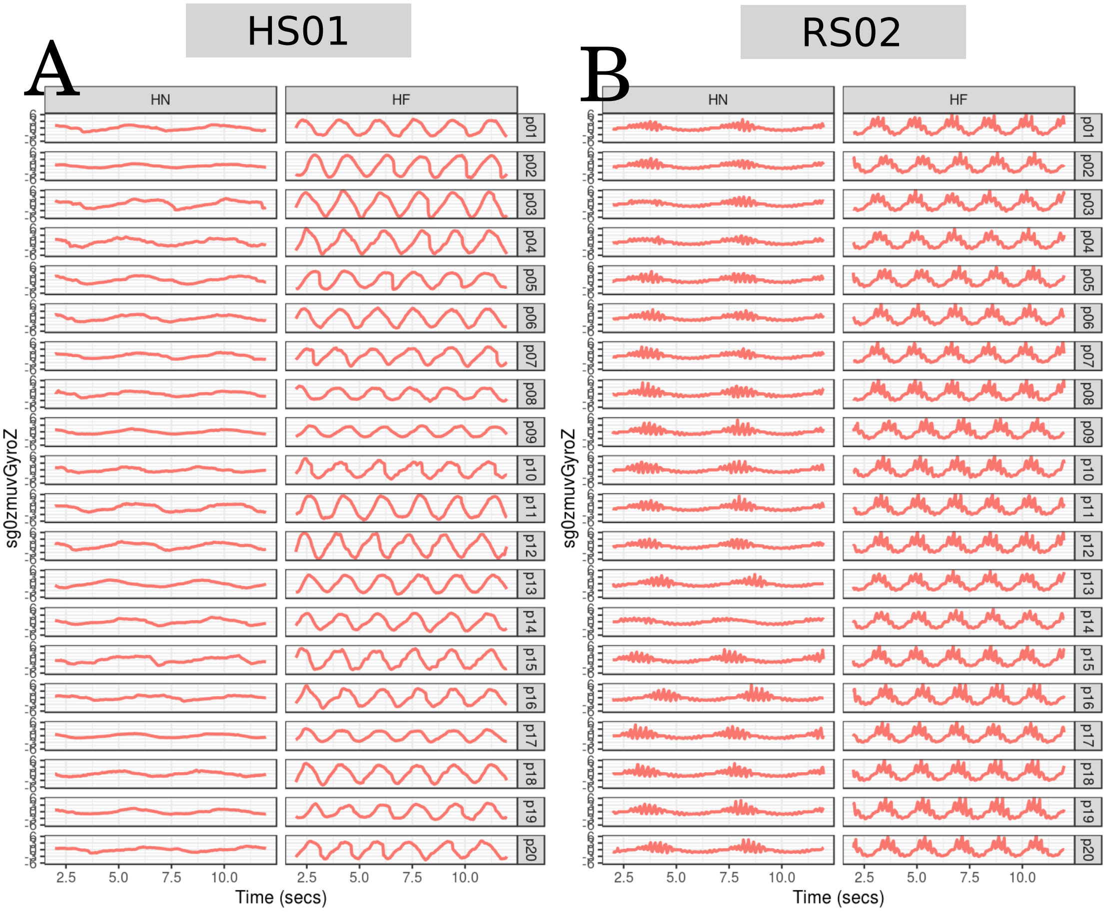

Fig. E.1 **Time series for horizontal arm movements (sg0)** Time series for sg0zmuvGyroZ for twenty participants ($p01$ to $p20$) for horizontal movements in normal (HN) and horizontal faster (HF) velocity with sensors attached to the participant wrist (HS01) and to the humanoid wrist (RS02). R code to reproduce the figure is available at .

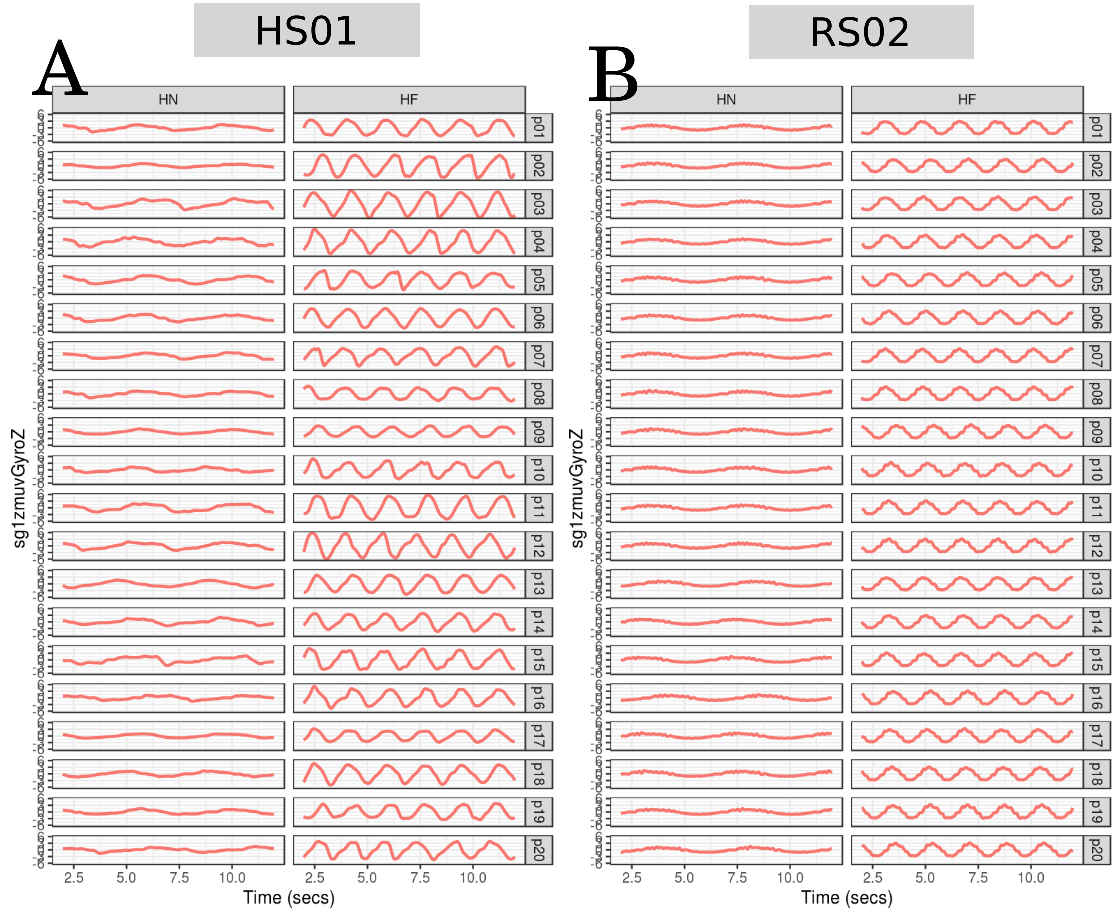

Fig. E.2 **Time series for horizontal arm movements (sg1)** Time series for sg0zmuvGyroZ for twenty participants ($p01$ to $p20$) for horizontal movements in normal (HN) and horizontal faster (HF) velocity with sensors attached to the participant wrist (HS01) and to the humanoid wrist (RS02). R code to reproduce the figure is available at .

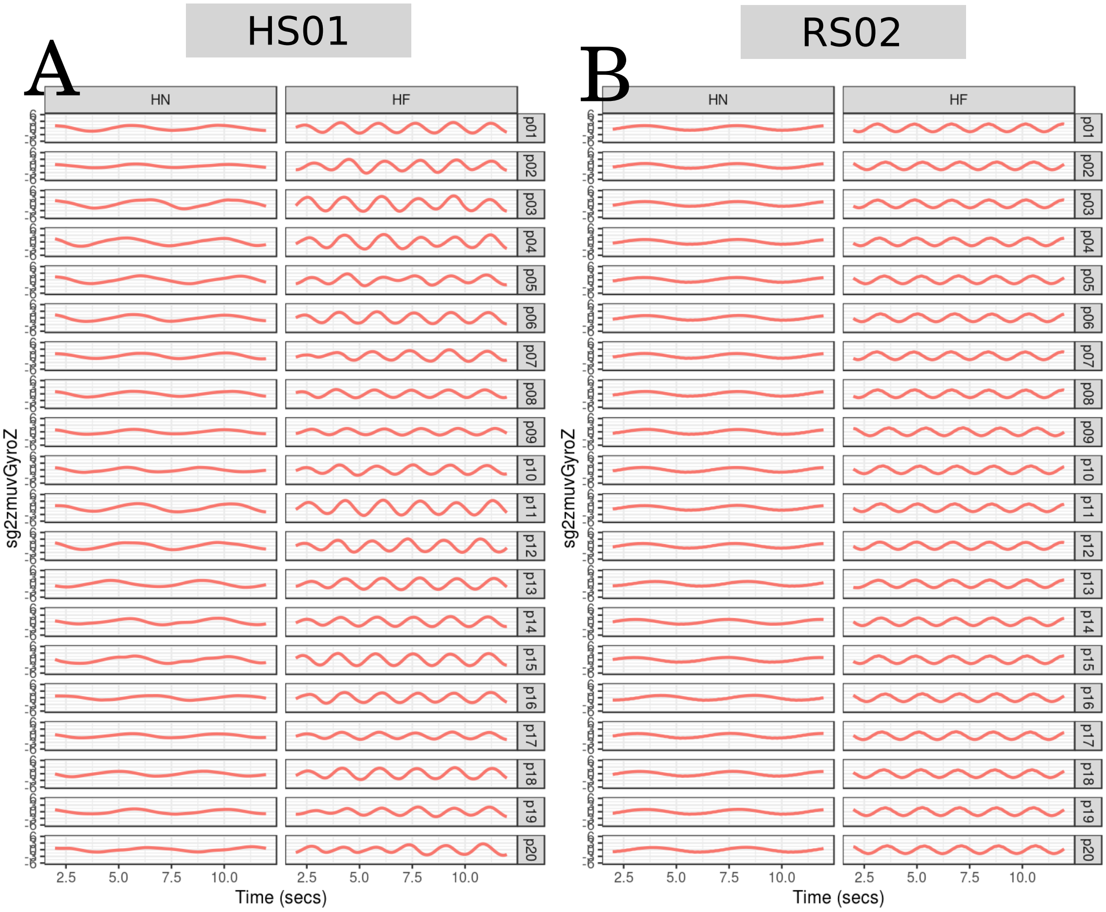

Fig. E.3 **Time series for horizontal arm movements (sg2)** Time series for sg0zmuvGyroZ for twenty participants (p01 to p20) for horizontal movements in normal (HN) and horizontal faster (HF) velocity with sensors attached to the participant wrist (HS01) and to the humanoid wrist (RS02). R code to reproduce the figure is available at .

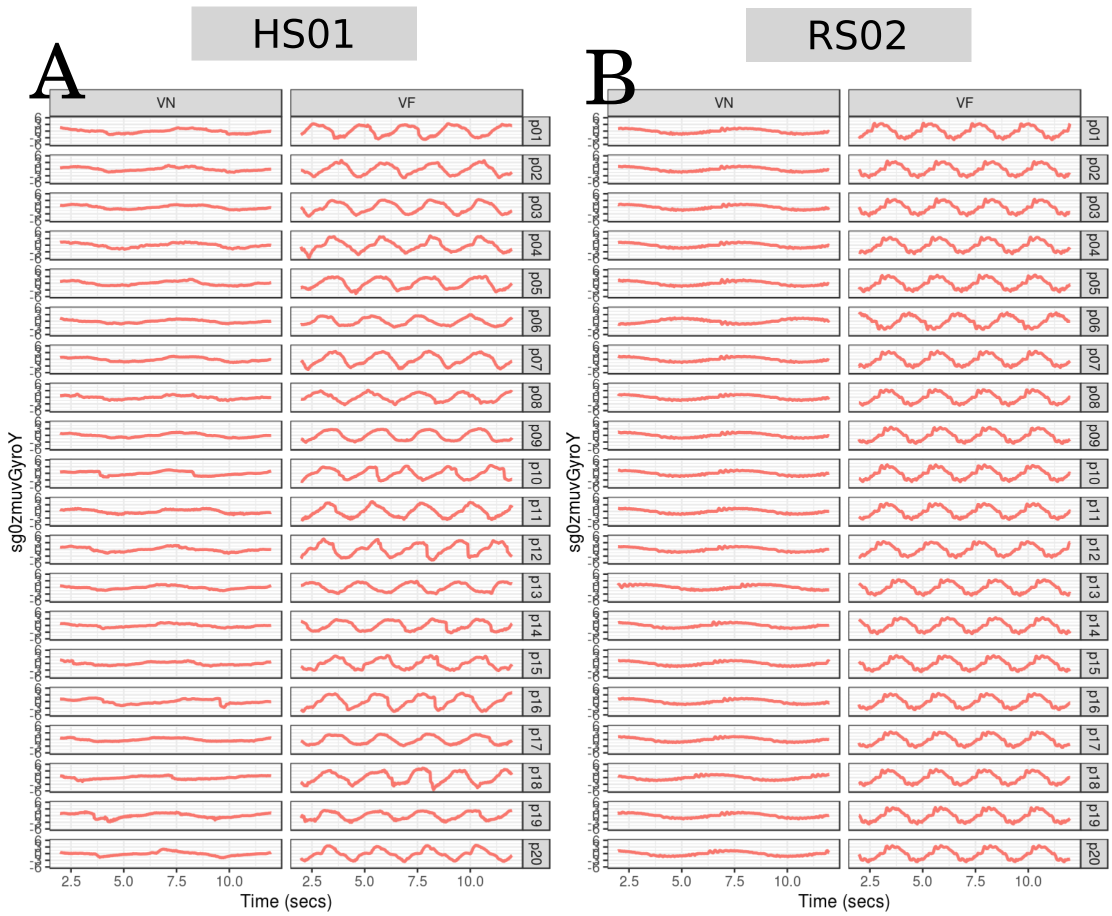

Fig. E.4 **Time series for vertical arm movements (sg0)** Time series for sg0zmuvGyroY for twenty participants (*p*01 to *p*20) for vertical movements in normal (HN) and horizontal faster (HF) velocity with sensors attached to the participant wrist (HS01) and to the humanoid wrist (RS02). R code to reproduce the figure is available at .

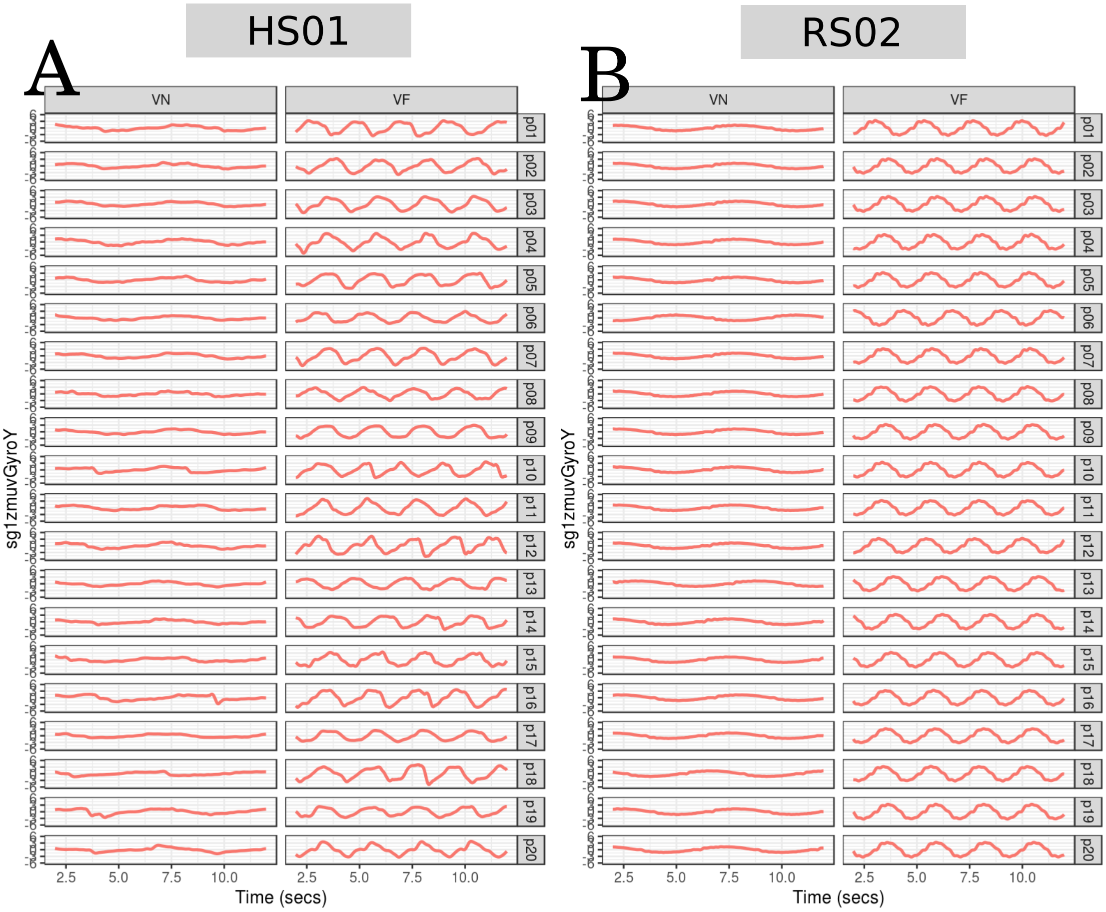

Fig. E.5 **Time series for vertical arm movements (sg1)** Time series for sg0zmuvGyroY for twenty participants ($p01$ to $p20$) for horizontal movements in normal (HN) and horizontal faster (HF) velocity with sensors attached to the participant wrist (HS01) and to the humanoid wrist (RS02). R code to reproduce the figure is available at .

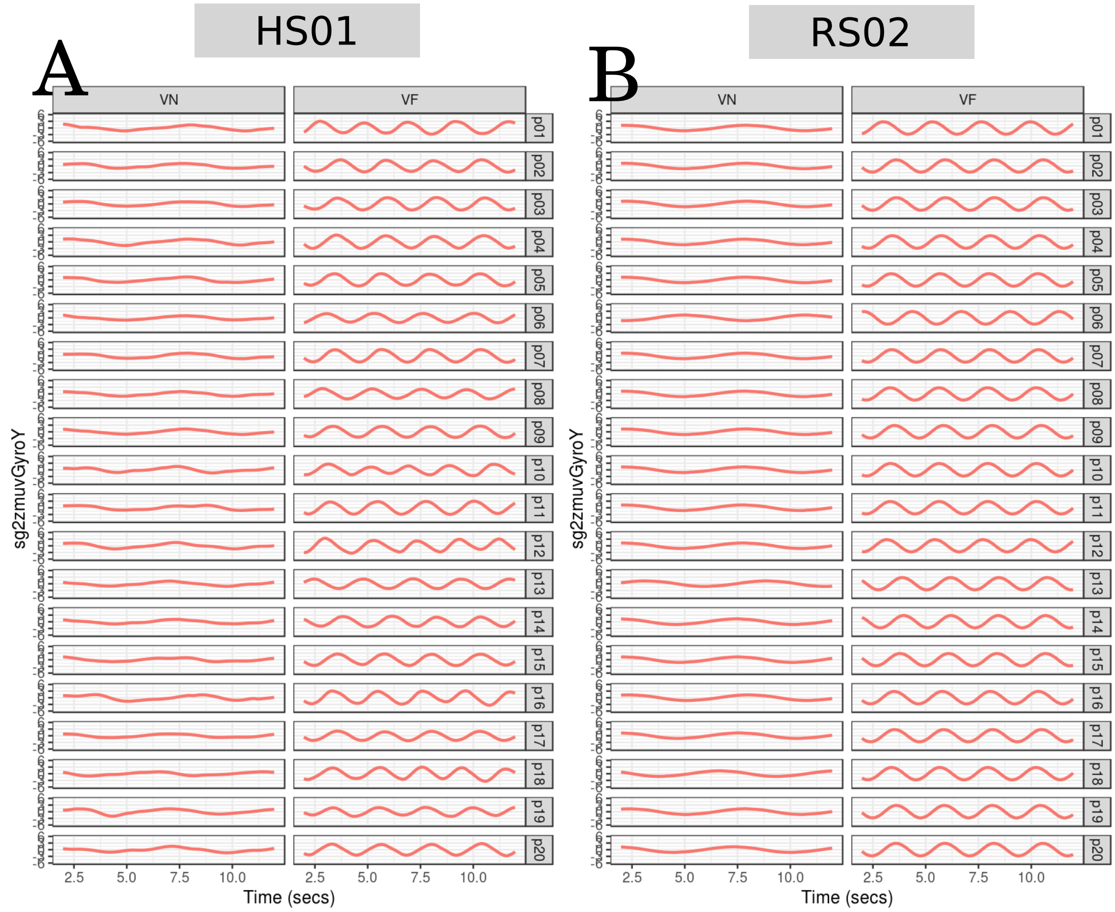

Fig. E.6 **Time series for vertical arm movements (sg2)** Time series for sg0zmuvGyroY for twenty participants (*p*01 to *p*20) for vertical movements in normal (HN) and horizontal faster (HF) velocity with sensors attached to the participant wrist (HS01) and to the humanoid wrist (RS02). R code to reproduce the figure is available at .

E.2 Embedding parameters

E.2.1 Minimum dimension embedding values

Minimum embedding dimensions for horizontal and vertical arm movements are presented in Figs. E.7 and E.8, respectively. For remained results with window size lengths of time series data, we refer the reader to download the data and code at Xochicale (2018).

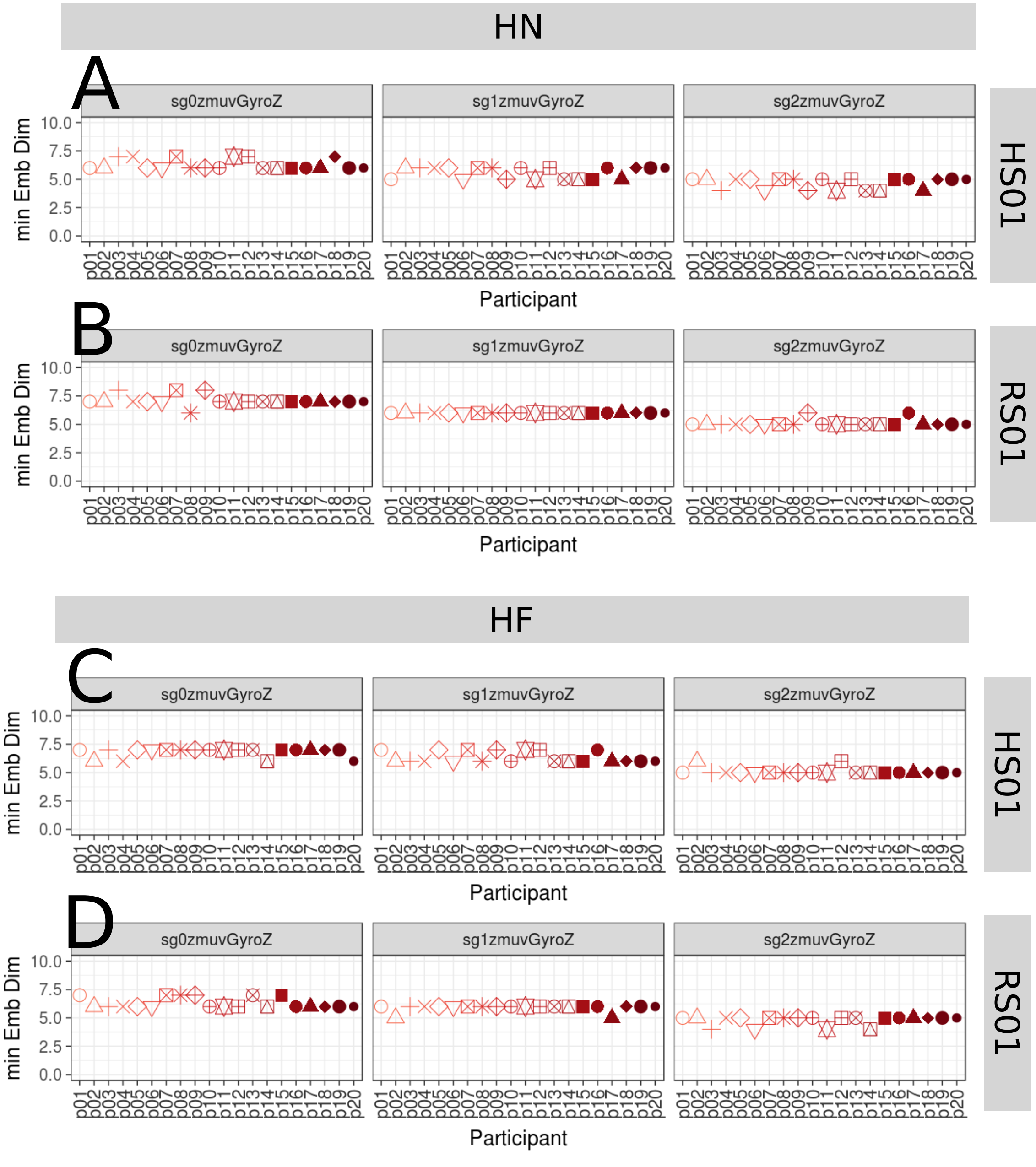

Fig. E.7 **Minimum embedding dimensions for horizontal arm movements.** (A, B) Horizontal Normal (HN), (C, D) Horizontal Faster (HF) movements, (A, C) sensor attached to participants (HS01), and (B, D) sensor attached to robot (RS01). Minimum embedding dimensions are for twenty participants (p01 to p20) with three smoothed signals (sg0zmuvGyroZ, sg1zmuvGyroZ and sg2zmuvGyroZ) and window lenght of 10-sec (500 samples). R code to reproduce the figure is available at .

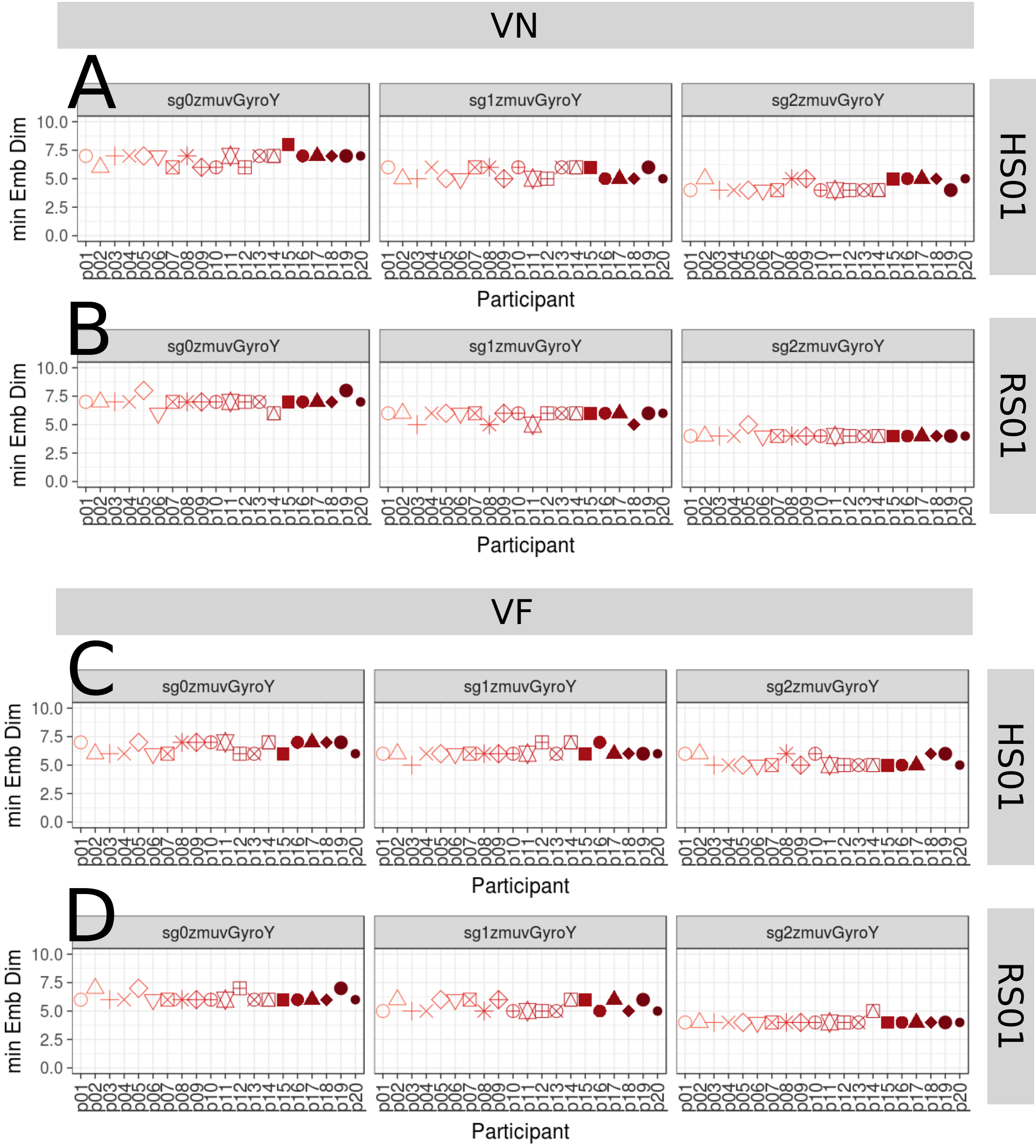

Fig. E.8 **Minimum embedding dimensions for vertical arm movements.** (A, B) Vertical Normal (VN), (C, D) Vertical Faster (VF) movements, (A, C) sensor attached to participants (HS01), and (B, D) sensor attached to robot (RS01). Minimum embedding dimensions are for twenty participants (p01 to p20) with three smoothed signals (sg0zmuvGyroY, sg1zmuvGyroY and sg2zmuvGyroY) and window length of 10-sec (500 samples). R code to reproduce the figure is available at .

E.2.2 Minimum delay embedding values

First minimum AMI values for horizontal and vertical arm movements are presented in Figs. E.9 and E.10, respectively. For remained results with window size lengths of time series data, we refer the reader to download the data and code at Xochicale (2018).

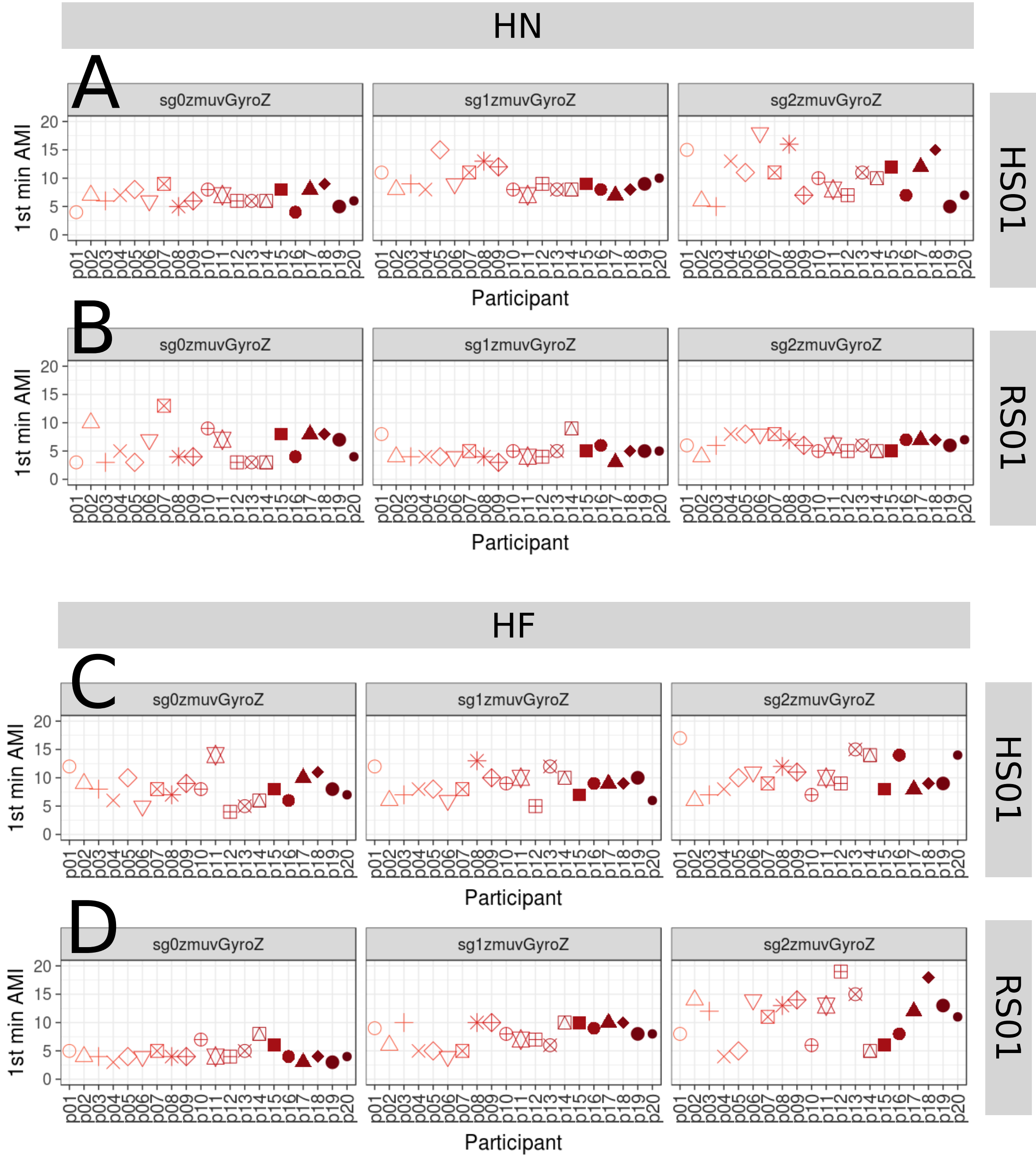

Fig. E.9 **First minimum AMI values for horizontal arm movements.** (A, B) Horizontal Normal (HN), (C, D) Horizontal Faster (HF) movements, (A, C) sensor attached to participants (HS01), and (B, D) sensor attached to robot (RS01). First minimum AMI values are for twenty participants (p01 to p20) with three smoothed signals (sg0zmuvGyroZ, sg1zmuvGyroZ and sg2zmuvGyroZ) and window lenght of 10-sec (500 samples). R code to reproduce the figure is available at .

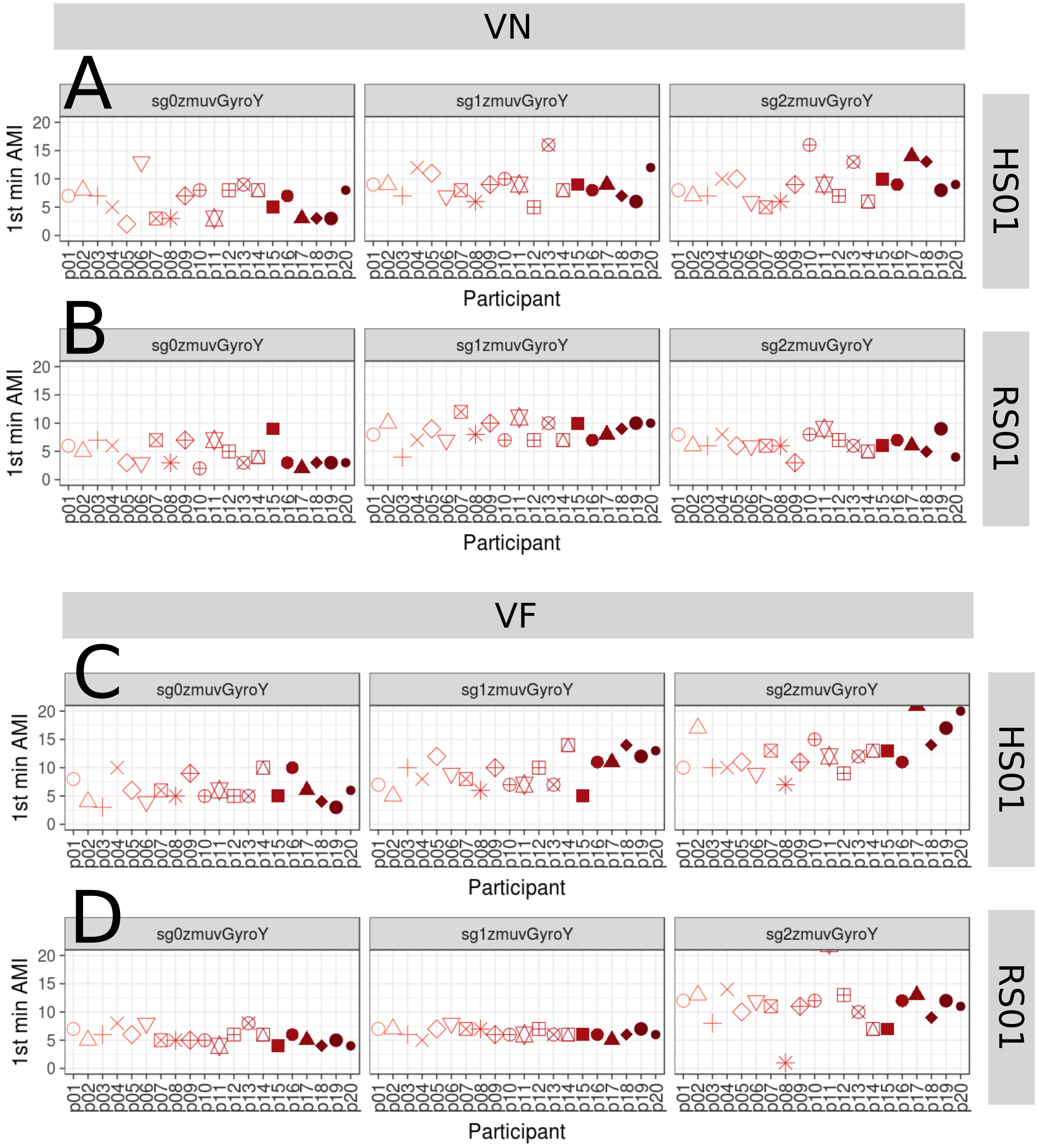

Fig. E.10 **First minimum AMI values for vertical arm movements.** (A, B) Vertical Normal (VN), (C, D) Vertical Faster (VF) movements, (A, C) sensor attached to participants (HS01), and (B, D) sensor attached to robot (RS01). First minimum AMI values are for twenty participants (p01 to p20) with three smoothed signals (sg0zmuvGyroZ, sg1zmuvGyroZ and sg2zmuvGyroZ) and window lenght of 10-sec (500 samples). R code to reproduce the figure is available at .

E.3 RSSs

Reconstructed state spaces of participant $p01$, $p02$ and $p03$ for horizontal arm movements (Figs. E.11 and E.12) and vertical arm movements (Figs. E.13 and E.14). For remained results with window size lengths of time series data, we refer the reader to download the data and code at Xochicale (2018).

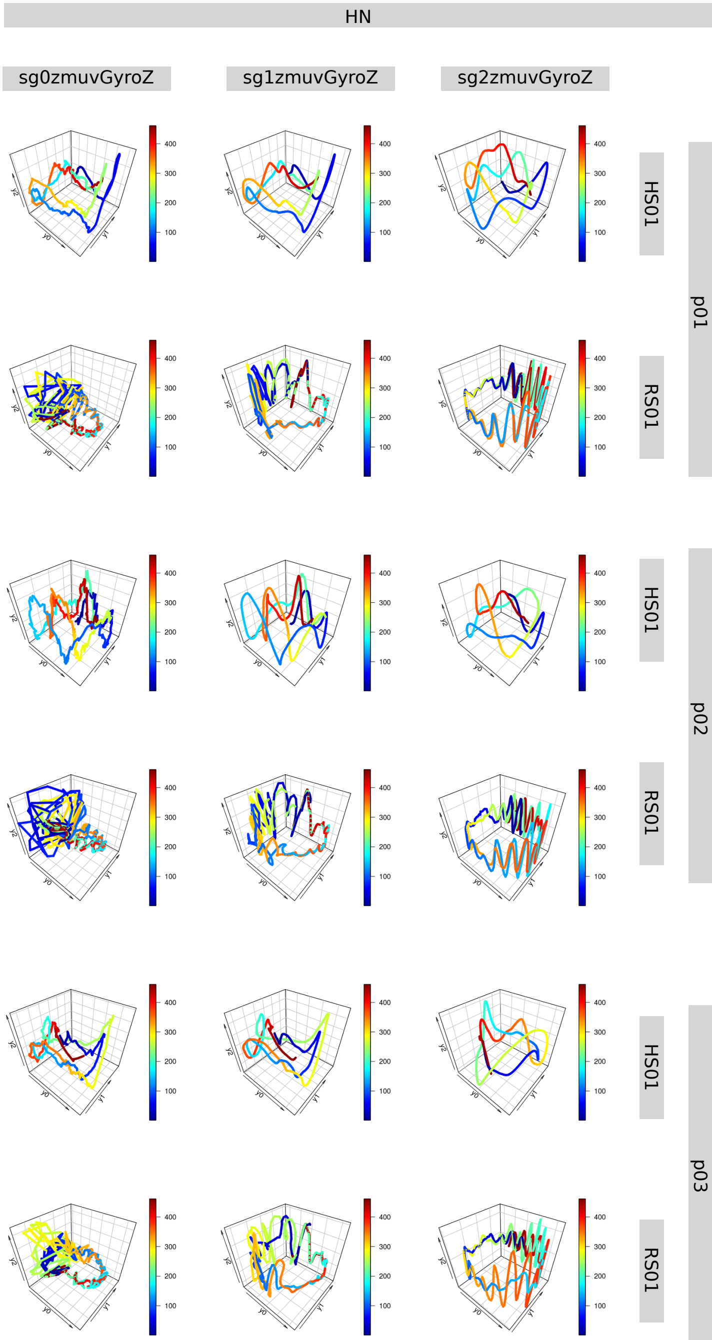

Fig. E.11 **RSSs for horizontal normal arm movements.** Reconstructed state spaces of participant $p01$, $p02$ and $p03$ for horizontal movements with raw-normalised (sg0zmuvGyroZ), normalised-smoothed 1 (sg1zmuvGyroZ) and normalised-smoothed 2 (sg2zmuvGyroZ) time series of the sensors attached to the participant (HS01) and other sensor attached to the robot (RS01). Reconstructed state spaces were computed with embedding parameters $\overline{m_0} = 6$, $\overline{\tau_0} = 8$. R code to reproduce the figure is available at .

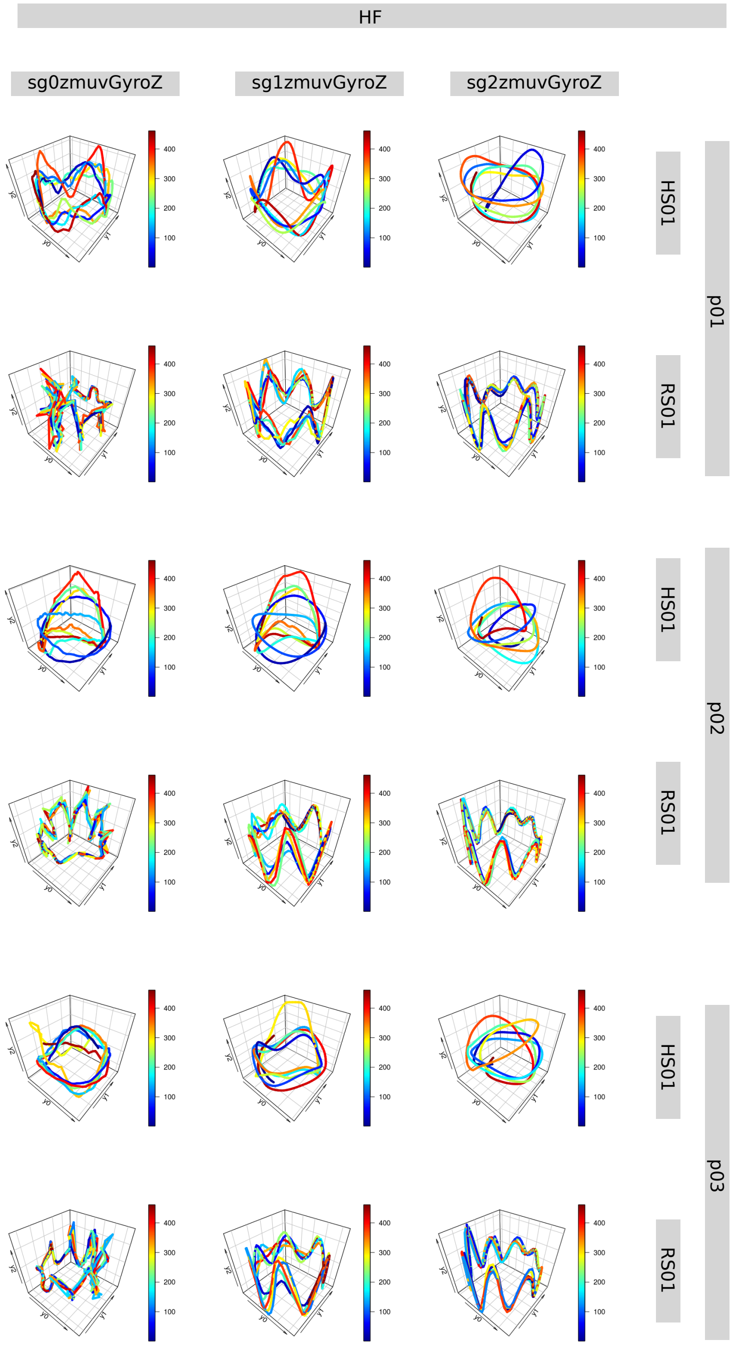

Fig. E.12 **RSSs for horizontal faster arm movements.** Reconstructed state spaces of participant $p01$, $p02$ and $p03$ for horizontal faster movements with raw-normalised (sg0zmuvGyroZ), normalised-smoothed 1 (sg1zmuvGyroZ) and normalised-smoothed 2 (sg2zmuvGyroZ) time series of the sensors attached to the participant (HS01) and other sensor attached to the robot (RS01). Reconstructed state spaces were computed with embedding parameters $\overline{m_0} = 6$, $\overline{\tau_0} = 8$. R code to reproduce the figure is available at .

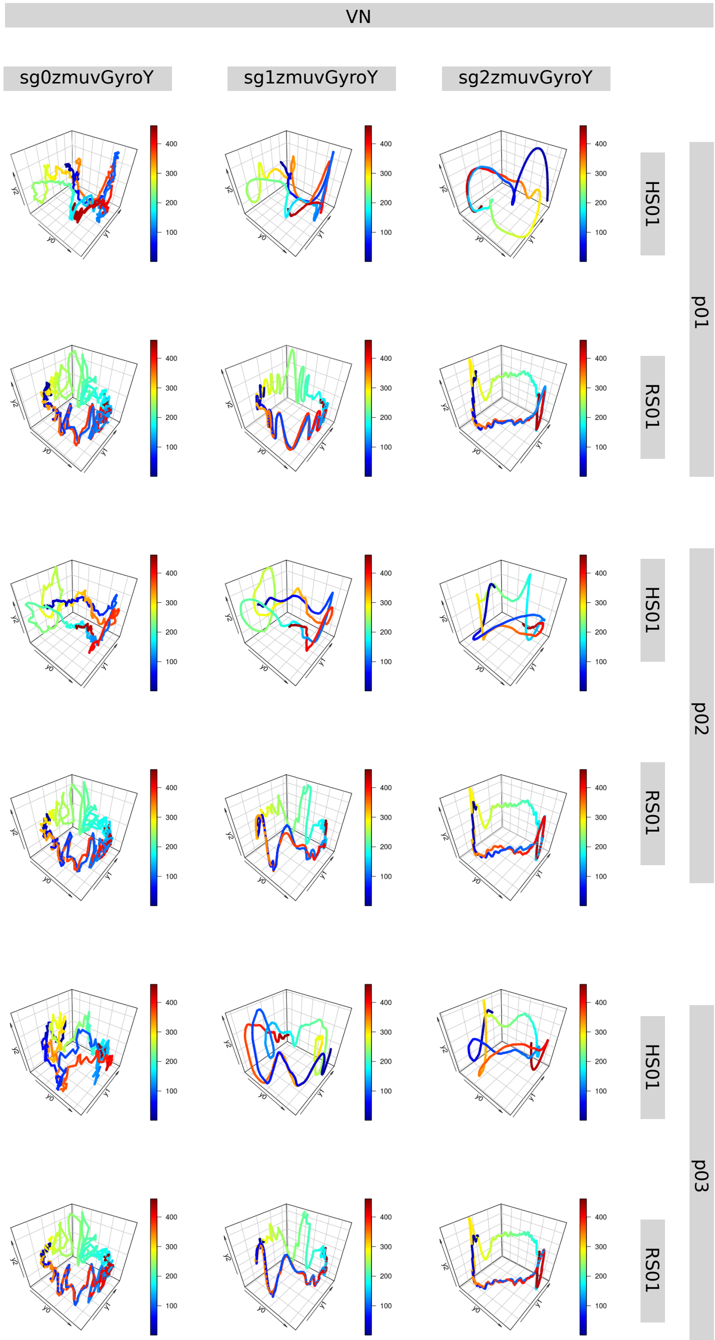

Fig. E.13 **RSSs for vertical normal arm movements.** Reconstructed state spaces of participant $p01$, $p02$ and $p03$ for horizontal movements with raw-normalised (sg0zmuvGyroY), normalised-smoothed 1 (sg1zmuvGyroY) and normalised-smoothed 2 (sg2zmuvGyroY) time series of the sensors attached to the participant (HS01) and other sensor attached to the robot (RS01). Reconstructed state spaces were computed with embedding parameters $\overline{m_0} = 6$, $\overline{\tau_0} = 8$. R code to reproduce the figure is available at .

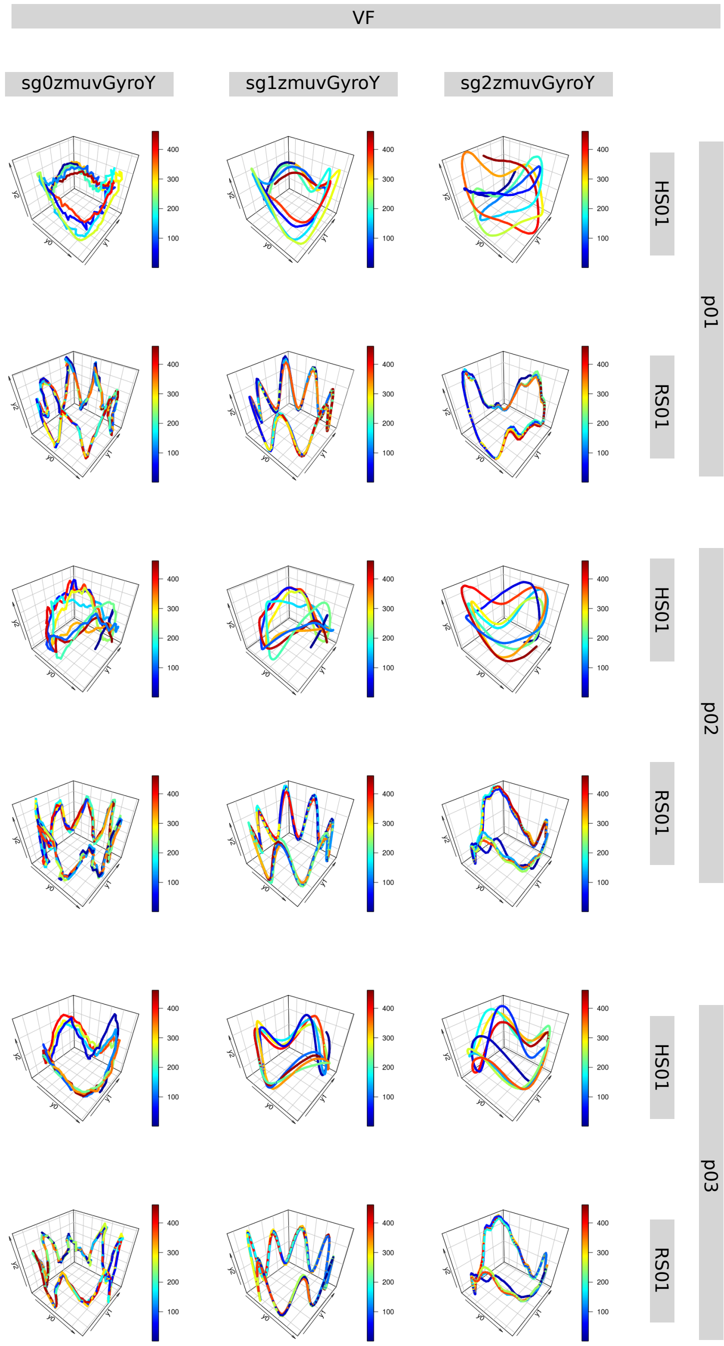

Fig. E.14 **RSSs for vertical faster arm movements.** Reconstructed state spaces of participant $p01$, $p02$ and $p03$ for horizontal faster movements with raw-normalised (sg0zmuvGyroY), normalised-smoothed 1 (sg1zmuvGyroY) and normalised-smoothed 2 (sg2zmuvGyroY) time series of the sensors attached to the participant (HS01) and other sensor attached to the robot (RS01). Reconstructed state spaces were computed with embedding parameters $\overline{m_0} = 6$, $\overline{\tau_0} = 8$. R code to reproduce the figure is available at .

E.4 RPs

Recurrence Plots participant $p01$, $p02$ and $p03$ for horizontal arm movements (Figs. E.15, E.16) and vertical arm movements (Figs. E.17, E.18). For remained results with window size lengths of time series data, we refer the reader to download the data and code at Xochicale (2018).

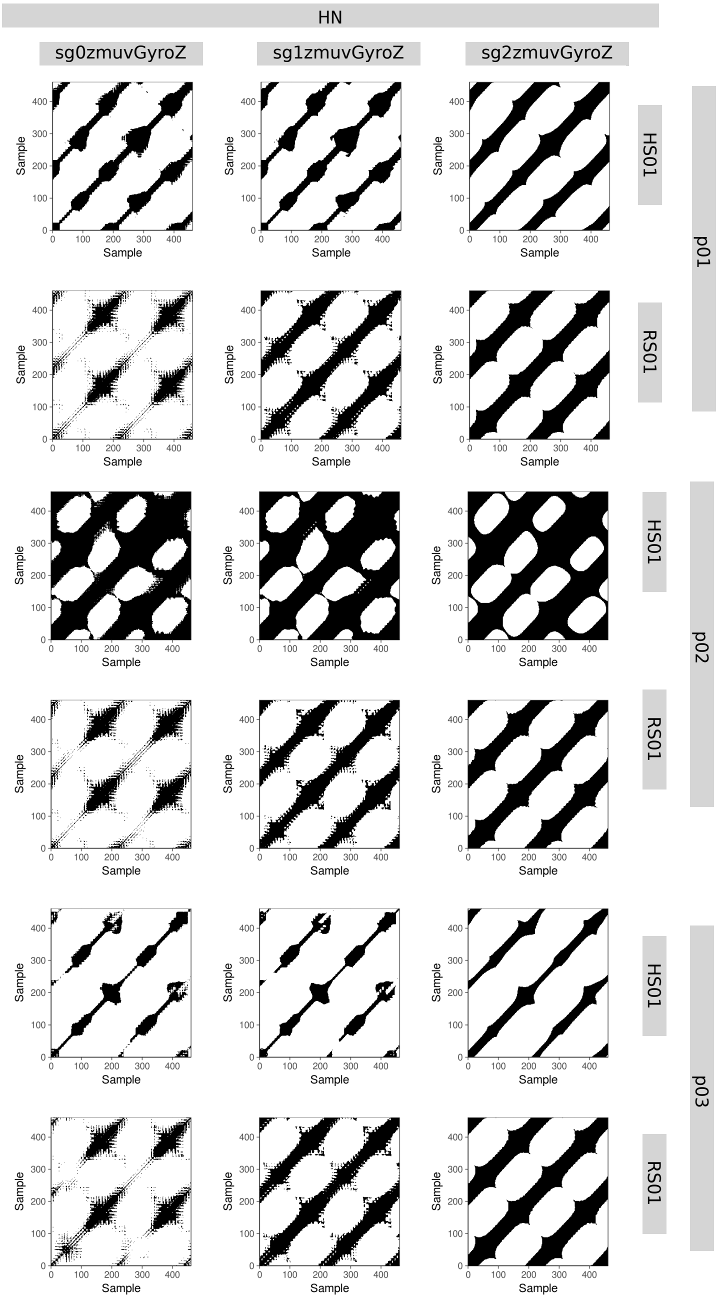

Fig. E.15 **RPs for horizontal normal arm movements.** Recurrence plots of participant $p01$, $p02$, $p03$ for horizontal normal movements with time series of raw-normalised (sg0zmuvGyroZ), normalised-smoothed 1 (sg1zmuvGyroZ) and normalised-smoothed 2 (sg2zmuvGyroZ), and sensors attached to the participant (HS01) and to the robot (RS01). Recurrence plots were computed with embedding parameters $\overline{m_0} = 6$, $\overline{\tau_0} = 8$ and recurrence threshold $\epsilon = 1$. R code to reproduce the figure is available at .

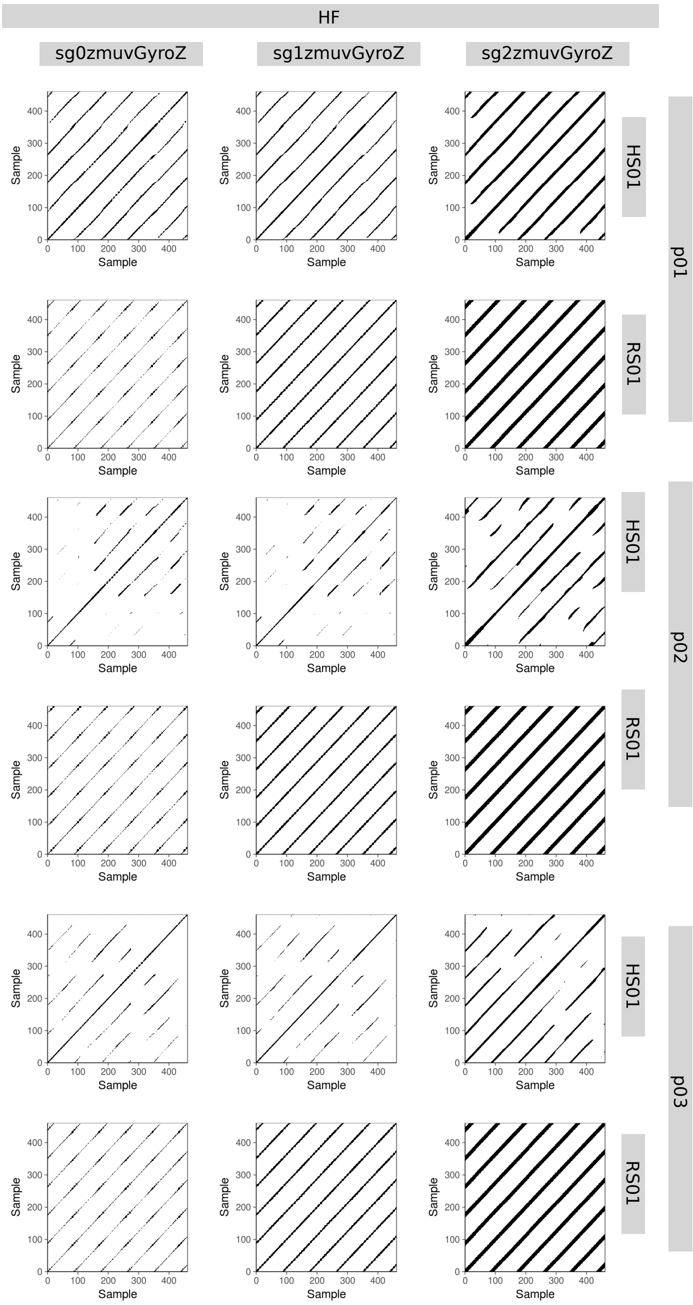

Fig. E.16 **RPs for horizontal faster arm movements.** Recurrence plots of participant $p01$, $p02$, $p03$ for horizontal faster movements with time series of raw-normalised (sg0zmuvGyroZ), normalised-smoothed 1 (sg1zmuvGyroZ) and normalised-smoothed 2 (sg2zmuvGyroZ), and sensors attached to the participant (HS01) and to the robot (RS01). Recurrence plots were computed with embedding parameters $\overline{m_0} = 6$, $\overline{\tau_0} = 8$ and recurrence threshold $\epsilon = 1$. R code to reproduce the figure is available at .

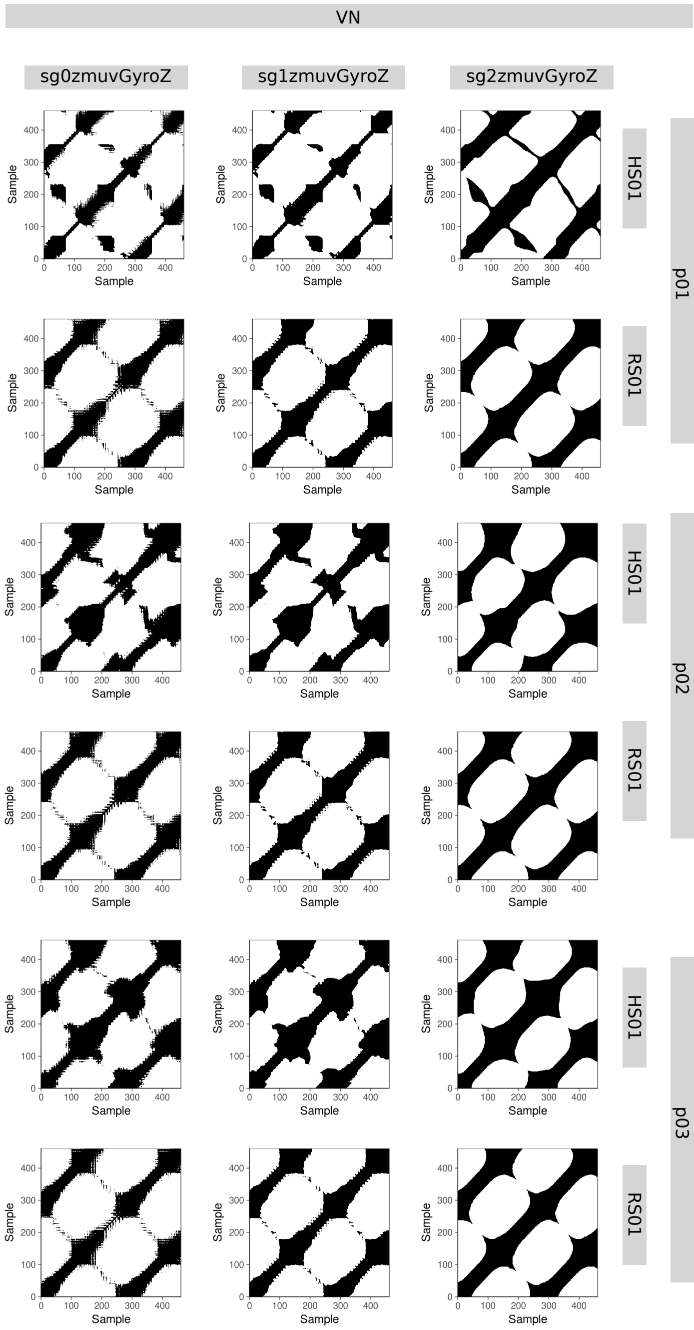

Fig. E.17 **RPs for vertical normal arm movements.** Recurrence plots of participant $p01$, $p02$, $p03$ for vertical normal movements with time series of raw-normalised (sg0zmuvGyroY), normalised-smoothed 1 (sg1zmuvGyroY) and normalised-smoothed 2 (sg2zmuvGyroY), and sensors attached to the participant (HS01) and to the robot (RS01). Recurrence plots were computed with embedding parameters $\overline{m_0} = 6$, $\overline{\tau_0} = 8$ and recurrence threshold $\epsilon = 1$. R code to reproduce the figure is available at .

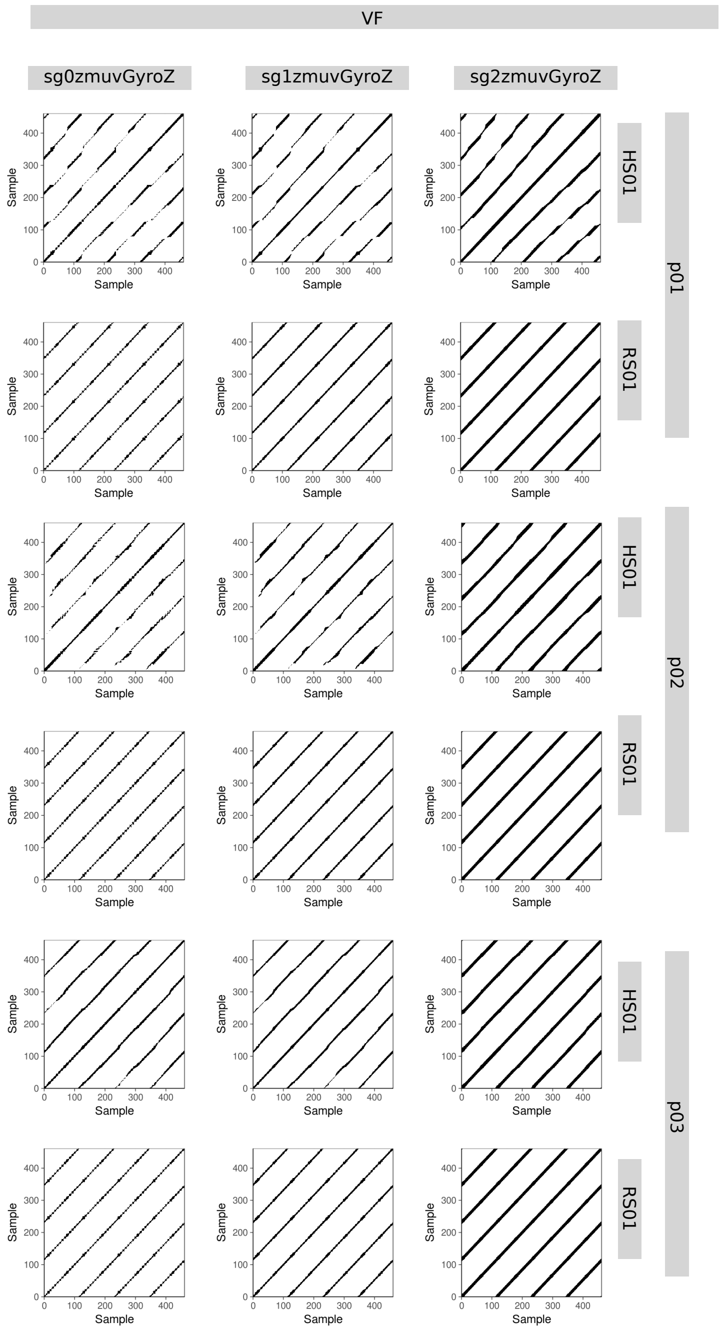

Fig. E.18 **RPs for vertical faster arm movements.** Recurrence plots of participant $p01$, $p02$, $p03$ for vertical faster movements with time series of raw-normalised (sg0zmuvGyroY), normalised-smoothed 1 (sg1zmuvGyroY) and normalised-smoothed 2 (sg2zmuvGyroY), and sensors attached to the participant (HS01) and to the robot (RS01). Recurrence plots were computed with embedding parameters $\overline{m_0} = 6$, $\overline{\tau_0} = 8$ and recurrence threshold $\epsilon = 1$. R code to reproduce the figure is available at .

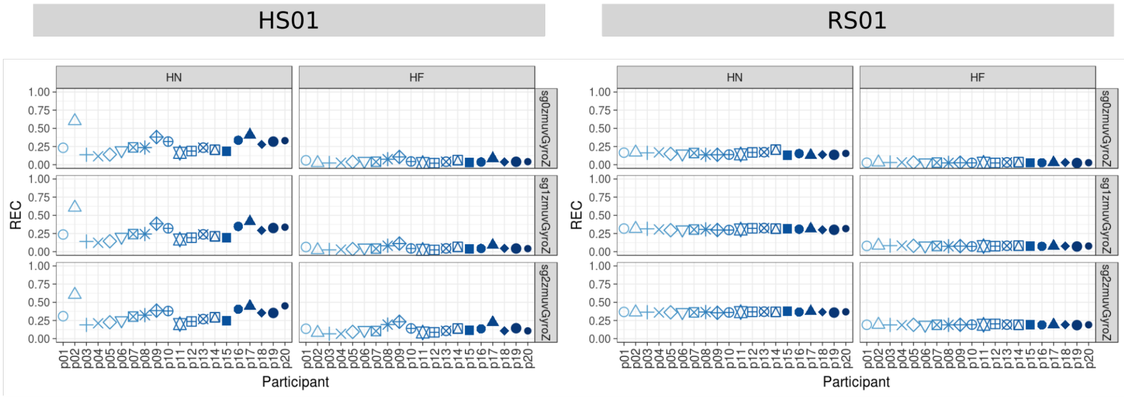

Fig. E.19 **REC values for horizontal arm movements.** REC values (representing % of black dots in the RPs) for 20 participants performing HN and HF movements with sensors HS01, RS01 and three smoothed-normalised axis of GyroZ (sg0zmuvGyroZ, sg1zmuvGyroZ and sg2zmuvGyroZ). REC values were computed with embedding parameters $\overline{m_0} = 6$, $\overline{\tau_0} = 8$ and recurrence threshold $\epsilon = 1$. R code to reproduce the figure is available at .

E.5 RQAs

E.5.1 REC values

REC values, representing the % of black dots in the RPs, are shown in Figs. E.19 and E.20.

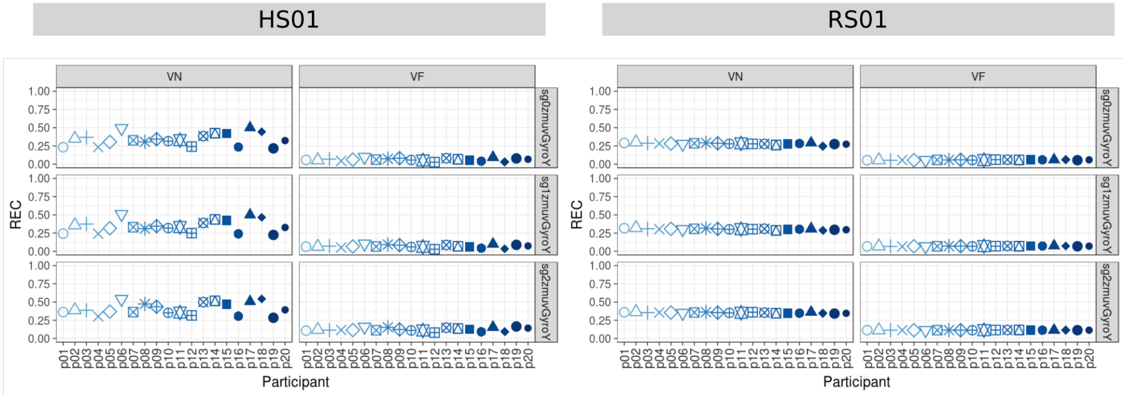

Fig. E.20 **REC values for vertical arm movements.** REC values (representing % of black dots in the RPs) for 20 participants performing VN and VF movements with sensors HS01, RS01 and three smoothed-normalised axis of GyroY (sg0zmuvGyroY, sg1zmuvGyroY and sg2zmuvGyroY). REC values were computed with embedding parameters $\overline{m_0} = 6$, $\overline{\tau_0} = 8$ and recurrence threshold $\epsilon = 1$. R code to reproduce the figure is available at .

E.5.2 DET values

DET values, representing predictability and organisation of the RPs. are shown in Figs. E.21 and E.22.

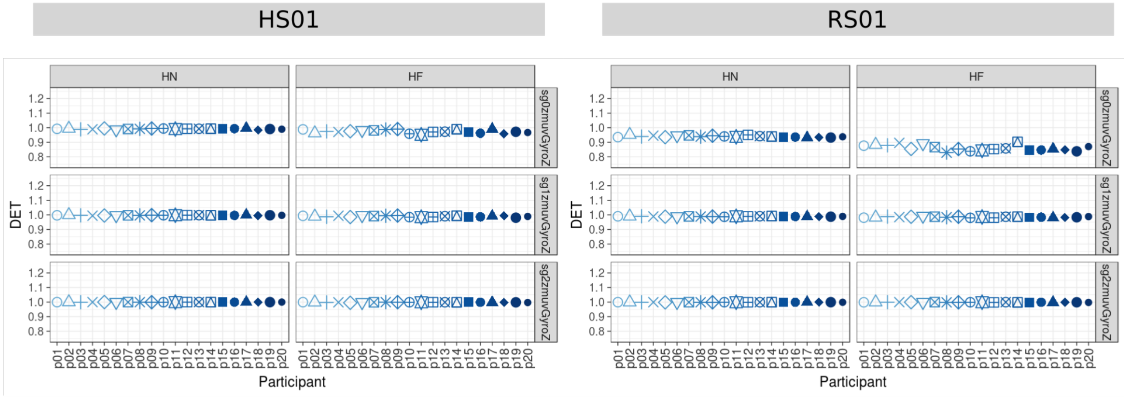

Fig. E.21 **DET values for horizontal arm movements.** DET values (representing predictability and organisation of the RPs) for 20 participants performing HN and HF movements with sensors HS01, RS01 and three smoothed-normalised axis of GyroZ (sg0zmuvGyroZ, sg1zmuvGyroZ and sg2zmuvGyroZ). DET values were computed with embedding parameters $\overline{m_0} = 6$, $\overline{\tau_0} = 8$ and recurrence threshold $\epsilon = 1$. R code to reproduce the figure is available at .

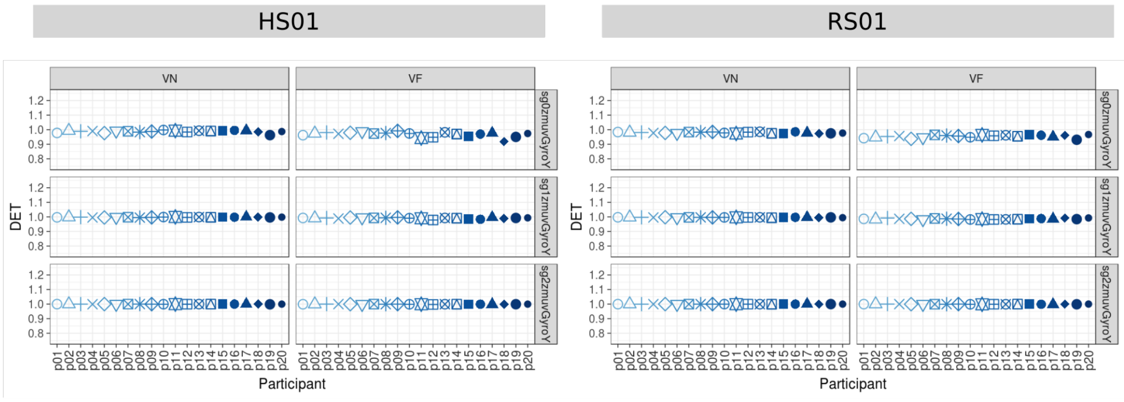

Fig. E.22 **DET values for vertical arm movements.** DET values (representing predictability and organisation of the RPs) for 20 participants performing VN and VF movements with sensors HS01, RS01 and three smoothed-normalised axis of GyroY (sg0zmuvGyroY, sg1zmuvGyroY and sg2zmuvGyroY). DET values were computed with embedding parameters $\overline{m_0} = 6$, $\overline{\tau_0} = 8$ and recurrence threshold $\epsilon = 1$. R code to reproduce the figure is available at .

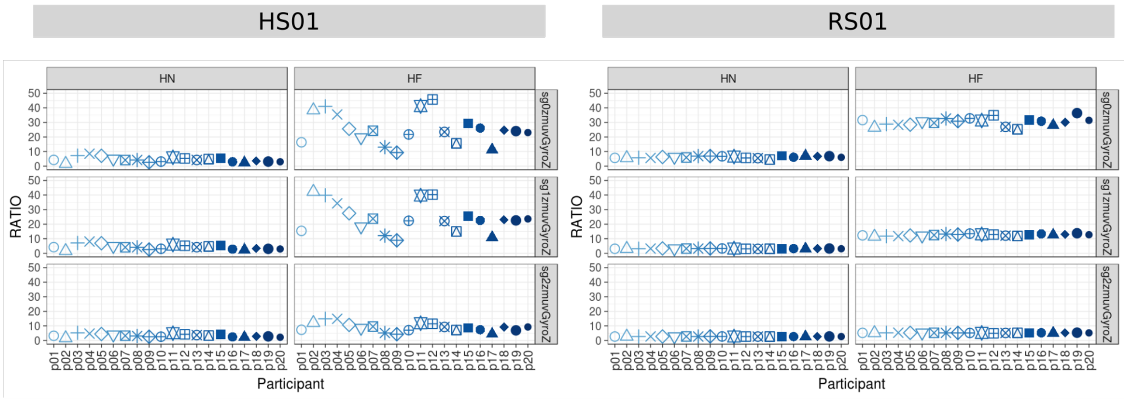

Fig. E.23 **RATIO values for horizontal arm movements.** RATIO (representing dynamic transitions) for 20 participants performing HN and HF movements with sensors HS01, RS01 and three smoothed-normalised axis of GyroZ (sg0zmuvGyroZ, sg1zmuvGyroZ and sg2zmuvGyroZ). RATIO values were computed with embedding parameters $\overline{m_0} = 6$, $\overline{\tau_0} = 8$ and recurrence threshold $\epsilon = 1$. R code to reproduce the figure is available at .

E.5.3 RATIO values

RATIO values, representing dynamic transitions, are shown in Figs. E.23 and E.24.

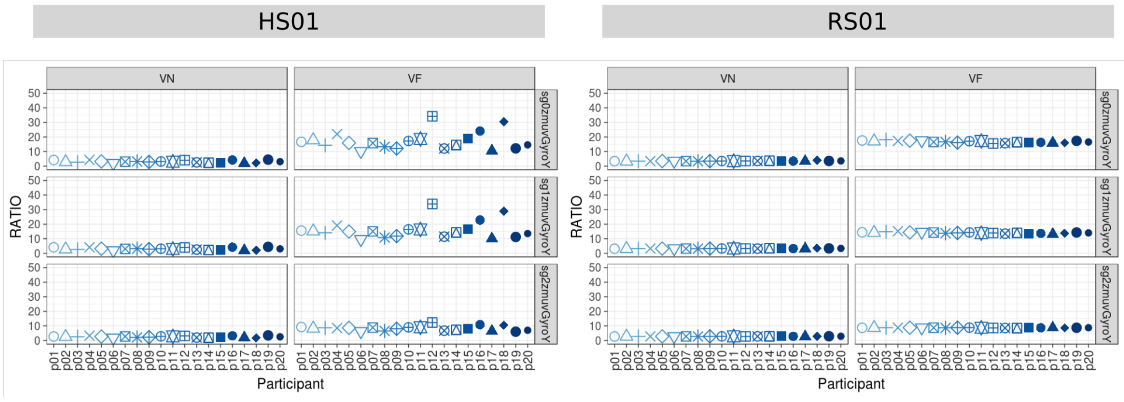

Fig. E.24 **RATIO values for vertical arm movements.** RATIO (representing dynamic transitions) for 20 participants performing VN and VF movements with sensors HS01, RS01 and three smoothed-normalised axis of GyroY (sg0zmuvGyroY, sg1zmuvGyroY and sg2zmuvGyroY). RATIO values were computed with embedding parameters $\overline{m_0} = 6$, $\overline{\tau_0} = 8$ and recurrence threshold $\epsilon = 1$. R code to reproduce the figure is available at .

E.5.4 ENTR values

ENTR values, representing the complexity of the ructure in time series, are shown in Figs. E.25 and E.26.

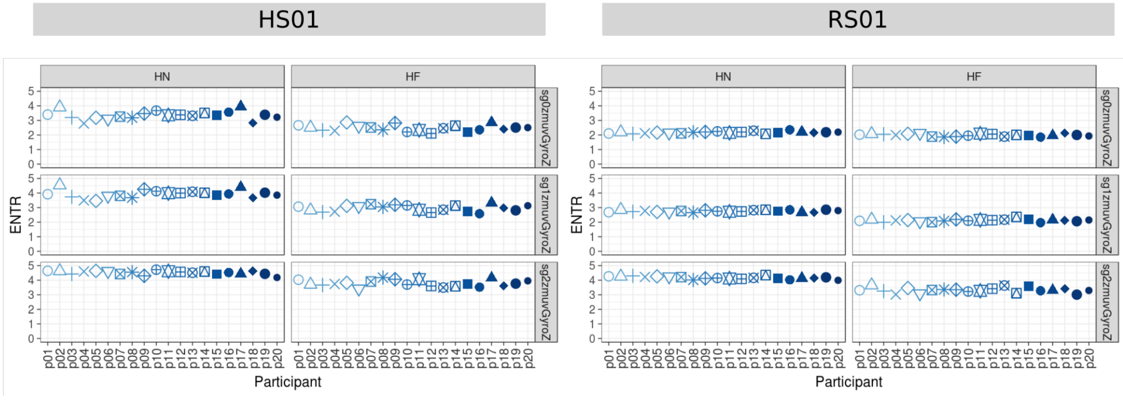

Fig. E.25 **ENTR values for horizontal arm movements.** ENTR values (representing the complexity of the deterministic structure in time series) for 20 participants performing HN and HF movements with sensors HS01, RS01 and three smoothed-normalised axis of GyroZ (sg0zmuvGyroZ, sg1zmuvGyroZ and sg2zmuvGyroZ). ENTR values were computed with embedding parameters $\overline{m_0} = 6$, $\overline{\tau_0} = 8$ and recurrence threshold $\epsilon = 1$. R code to reproduce the figure is available at .

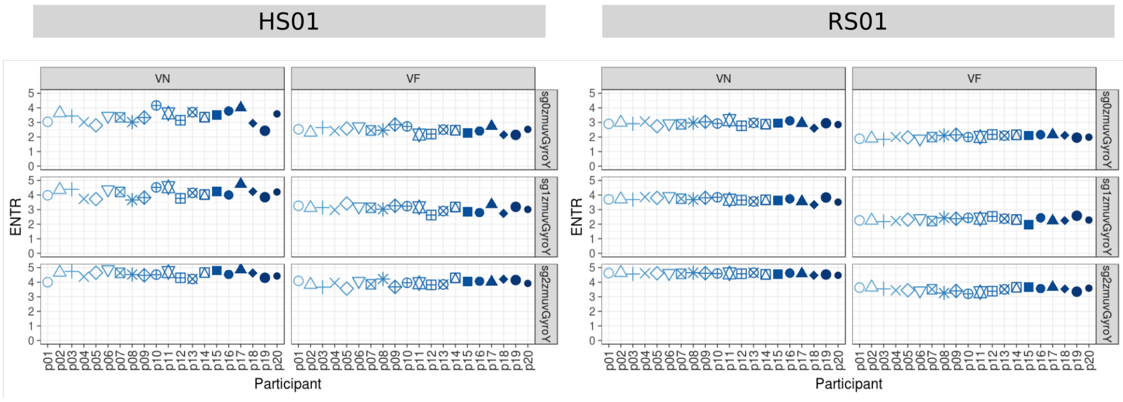

Fig. E.26 **ENTR values for vertical arm movements.** ENTR values (representing the complexity of the deterministic structure in time series) for 20 participants performing VN and VF movements with sensors HS01, RS01 and three smoothed-normalised axis of GyroY (sg0zmuvGyroY, sg1zmuvGyroY and sg2zmuvGyroY). ENTR values were computed with embedding parameters $\overline{m_0} = 6$, $\overline{\tau_0} = 8$ and recurrence threshold $\epsilon = 1$. R code to reproduce the figure is available at .

Appendix F

Open Access Code and Data

F.1 Code and data organisation

Code path has ten directories which have a descriptive name of their content:

`0_machineinfo/`

`1_dependencies/`

`2_libraries_functions/`

`3_anthropometrics/`

`4_figs_ch3/`

`5_creation_of_curated_timeseries/`

`6_figs_ch4/`

`7_figs_ch5/`

`8_figs_ch6/`

`x_surrogate/`

Code path is available at . Data is organised in paths for row data time series and preprocessed datsets .

F.2 How results can be replicated

This thesis has been written in GNU Linux Operating System. Therefore, for its replication it is suggested that users install Ubuntu 14.04.5 LTS or Ubuntu 16.04.2 LTS (other GNU Linux distributions can also work). Additionally, it is suggested installing the latest version of R with all its dependencies and GNU Octave, version 4.0.2 (follow the alphabetic order of the scripts to install all dependencies).

For figure replication, the paths are organised with three paths: `code/` contains R scripts that create figures in `scr/`, and `vector/` contains the vector files.